Lipid ligand - protein receptor interactions characterised by a resonant mirror biosensor

by

Pieter Jakobus Vrey

Submitted in partial fulfilment of the requirements for the degree

Master of Science

in the
Department of Biochemistry
Faculty of Natural and Agricultural Sciences
University of Pretoria
Pretoria

April 2004

ACKNOWLEDGEMENTS

- Prof. Jan Verschoor, my promoter: without your leadership, discussions and trust, this dissertation would not have been possible.
- Dr. Annemieke ten Bokum: apart from the numerous helpful discussions, your friendship in South Africa and Holland was invaluable to me.
- Personnel of the Immunology Department, Erasmus University, Rotterdam under leadership of Prof. Dr. Rob Benner: my stay in Holland would have been worthless and gloomy without your discussions, leadership and friendship.
- Mrs. Sandra van Wyngaardt: for the HPLC analysis and for always being there to lend a helping hand in the lab.
- Dr. Bart Jacobs: who kindly provided me with GBS patient sera from Holland.
- Dr. Caswell Hlongwane and Mr. Clement Stander who assisted me with MALDI-TOF and EI-MS.
- Dr. Lynne Collett: for helpful discussions concerning TLC.
- Fellow students of the Biochemistry Department: for sharing the trials and tribulations that sprouted in the labs and hallways.
- My dearest friends: who put up with my sour moods and incessant complaining.
- My parents: to whom I owe so much and tell them so little.
- Marsha: my love, you have taught me to believe in myself. Without you, my achievements in life would be greatly diminished.
- The National Research Foundation and the Medical Research Council of South Africa for funding and bursaries.

CONTENTS

LIST OF TABLES

LIST OF FIGURES

LIST OF ABBREVIATIONS

Å	Angstrom
Ab	antibody
Ag	antigen
$AgNO_3$	silver nitrate
AIDS	acquired immune deficiency syndrome
anti-Id	anti-idiotype
BCG	Bacillus Calmette Guerin
BIA	biomolecular interaction analysis
°C	degrees Celsius
$CaSO_4$	calcium sulphate
CD	cluster of differentiation
cm	centimeters
CMD	carboxymethyl dextran
CPC	cetyl pyridinium chloride
CSIR	Council for Scientific and Industrial Research
CTx	cholera toxin
CTxB	cholera toxin B-subunit (choleragenoid)
Da	Dalton
DHB	2,5-dihydroxybenzoic acid
DNA	deoxyribonucleic acid
EDC	1-ethyl-3-(3-dimethylaminopropyl)-carbodiimide
EDTA	ethylene diamine tetra-acetic acid
EI-MS	electron-impact mass spectrometry
ELISA	enzyme-linked immunosorbent assay
eV	electronvolt
G	ligand
GBS	Guillain-Barré syndrome
GC-MS	gas chromatography mass spectrometry
G_{D1a}	ganglioside G_{D1a}
G_{D1b}	ganglioside G_{D1b}
G_{M1}	ganglioside G_{M1}
G_{M3}	ganglioside G_{M3}
GSCN	guanidine thiocyanate
HCl	hydrochloric acid
HDL	high-density lipoproteins
HIV	human immune deficiency virus
HPLC	high-pressure liquid chromatography
HSP	heat shock protein
IAsys	interaction analysis system
Id	idiotype

Ig	immunoglobulin
ITC	isothermal titration calorimetry
IVIg	intravenous immunoglobulin
K_A	association equilibrium constant
k_{ass}	association rate constant
K_D	dissociation equilibrium constant
k_{diss}	dissociation rate constant
$KHCO_3$	potassium bicarbonate
KOH	potassium hydroxide
k_{on}	apparent on-rate for monophasic association
$k_{on(1)}$	first order apparent on-rate for biphasic association
$k_{on(2)}$	second order apparent on-rate for biphasic association
kV	kilovolt
L	ligate
LAM	lipoarabinomannan
LDL	low density lipoproteins
L_{M1}	ganglioside L_{M1}
LPS	lipopolysaccharides
M	molar
MA	mycolic acids
mA	milliamperes
MALDI-TOF	matrix-assisted laser desorption/ionisation time-of-flight
mg	milligrams
MHC	major histocompatibility complex
min	minutes
mM	millimolar
mm	millimeters
MS	mass spectrometry
NaCl	sodium chloride
NaN_3	sodium azide
NaOH	sodium hydroxide
NHS	N-hydroxysuccinimide
nm	nanometers
ODM	octadecylmercaptan
%	percentage
PBS	phosphate buffered saline
PBS/AE	phosphate buffered saline containing sodium azide and EDTA
PC	L-α-phosphatidylcholine
PLC	preparative thin layer chromatography
PPD	purified protein derivative
psi	pounds per square inch
R_0	initial biosensor response
R_{eq}	equilibrium biosensor response
R_t	biosensor response at time **t**

SLE	systemic lupus erythematosus
std	standard
TB	tuberculosis
T_C cells	cytotoxic T-cells
TCR	T-cell antigen receptor
TFA	trifluoracetic acid
T_H cells	T helper cells
TLC	thin layer chromatography
TMDM	(trimethylsilyl)diazomethane
Tris	tris (hydroxymethyl) aminomethane
T_S cells	suppressor T cells
µg	micrograms
µl	microliters
UV	ultra violet
V	volt
v/v	volume per volume
w/v	weight per volume

CHAPTER 1
LITERATURE REVIEW: LIPIDS AND AUTO-IMMUNITY

1.1 Auto-immunity

Pathogenic microbes surround us every day of our lives, waiting for a chance to infect us. Fortunately, humans possess a complex and effective immune system to combat such pathogenic infections. However, when any immune system, human or animal, loses the ability to differentiate between foreign and self-tissues, cells or molecules, a condition called auto-immunity results. In other words, the host's own immune system acts against its own tissues in a sort of a natural suicide.

Auto-immunity can result from the cellular arm of adaptive immunity by virtue of T-lymphocytes (T-cells) (Hood *et al.*, 1989), or from the humoral arm of adaptive immunity by virtue of antibodies (Calvanico, 1993) or a combination of both (Oldstone *et al.*, 1986). Specific recognition is achieved in both arms of the adaptive immune response by antigen specific receptors, be it the antibodies themselves or T-cell antigen receptors anchored in the membranes of T-cells. These antigen specific receptors are generated randomly by the bone marrow (B-cells) and thymus (T-cells) during the ontogeny of the animal/human. This process, affected by gene recombination, produces antibodies and T-cells reacting to both foreign and self-structures. Almost every conceivable antigen can be recognised by the variety of antibodies and T-cells generated. In the thymus and bone marrow, T- and B-cells respectively are sorted to eliminate the auto-antibodies and T-cells reactive to self, before they are released into circulation (Cooper, 1986; Schwartz, 1986; Singer *et al.*, 1986). Sometimes however, as a consequence of an infection or genetic predisposition, auto-antibodies and auto-reactive T-cells manifest in the body (Schwartz, 1986). Although difficult to demonstrate in case-controlled studies, it has also been shown that vaccinations and surgery can lead to the generation of auto-immunity (Winer *et al.*, 1988; Hughes, 1990).

Many examples of auto-immunity exist. Auto-antibodies called rheumatoid factors circulate in rheumatoid arthritis as well as tuberculosis patients. These auto-antibodies recognise the F_c region epitopes of denatured IgG (Abe *et al.*, 1984; Pasquali *et al.*, 1984).

In systemic lupus erythematosus (SLE), auto-antibodies are generated against naked deoxyribonucleic acid (DNA) (Abdou *et al.*, 1981; Zouali & Eyquem, 1983), and patients with acute viral hepatitis have antibodies against membrane bound liver specific lipoprotein (Tsubouchi *et al.*, 1985). Protein receptors have also been the target of auto-antibodies as in the cases of myasthenia gravis where auto-antibodies recognise the acetylcholine receptor (Dwyer *et al.*, 1983) and in juvenile hypoglycaemia where insulin receptors are targeted (Maron *et al.*, 1983). Auto-antibodies against lipids also exist but this will be discussed in detail later (*see* par 1.8).

The mechanism of how these auto-immune diseases come into existence is largely unknown. The general aim of this study is to make a contribution towards the knowledge of the mechanisms of auto-immunity, by investigating possible molecular targets for auto-antibodies and how these antibodies are regulated in the antibody idiotype network.

1.2 Idiotype-anti-idiotype relationships

It seems that B-cells and T-cells are opposed by counteracting B- and T-cells of which the receptors are in a mutual idiotope-paratope relationship, i.e. they can bind specifically to the antigen binding sites of one another. Antibody receptors have different kinds of antigenic determinants: isotypic, allotypic and idiotypic, located on different regions of the antibody. Isotypic determinants are present in the germ line of all species, determine the isotype (IgG, IgM, IgD, IgA, IgE) of the antibody and are located throughout the constant domains of both the heavy and the light chains (Van Loghem & Biewenga, 1983). Allotypic determinants determine the allelic variability within species and are located also on both the heavy and light chain's constant regions (Roux & Metzger, 1982). The hyper variable V-region of the antibody that determines antigen-binding specificity contains the idiotypic determinants that comprise the idiotype (Id) of the antibody (Clem & Leslie, 1982; Roux & Metzger, 1982). The idiotype of every antibody is expressed by the combination of variable (V), diversity (D) and joining (J) exons (Kearney *et al.*, 1989) and is located in the F_{ab} region of the antibody where both heavy and light chains participate in the formation of the idiotype (Clem & Leslie, 1982). Regulatory idiotopes are located next to the antigen-binding site, also named the combining site or the paratope (Bona & Bonilla, 1990). Figure 1.1 illustrates the orientation of the antigenic determinants of antibodies.

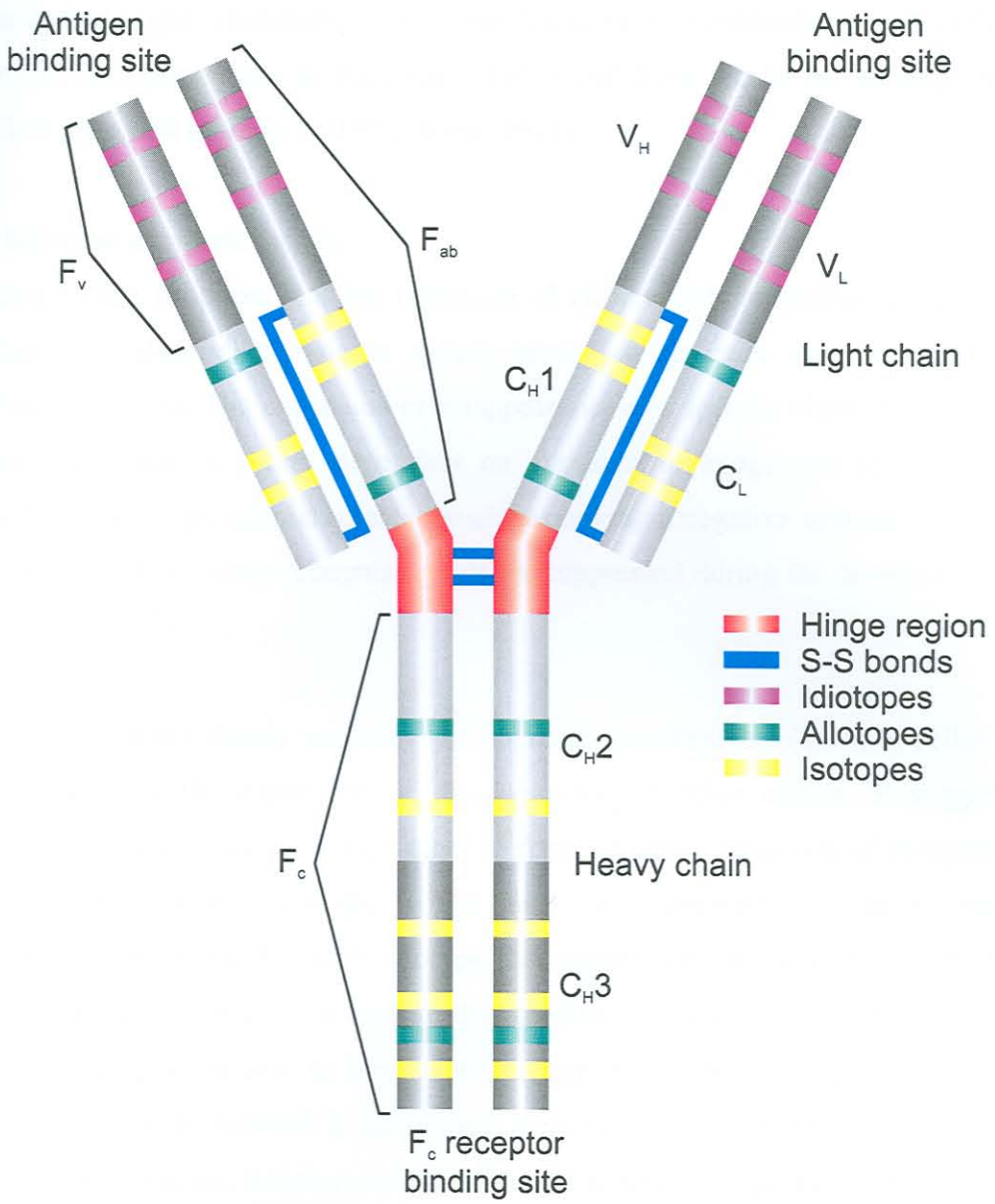

Figure 1.1: Diagram of an immunoglobulin structure indicating the locations of isotopic, allotopic and idiotopic antigenic determinants. Constant and hyper variable domains are indicated as well as the hinge region and disulphide bonds. Fragments (F_v, F_{ab}, F_c) obtained with enzymatic digestion are also indicated. (Source: Benner *et al.*, 1996)

It is universally accepted that antibodies bind antigens via their paratopes, but antibodies exist that can bind to the antigenic determinants of these antibodies and act as receptors for the antibodies. Of specific interest are the antibodies that bind to the idiotype of antibodies and are named anti-idiotypes (anti-Id). In an Id-anti-Id interaction, the antibody carrying the recognised idiotype is designated Ab1 and the antibody recognising the idiotype via its paratope is designated Ab2 (Bona & Bonilla, 1990).

Idiotype-anti-idiotype relationships have been found in both antibodies and T-cell antigen receptors (TCR) (Eichmann & Rajewsky, 1975) and have led to the idiotype network theory first proposed by Jerne in 1974 (Jerne, 1974).

1.3 Idiotype network theory

The clonal theory proposes that the repertoire of all available antibodies arises from the generation of independent random clones according to each clone's specific gene recombination events. The expansion or disappearance of a specific clone is not influenced by other clones but is purely dependent on exposure to exogenous antigen (Bona & Bonilla, 1990). Foreign antigen selects the clones having a negative imprint of the antigen and expands it, while clones recognising self are suppressed during the development of the animal (Bona, 1987).

The idiotype network theory proposes the opposite: lymphocytes (T- or B-cells) have a great influence on the expansion or disappearance of other clones. It suggests that lymphocytes communicate with each other to form an entire repertoire of receptors, each bearing its own unique idiotype, which may be expressed by antigen receptors. Furthermore, it proposes that each idiotype has, somewhere in the idiotype repertoire, a complementary paratope able to bind to that specific idiotype which in turn has another complementary paratope able to bind to its idiotype (Bona & Bonilla, 1990). The factor that limits the idiotype network is the number of genes encoding permutations available in the genome of a species, which is unlimited for all practical purposes. This constitutes an open network.

The network theory suggests that the immune system looks towards itself for the generation of specificity and diversity, rather than to the outside. However, we know that the immune system responds to exposure to exogenous antigens (Nutman *et al.*, 1984). The moulded interface of Id-anti-Id interactions is a pattern of physical non-covalent macromolecular forces and is imperfect (Bona & Bonilla, 1990). This means that absolute complementarity between idiotypes and anti-idiotypes does not exist and for each idiotype there would be a spectrum of different structures of varying degrees of complementarity and hence also varying degrees of affinity. This flexibility in complementarity permits the interaction with foreign epitopes. Considering that antibodies (or T-cell receptors) cannot differentiate between each of its whole array of possible epitopes (which could be an

antibody or a receptor-bound peptide), it seems logical that it would also not be able to distinguish between an internal self epitope and an external foreign epitope. In turn, this suggests that all possible epitopes can be recognised by the immune system, whether they originate from outside or inside the animal.

The ability of an anti-Id antibody to bind slightly different idiotopes suggests that the idiotype is multispecific. Another type of multispecifity is that each idiotype can be recognised by different anti-idiotypes. Some of these anti-idiotypes might bind within the antigen-binding site of an antibody and would therefore be the internal image of an antigen, but some anti-idiotypes may recognise the idiotypic structures outside the antigen-binding site in such a way as to regulate the binding of a foreign antigen or an internal image. Two anti-idiotype antibodies can therefore be defined: Ab2α that binds to idiotypic determinants outside the paratope and Ab2β that acts as an internal image of the antigen (Bona & Bonilla, 1990). This concept is illustrated in Figure 1.2.

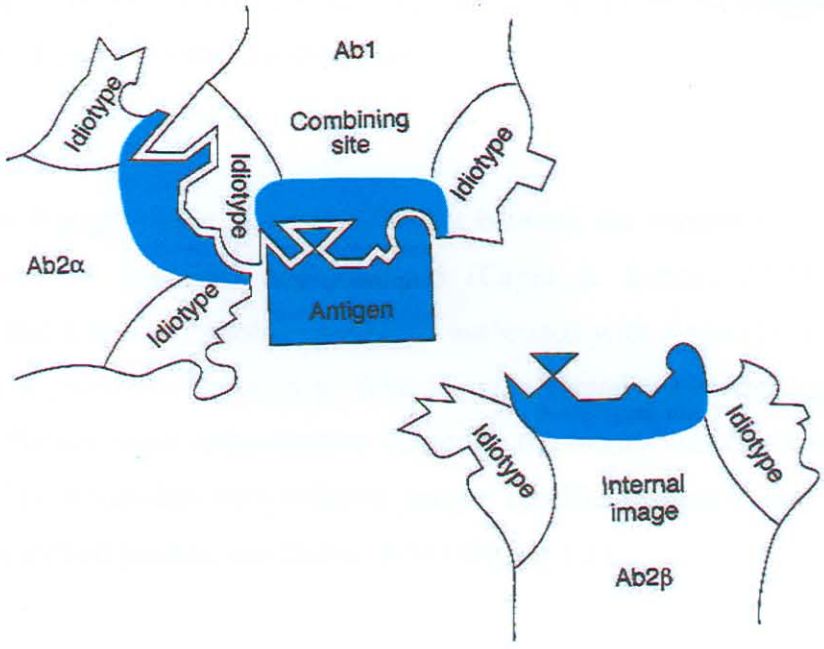

Figure 1.2: Idiotypes and anti-idiotypes. Ab1 provides complementarity for its specific antigen via its paratope. Ab1 contains several idiotypes recognisable by different anti-Id antibodies or Ab2. Ab2α binds to an idiotype of Ab1 that is outside the antigen-binding site and does not interfere with the binding of antigen to Ab1. Ab2β mimics the structure of the antigen and is therefore the internal image of the antigen. (Source: Bona & Bonilla, 1990)

Experimental evidence to support the idiotype network theory exists. Immunisation with antibodies or antigens induces the interaction of antibodies (Ab2) with other antibodies (Ab1) and is called immunomodulation (Dietrich *et al.*, 1993; Hall, 1993). It has been noted that levels of anti-idiotypes and idiotypes fluctuate inversely; in other words, when the concentration of the one is high, the concentration of the other is low (Seto, 1980). Idiotopes have been identified on both B-cells (Munthe *et al.*, 1999) and T-cells (Somasundaram *et al.*, 1995). The same idiotopes can be recognised by both B- and T-cells, which indicates the immunoregulatory function of the idiotype network (Perez, *et al.*, 2002a). Idiotypes or anti-idiotypes are transferred from pregnant animals across the placenta to the neonatal offspring and can influence idiotype expression in the offspring (Lemke *et al.*, 1998).

The network theory also postulates that the immune system, and therefore all idiotypes, is in a constant state of dynamic equilibrium of Id-anti-Id interactions (Bona & Bonilla, 1990). This regulatory mechanism may explain why the response to external epitopes can be launched quickly and effectively, and why an imbalance in the system may lead to severe conditions like auto-immune disorders.

1.4 Parallel sets

Initially it was thought that a relationship exists between the antigen-binding site, hyper variable regions (V domains) and idiotopes (Capra & Kehoe, 1975). This theory hypothesised that a specific idiotope would be associated with a specific antigen-binding site and have a particular specificity. When it was demonstrated that antibodies with different specificities share cross-reactive idiotopes, the theory was challenged (Oudin & Cazenave, 1971). Antibodies with different antigen specificities that shared cross-reactive idiotopes were termed parallel sets (Jerne, 1974) (Figure 1.3).

The discovery of these parallel sets was based on two important conclusions drawn from the interactions of rabbit antibodies to ovalbumin from different species. First, as the antibodies were specific to their antigens, they had to originate from distinct clones. Second, because these different antibodies shared idiotopes among them, they were probably related to one another via a common ancestor (Oudin & Cazenave, 1971).

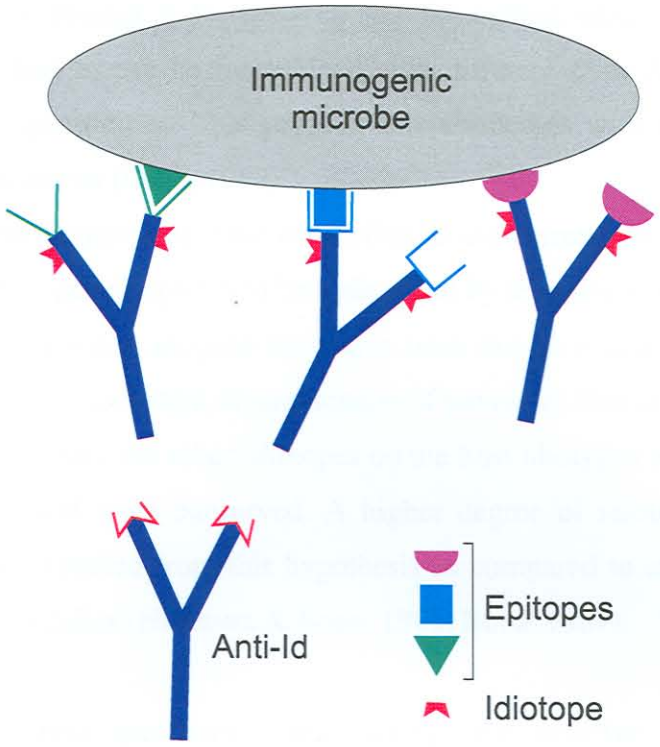

Figure 1.3: Parallel sets. Antibodies with different specificities carry identical or cross-reactive idiotopes. These parallel sets of antibodies probably originated from a common ancestral gene.

Evidence supporting these conclusions was accumulated in subsequent studies. It was shown that goat antibodies specific to human normal and sickle cell haemoglobin have cross-reactive idiotopes (Karol *et al.*, 1978) and that monoclonal antibodies specific to different sugars in lipopolysaccharides of bacteria shared idiotopes (Hiernaux & Bona, 1982). Evidence was also obtained that indicated that idiotopes could be shared by antibodies that are specific to different epitopes of multivalent antigens as well as non-specific sets of antibodies (Bona, 1987).

There are three main hypotheses to explain these so-called parallel sets:

1. Because the idiotype repertoire is larger than the paratope repertoire it was proposed that antibody sets might overlap in idiotype specificity but not in antigen specificity (Jerne, 1974). Idiotypes consist of a number of idiotopes, of which one or more might be shared between antibodies of different specificities. Idiotype diversity might be determined by different 'minigenes' like the *D*-segment (of *V-D-J* recombination), without having an effect on the antigen specificity (Meek *et al.*, 1984).

2. A heavy chain expressing a V_H gene coding for certain idiotopes, may pair with different light chains or can be recombined with different D or J_H segments to form different antigen specificities. This suggests that antibodies with any specificity may share the same idiotopes (Bona, 1987).
3. A common ancestral gene may have diversified to the current pool of V genes due to somatic mutation or gene duplication brought about by selective evolutionary pressure. Diversification of possible antigens may have been due to evolutionary pressure that would have led to a concomitant diversification of paratopes that can bind the antigens. Gene segments encoding the other idiotopes on the host idiotypes were not affected by selective pressure and were conserved. A higher degree of idiotope sharing among antibodies can be expected from this hypothesis as compared to antibodies expressed by different gene families (Hiernaux & Bona, 1982; Bona, 1987).

Antibodies with different specificities, but having cross-reactive idiotopes, may be regulated by antibodies or T-cells specific for the shared idiotype. A degree of relatedness in the immune system genes is implied by cross-reactive idiotypes that may be utilised for cross-regulation (Bona, 1987). The existence of regulatory idiotopes provides an elegant explanation for some of the complexities of the immune system.

1.5 Induction of auto-immunity through idiotypic interactions

Antibodies that can recognise antigens through their paratopes and that can be recognised by other paratopes via their idiotopes provide a basis for auto-immunity. Along with the knowledge of a virtually infinite repertoire of idiotopes, recognition of self-structures seems inevitable. Self-recognition of idiotopes would lead to the expansion of clones and a specific immune response to self-structures (Bona, 1987).

Evidence for self-recognition of idiotypes was first presented in 1974 by Rodkey (1974) and confirmed in 1979 by Wuilmart *et al.* (1979) who reported that antibodies isolated from animals, and injected again into the same animals when they ceased antibody production, induced auto-anti-Id antibodies against the injected idiotypes. Advancing the understanding of auto-immunity a step further, it was shown that auto-anti-Id antibodies were produced under normal circumstances when an immune system responds to a foreign antigen (Kluskens & Köhler, 1974; Cosenza, 1976).

Through the interaction of anti-Id antibodies as well as anti-Id T-cells, microbes can be the triggering mechanism of auto-immunity. This can happen in five ways (Figure 1.4):

1. An auto-antigen cross-reacts with an auto-anti-Id lymphocyte and an idiotope of the antigen specific lymphocyte (Johnson *et al.*, 1985).
2. The antibody recognising the antigen, shares a cross-reactive idiotope with the auto-lymphocyte. The idiotypes of the auto-lymphocyte and the antigen specific antibody are recognised by an anti-Id lymphocyte (Naparstek *et al.*, 1985).
3. The antibody recognising the antigen is anti-Id to an auto-lymphocyte (Holmdahl *et al.*, 1987).
4. Auto-antibodies have idiotopes cross-reacting with viral epitopes by anti-viral antibodies. Viral receptors on the surfaces of cells susceptible to infection would cross-react with the anti-viral antibody (Plotz, 1983).
5. Auto-antibodies against hormones are activated by viral infection of a hormone-secreting cell. This autoantibody would trigger anti-Id antibodies that would in turn, be reactive to the hormone receptor on target cells. Auto-antigenicity to hormones and their receptors would thus be propagated through the idiotype network (Cooke *et al.*, 1984).

1.6 Regulation of the idiotypic network

It has been shown that idiotopes are expressed on the immunoglobulin antigen receptor of B-cells (Claflin *et al.*, 1974; Köhler, 1975) as well as on the antigen receptor of T-cells (Binz & Wigzell, 1975; Eichmann & Rajewsky, 1975). It seems that T-cell receptors share idiotopes with antibodies with the same antigen specificity. How this comes about is unclear, but results have shown that there is no genetic link between idiotopes on antibodies and T-cell receptors (Kurosawa *et al.*, 1981; Kraig *et al.*, 1983). This hypothesis implies that there must be an intermediary element linking antibodies and T-cells that share idiotopes (Bona, 1987).

One theory suggests a mechanism of how the idiotype network may be regulated (personal communication, Prof. J.A. Verschoor). This theory also incorporates how an intermediate element between identical idiotopes on antibodies and T-cells may regulate the network.

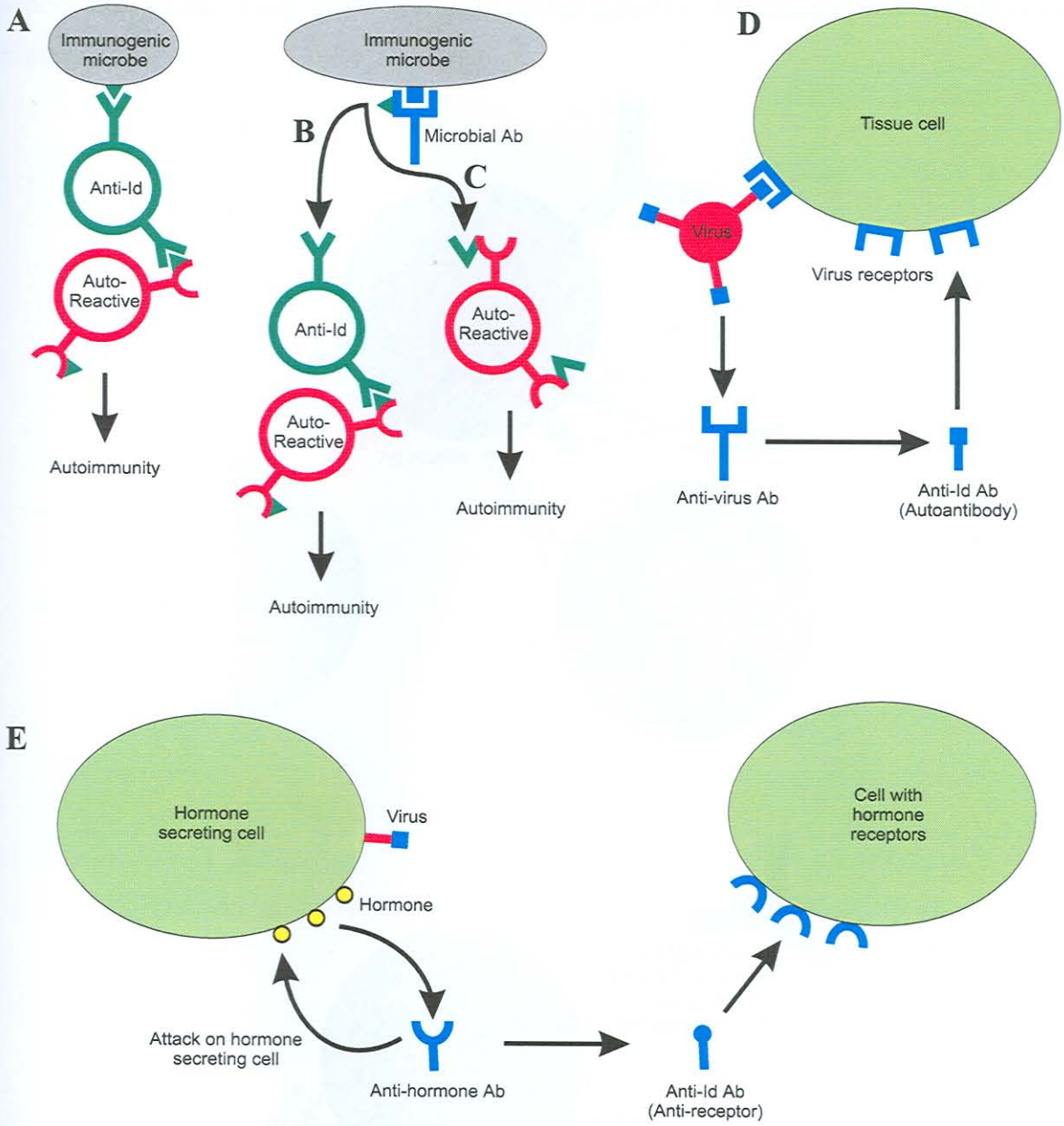

Figure 1.4: Microbial induction of auto-immunity through idiotypic mechanisms. **(A)** Microbial antigen cross-reacts with auto-reactive idiotype via anti-Id. **(B)** Microbial antibody cross-reacts with auto-reactive idiotype via anti-Id. **(C)** Microbial antibody is recognised by auto-reactive lymphocytes. **(D)** Auto-reactive anti-Id antibody is generated by anti-viral antibodies recognising a virus. Anti-Id recognises the viral receptor. **(E)** Viral determinants enhance auto-immunogenicity. (Source: Plotz, 1983; Roiit & Cooke, 1986)

It is universally accepted that antigen (Ag) primes antibody-producing B-cells. The Ag receptors of the B-cells are processed internally and expressed on major histocompatibility complex (MHC) class I and presented to $CD8^+$ cytotoxic T-cells (T_C cells). Cytotoxic T-cells would act as suppressors of these B-cells if no antigen were present. If antigen were present, it would be recognised by the B-cell receptor, internalised, processed and expressed on MHC class II. These antigenic determinants would be recognised by $CD4^+$ T

helper cells (T_H cells) that would stimulate the upregulation of antibody producing B-cells (Figure 1.5A).

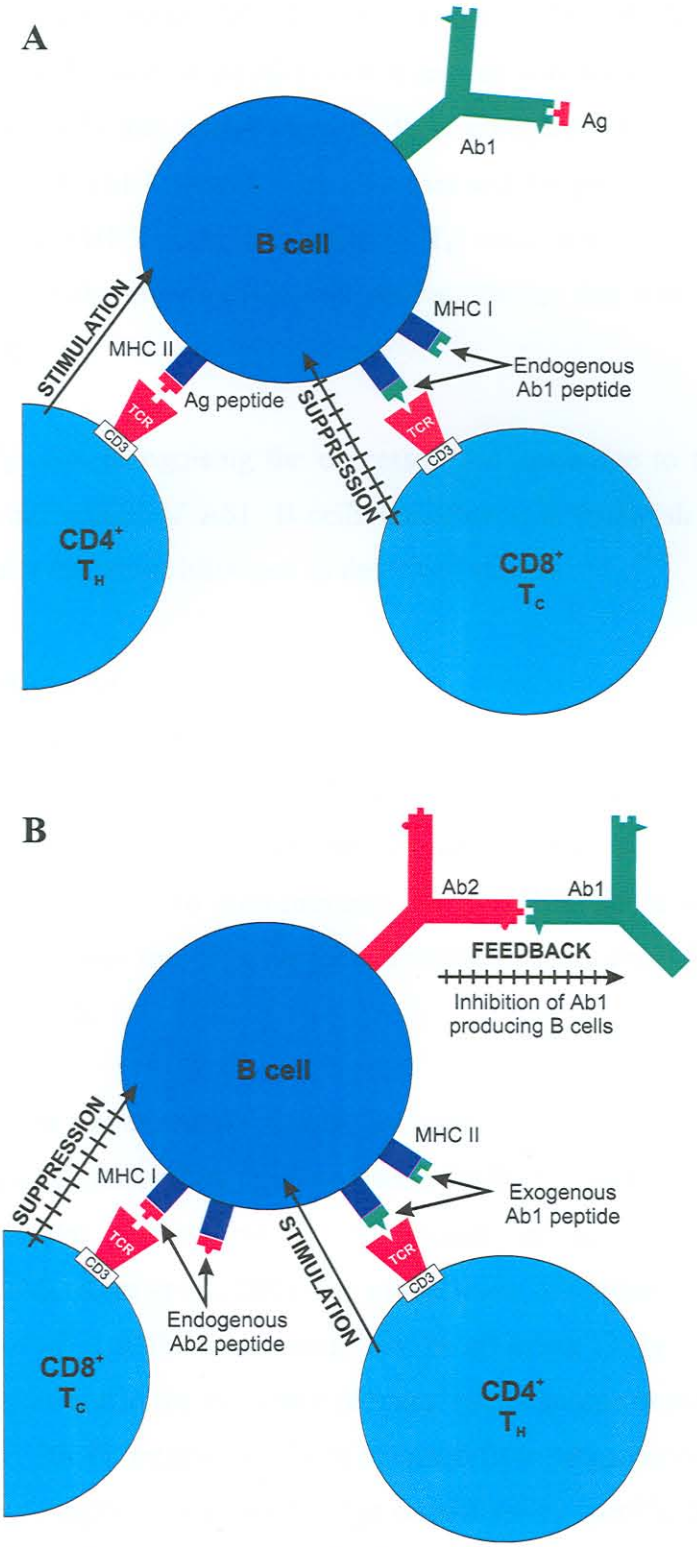

Figure 1.5: Regulation of the B-cells via idiotype network interactions. **(A)** Upregulation of antibody producing B-cells is stimulated by T_H cells after recognition of antigen by an existing idiotope. **(B)** Regulation of the idiotype network via suppressor T cells (T_S cells) mediated suppression and feedback inhibition.

The secreted antibodies (Ab1) contain regulatory idiotopes outside their paratopes as well as antigen counter-image idiotopes within their paratopes. B-cell receptors of different clones (Ab2α or Ab2β) would be able to recognise the different idiotopes. The endogenously expressed Ab2α or Ab2β B-cell receptors will also be presented in MHC class I context to T_C cells that would suppress their upregulation during the absence of Ab1. In the presence of Ab1 however, Ab1 idiotopes will be processed by the anti-Id B-cell and presented in MHC class II context to T_H cells that would stimulate B-cell upregulation and hence also the production of Ab2 antibodies that would keep Ab1 under control. (Figure 1.5B).

The suppressing T_S cells recognising the expressed Ab2 paratope to the Ab1 paratope, would be the internal image of Ab1. B-cells therefore, can establish the link between antibodies and T-cells that share idiotopes as described above.

1.7 Immunomodulation

Analysis of the kinetics of the patterned fluctuation of autoantibody concentrations (Varela *et al.*, 1991) indicates that autoreactivity is strictly regulated by the idiotype network under physiological conditions (Lacroix-Desmazes *et al.*, 1996). A disturbance in this homeostatic control may lead to auto-immune disease (Dietrich *et al.*, 1993), but the administration of antibodies may lead to the recovery of the normal fluctuation patterns (Marchalonis *et al.*, 1992).

Auto-immune diseases are currently treated by suppressing the development of auto-immune clones. This is most often done non-specifically by administration of immuno-suppressive drugs like cyclosporin A (Bambauer *et al.*, 2000), steroids and cyclophosphamide (McIntyre *et al.*, 2001), or monoclonal antibodies to leukocyte surface antigens (Adorini *et al.*, 1990). Intravenous immunoglobulin (IVIg) administration has been shown to be effective in the treatment of many auto-immune disorders (Perez, *et al.*, 2002b; Wolfe *et al.*, 2002). Intravenous Ig is obtained from large pools of human plasma donors (15 000+) and represents a broad range of antibodies specific to foreign antigens and auto-antibodies. Also non-specific in action, mechanisms vary from F_c receptor ligandation or blockage (Fehr *et al.*, 1982), inhibition of antibody synthesis via T/B-cell receptor mediated inhibition (Delfraissy *et al.*, 1985) and idiotype network interference via idiotype recognition (Rossi *et al.*, 1989).

Due to the pool size, IVIg treatment is able to provide the patient with a large number of anti-Id antibodies. The anti-Id antibodies complex with the complementary idiotype antibodies and hopefully an anti-idiotype exist in the total IVIg pool that recognises the idiotype responsible for the auto-immune disorder (Hall, 1993). With an increase in pool size, the probability for a complementary anti-Id antibody also increases. Apart from preventing idiotype antibodies specific for the autoantigen, the anti-Id antibodies may also bind to surface immunoglobulin on B-cells and lower further production of the auto-antibody (Sultan *et al.*, 1984). Besides the idiotype network, IVIg also interact with T-cells, natural killer cells and the complement cascade (Hall, 1993).

1.8 Molecular mimicry and lipid antigens

When cross-reactive antigens originate from foreign and host tissue sources, the term 'molecular mimicry' applies (Damian, 1964). Cross-reactivity and molecular mimicry are frequent events in antibody recognition of proteins or peptides. However, it has been shown that antibodies to peptides can cross-react with similar looking carbohydrates (Kieber-Emmons, 1998; Sparbier & Walden, 1999) and that glycopeptide specific T-cells bind both peptides and carbohydrates (Deck *et al.*, 1999). The term mimotope applies to this case because the carbohydrates mimic the conformational structure of the peptides.

Antibodies to other types of antigens like glycolipids (Ilyas *et al.*, 1985) and lipids (Alving & Swartz Jr, 1991) also exist. It has been shown that humans have naturally occurring antibodies to cholesterol (Alving & Wassef, 1999) and these can react not only with cholesterol but also with lipoproteins like low-density lipoproteins (LDL) and high-density lipoproteins (HDL) (Dijkstra *et al.*, 1996). Though most viruses entering the body have proteinaceous coats, bacteria have predominantly lipid and glycolipid cell walls and capsules. Therefore it is understandable that antibodies may exist not only against the surface proteins of these pathogens but also their exposed lipid and glycolipid surfaces. This makes the study of lipid antigens and their antibodies extremely important, especially since so many similar lipids are shared between humans and pathogens.

Molecular mimicry has been shown to exist between lipopolysaccharides (LPS) of certain bacteria and gangliosides in the myelin sheaths of nerve cells (Harvey *et al.*, 2001). Molecular mimicry in cases such as these is a classic cause for auto-immune diseases where antibodies directed against an infectious agent turn upon the host due to similarity of

the host's structures to those of the infectious agent. As shown in Figure 1.4, molecular mimicry of a host structure by a foreign antigen could induce auto-immunity via the idiotype network. But how would one go about studying the relationship between antigen implicated in auto-immunity, Id and anti-Id antibodies?

1.9 Problems of detection of idiotype-anti-idiotype relationships

Polyclonal anti-Id antibodies are usually produced by injecting an animal with an antibody isolated from another test animal or human (Page *et al.*, 1985; Jean-Francois *et al.*, 1993). The immune system of the animal injected with the antibody raises polyclonal antibodies against the injected foreign antibody from which anti-idiotypic antibodies can be isolated. Polyclonal antibodies are purified by standard techniques including ammonium sulphate precipitation, simple matrix chromatography, protein A or G chromatography and affinity chromatography (Diamandis & Christopoulos, 1996). Monoclonal anti-Id antibodies are produced by the classic fusion of an anti-Id B-lymphocyte from the spleen with an immortal myeloma cell line (Guillet *et al.*, 1984; Losman *et al.*, 1995; Diamandis & Christopoulos, 1996). Anti-idiotype antibodies can also be produced by cloning and expression of a recombinant chimeric anti-Id antibody (Hastings *et al.*, 1992) or by cloning and expression of phage display antibody libraries (Zhang *et al.*, 2002). For studies of the structure-function relationship of the paratope or idiotype of antibodies, antigen binding site engineering can be used (Diamandis & Christopoulos, 1996). The specific *V* genes expressing the variable domains of the antibody can be isolated, sequenced and modelled using structural modelling. The variable regions can also be expressed and used for binding and inhibition studies.

Characterisation of anti-Id antibodies is extremely important in order to determine and quantify the functions of the antibody, especially when regulatory processes that depend on dynamic equilibrium states need to be determined. In order to characterise these antibodies, a sensitive detection method is necessary. Many different immunoassay techniques are available (Diamandis & Christopoulos, 1996) and many of them are employed in the detection of anti-Id antibodies (Dar & Seth, 1993), but different enzyme immunoassays or enzyme-linked immunosorbent assay (ELISA) techniques are probably the most common (Thurmond *et al.*, 1998; Yu & Chu, 1999).

The basis of immunoassays is to combine a sensitive detection method with the specificity of antibodies. This necessitates labelling of antibodies in one form or another. Labelling techniques, whether they are isotopic, enzymatic, fluorescent, chemiluminescent or bioluminescent, all run the risk of interfering with the function or specificity of antibodies. Another limitation of characterising antibodies with standard immunoassay techniques is that the endpoint state after Id-anti-Id interaction is measured, rather than the real-time interaction. Enzyme-linked immunosorbent assays itself are easy and reliable but have a number of restrictions in the commonly used formats. Sandwich ELISA is affected by the epitope multivalency of the measured antibody or antigen for detection that limits its sensitivity. Layered ELISA depends on the reaction of the reporting antibody with the anti-Id and not the Id. Therefore layered ELISA is limited to anti-Id antibodies with an isotype different to that of the idiotype. This problem may be overcome by using a reporting antibody specific to an isotype different from the idiotype, but this cannot be applied when auto-anti-idiotypes need to be determined (Haimovich *et al.*, 1998). Biosensor technology may be able to circumvent most of these problems.

1.10 Biosensor technology in detection of idiotype-anti-idiotype relationships

Biosensors represent a new generation of advanced molecular sensing methodology applicable to a wide field of interactions (Nice & Catimel, 1999). In particular the resonant mirror, that combines the sensitivity of wave-guide sensors with the simplicity of surface plasmon resonance (Cush *et al.*, 1993), is well suited for the study of protein-protein interactions (Feldman *et al.*, 1998; Sheng *et al.*, 2000). It has already been applied successfully to study Id-anti-Id interactions (Haimovich *et al.*, 1998). Nevertheless, the technology still retains some problems. For example, when proteins are immobilised on a carboxymethyl dextran (CMD) surface via EDC/NHS chemistry, the three-dimensional mesh structure of CMD imposes sterical restrictions on the bound antibodies and cannot guarantee that all antigen-binding sites are available for interaction.

1.11 Lipid antigens and auto-immunity in biosensor technology

Lipids may be immobilised on sensor surfaces in their natural state, i.e. as a bilayer membrane structure. Biosensors have already been used for immobilising lipids on hydrophobic surfaces (Nakajima *et al.*, 2001), or immobilisation via liposome suspensions (Altin *et al.*, 2001). In 2000 a novel method was developed whereby lipids, specifically mycolic acids (MA) from *Mycobacterium tuberculosis*, can be immobilised on a biosensor

surface using liposome suspensions in order to characterise antibodies from patient sera (Siko, 2002). Conceivably this method can be applied to study lipid antigens in general, but specifically those that are involved in auto-immune disorders triggered by molecular mimicry. The implication that lipid antigens may influence the regulation of the immune system by destabilising Id-anti-Id equilibriums (Lundkvist *et al.*, 1993), suggests that many auto-immune diseases may be triggered in this way.

1.12 Auto-immunity in Guillain-Barré syndrome, tuberculosis and human immune deficiency virus/acquired immune deficiency syndrome

To study the role of lipid antigens in auto-immunity, a disease model is needed. The Guillain-Barré syndrome (GBS) provides a well-characterised model to study auto-immunity. The disease is triggered by bacterial LPS that closely mimic the structure of membrane gangliosides (glycolipids) of peripheral nerves (Ang, 2001). As a consequence, antibodies and macrophages recognize not only the invading bacteria but also the peripheral neuronal cells and launch a response against it. In other diseases, auto-immunity may provide similar mechanisms of induction and progression.

In tuberculosis (TB), the characteristic rheumatoid arthritis side-effect has been shown to be induced by mycobacterial heat shock protein (HSP), but it has been hypothesized that anti-collagen antibodies may also be triggered by MA located on the surface of infecting mycobacteria, to cause rheumatoid arthritis (Siko, 1999).

Evidence supporting the auto-immune mechanism of human immune deficiency virus's (HIV) progression to acquired immune deficiency syndrome (AIDS), is increasing almost daily (Süsal *et al.*, 1993; Süsal *et al.*, 1996). These publications also suggest that auto-immunity is a result of an upset in the balance of Id-anti-Id antibodies and speculate on the consequences this might have during vaccine trials. Advancing our knowledge in this respect might allow us to come a step closer to solutions for auto-immune diseases such as those mentioned here.

1.13 Aims

The eventual aim of this study is to investigate idiotype network related auto-immunity, specifically in cases where the antigen is a lipid. Specific aims include:

- Optimising a method for measuring lipid antigens on the biosensor, using mycolic acid (MA) antigens as an example
- Discriminating between specificities of antibodies to structurally closely related lipid antigens, specifically the subclasses of mycolic acids
- Determining the universality of the biosensor method developed for MA to other lipid antigens, specifically to those related to the Guillain-Barré syndrome (GBS)
- Demonstrating, in principle, how biosensor technology may be used to study idiotype anti-idiotype interactions in lipid-induced auto-immunity of GBS

CHAPTER 2

LIPID ANTIGEN IMMOBILISATION ON A BIOSENSOR SURFACE

2.1 Introduction

2.1.1 Biosensor technology

Antibody-antigen interactions are about molecular recognition. One way of characterising these interactions is to make use of biosensors. Biosensors are molecular sensors that detect and quantify molecular recognition by linking to a physical transduction technique to generate a measurable electronic signal that represents receptor-ligand interactions (qualitatively and/or quantitatively) in real-time (Cornell *et al.*, 1997; Thévenot *et al.*, 2001). Molecular recognition can be measured in complex biological samples as diverse as blood, urine, other bodily fluids and sewage effluent. Different types of biosensors exist, such as potentiometric (Reddy *et al.*, 2001), amperometric (Kulys & Vidziunaite, 2003), optic (Schneider *et al.*, 1997), conductimetric (Kim *et al.*, 2000), thermal (Ramanathan & Danielsson, 2001), acoustic (Barié & Rapp, 2001) and piezoelectric (Li *et al.*, 2002) biosensors. The resonant mirror biosensor (an optical biosensor) combines the simplicity and ease of use of surface plasmon resonance biosensors, with the improved sensitivity of wave-guide sensors (Cush *et al.*, 1993).

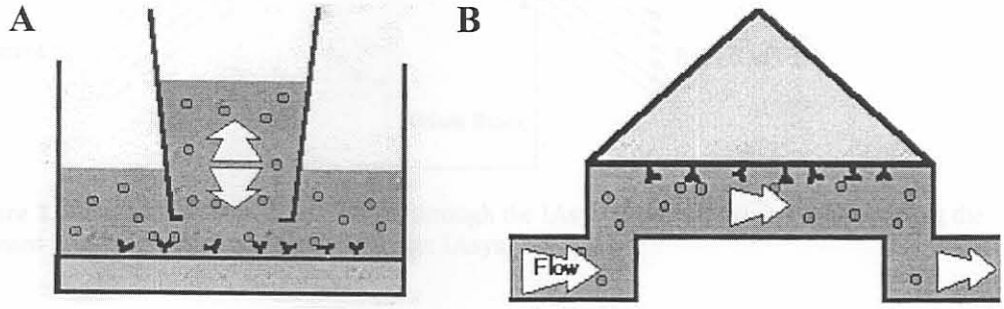

Figure 2.1: Two configurations of a molecular interaction chamber of a biosensor. **(A)** a micro cuvette or **(B)** a micro flow cell. (Source: http://www.cores.utah.edu/interaction/analyte.htm)

There are two different ways of introducing analyte in a sample to the ligand-coated sensor surface where the molecular recognition is to take place: a micro cuvette or a micro flow cell (Figure 2.1). Both types of systems have advantages and disadvantages, but the micro cuvette system is more appropriate for innovation and optimisation purposes due to easy access to the cuvette and the simplicity of the system (Nice & Catimel, 1999).

The IAsys Affinity Sensors system used in this study is a resonant mirror biosensor equipped with a binary cell (channel) micro cuvette system, allowing the comparison of two samples to one another. The cuvette is specially arranged to incorporate a prism through which laser light is projected from a moving source over a range of different angles. The laser light propagates through the prism and is reflected off the internal surfaces it encounters. At one specific angle, called the resonant angle, the light moves through the prism surface and into the layer next to the surface called the coupling layer (1000nm thick). Then it moves into the next layer called the resonant layer (100nm thick). The evanescent field is the region above the resonant layer where the electromagnetic field created by the laser light is affected by accumulation of ligates to the ligands (IAsys, 1995a, 1995b) (Figure 2.2). Accumulation or decrease of mass in the evanescent field alters the refractive index of the resonant structure, causing the resonant angle of the incident light to change. This change in angle is recorded in real-time by the IAsys software in arc seconds.

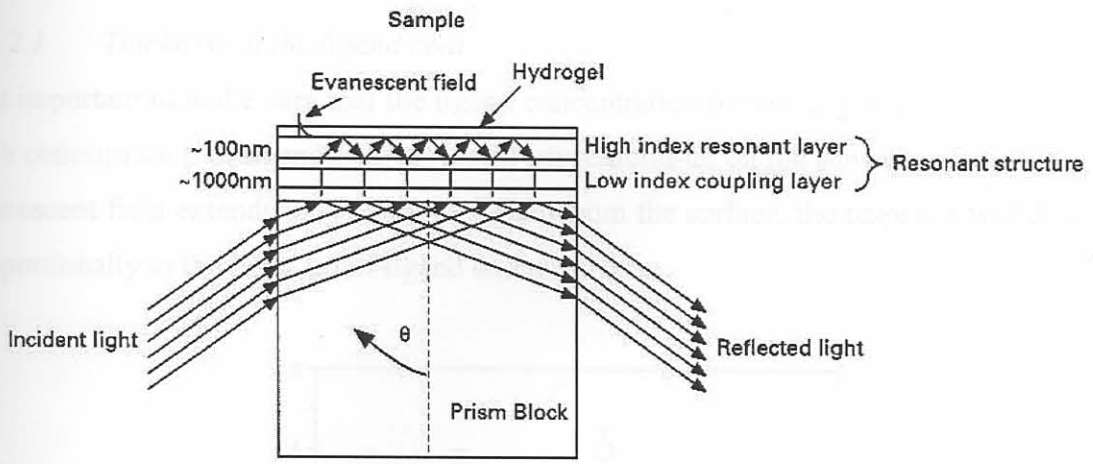

Figure 2.2: Optical pathway of laser light through the IAsys biosensor prism block showing the resonant layer and evanescent field. (Source: IAsys, 1995a)

The IAsys biosensor has twin internal aspirators that allow the removal of solutions from the cuvette cells without removing the cuvette from the biosensor. This expedites the pipetting of solutions. Integral stirrers ensure that the solutions are homogenous at all times and limit the effect of mass transfer through passive diffusion.

After chemical immobilisation of receptor molecules (ligands) to the sensor surface, the molecules specific for the receptors (ligates) can bind to the receptors. This interaction is called association and its strength is dependent on the affinity of the ligand for the ligate.

Displacement of the solution containing the ligate with buffer causes the ligate to dissociate from the ligands on the principle of diffusion from a higher to a lower concentration; this is called the dissociation phase. Because not all ligate molecules are removed during the dissociation phase the surface needs to be regenerated for another round of association/dissociation (IAsys 1995a, 1995b).

The system can be used for the determination of concentration, specificity of molecular recognition, kinetics of binding, co-operativity and quantitative parameters of association and dissociation interactions between ligand-ligate pairs (Nice & Catimel, 1999).

2.1.2 Practical considerations

During an interaction analysis, the factors that influence interactions must be considered. Because so much diversity exists in biomolecules, it is impossible to have a single protocol that will work for every sample.

2.1.2.1 Thickness of the ligand coat

It is important to make sure that the ligand concentration for coating is minimised. If a too high concentration of ligand is used, it will cause build-up on the sensor surface. Since the evanescent field extends only to about 100nm from the surface, the response will decrease proportionally to the build-up of ligand on the surface.

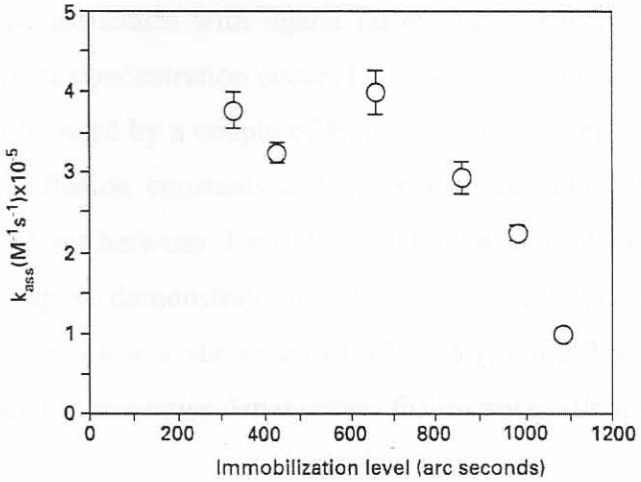

Figure 2.3: An example of the effect of ligand immobilisation level on the rate of association of a ligate on an IAsys biosensor CMD cuvette surface. (Source: IAsys, 1995b)

A plot of association constants versus mass of ligand immobilised demonstrates that this relationship is not linear, but that it plateaus already at low immobilisation levels and gradually loses responsivity (Figure 2.3). Therefore the ligand concentration should be optimised for immobilisation.

2.1.2.2 Type of cuvette surface

A variety of cuvette surfaces are available for different applications. In protein-protein interactions, a CMD surface is used most often as it provides an easy way to immobilise proteins onto the surface using EDC/NHS chemistry. However, sometimes the three-dimensional dextran surface might obstruct ligate molecules from associating with immobilised ligand molecules, thereby changing the kinetics of the sample. In cases where this is suspected, other types of surfaces can be used. Typically, carboxyl and aminosilane surfaces are used to orientate molecules in a specific way. An increasingly popular surface is the biotinylated surface that captures streptavidin-labelled molecules.

2.1.2.3 Mass transfer

Whenever a solution is flowing or moving over an adsorptive stationary layer, part of the mobile solution will also be stationary. In the biosensor, ligate must move through this 'unstirred' layer to associate with the ligand. The effect created by this movement is called mass transport. Under ideal conditions, ligate in the unstirred layer is replaced as soon as it is bound to the ligand, and also removed during dissociation before re-association can occur. But when ligate associates with ligand faster than it can be replaced, a transient lowering of surface ligate concentration occurs that also slows the association. These mass transfer effects are influenced by a couple of factors like kinetic rate constants, ligand and ligate concentration, diffusion constants and the stir speed. The integral stirrers of the IAsys biosensor can be set between 0 and 100%. Drawing a plot of the apparent on-rate (k_{on}) values versus stir speed demonstrates that the interactions between ligand and ligate is limited by mass transfer below a stir speed of 40-60% (Figure 2.4). Therefore, unless a slow stir speed is crucial to minimise denaturation for instance, stir speeds of 70%+ should be used.

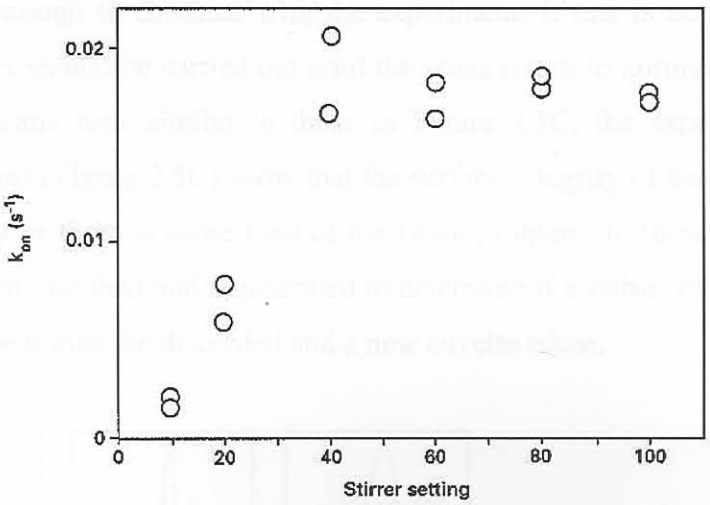

Figure 2.4: An example of the effect of stir speed on the apparent on-rate, k_{on}, of a ligate's association to a CMD surface immobilised ligand. (Source: IAsys, 1995b)

2.1.2.4 Regeneration

Using the same surface of immobilised ligand, it is possible to carry out a number of interaction analyses with different concentrations of ligate. Because dissociation is very seldom complete, the surface needs to be stripped of all the bound ligate and other non-specific impurities by a process of regeneration. Regeneration is done by adding a solution that lowers or increases the pH and thereby breaking the non-covalent interactions between the ligand and the ligate. Typical regeneration solutions are hydrochloric acid, formic acid, sodium carbonate or ethanol. Some regeneration buffers denature proteins under certain conditions, so care should be taken to optimise the regeneration solution type as well as concentration and pH.

2.1.2.5 Resonance scan diagnostics

A resonance scan is a measure of the integrity of the evanescent field and is a useful tool to determine the reliability of experimental data. It is important to note that the resonance scan profile will change during an experiment, especially during ligand immobilisation and regeneration when the structural composition at the surface changes most dramatically. It is important to take resonance scans during baseline events but also before and after immobilisation and between bindings. Normal scans are shown in Figure 2.5A. Scans that are sometimes obtained during an experiment that are also considered to be reasonable are shown in Figure 2.5B. Only when these scans return to smooth, defined peaks as in Figure 2.5A, during a phase where a stable surface is expected, can it be concluded that the

surface is stable enough to continue with the experiment. If this is not the case, washes with running buffer should be carried out until the scans return to normal. If this cannot be achieved or the scans look similar to those in Figure 2.5C, the experiment should be aborted. These scans (Figure 2.5C) show that the surface integrity of the cuvette is failing, the cuvette is dirty or there is some kind of hardware problem. In these cases the cuvette should be thoroughly washed and regenerated to determine if a stable, clean surface can be regained, otherwise it must be discarded and a new cuvette taken.

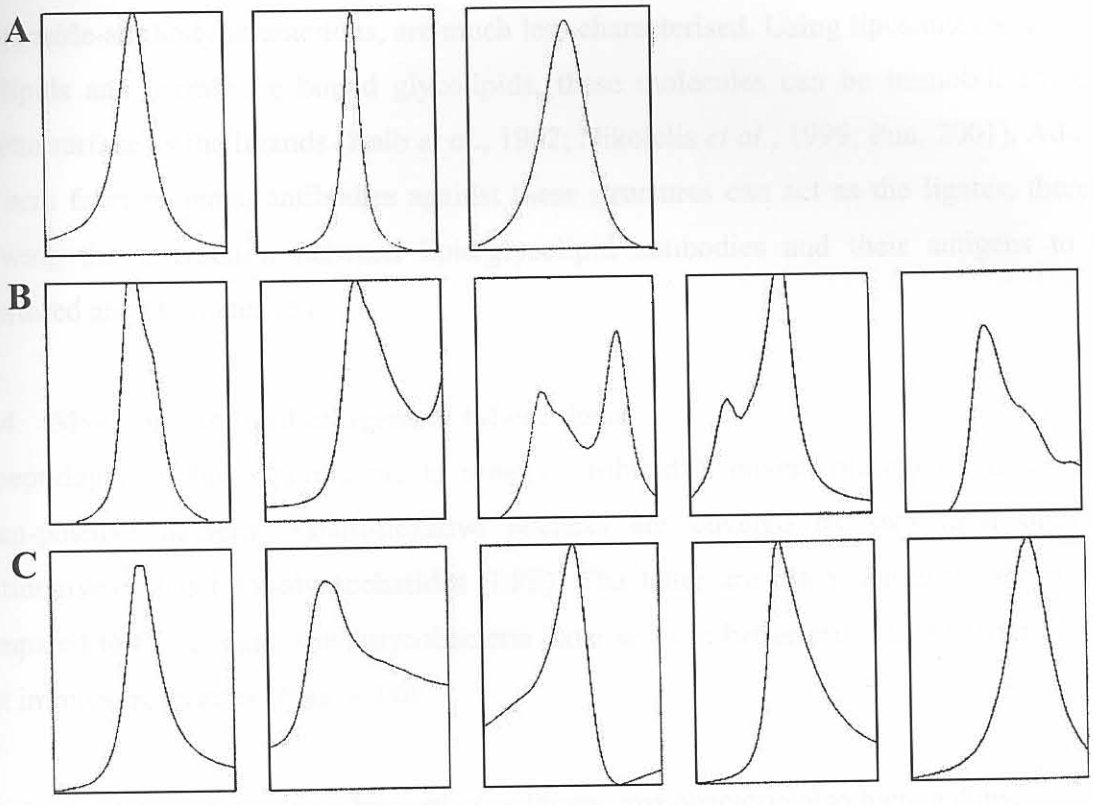

Figure 2.5: Examples of possible resonance scans of the IAsys biosensor cuvette surface obtained during an experiment that includes immobilisation, interaction analysis and regeneration. **(A)** Acceptable resonance scans obtained when the surface integrity is uniform and stable. **(B)** Resonance scans that may be seen when the surface is unstable. If these scans return to acceptable profiles during an expected stable event, the surface is still useful. **(C)** Abnormal resonance scans indicating dirty cuvettes or hardware problems. (Source: IAsys, 1995b)

2.1.2.6 Running buffer composition

All solutions have their own unique refractive indices that influence the angle of incidence light needed to obtain total internal reflection in the biosensor set-up. An important consequence is that the recorded response also change (abruptly) when solutions are exchanged in a biosensor cuvette. Accordingly, it is very important that the composition of running buffers used for test sample dilutions and wash steps during interaction analyses, be the same.

2.1.3 Biosensor applications in lipid-induced auto-immunity

The biosensor field is expanding rapidly. Protein-protein interactions were the first to be studied using a biosensor and are also the best characterised (Rubio *et al.*, 1997; Hirmo *et al.*, 1999; Altin *et al.*, 2001). Other interactions that have been tested before include DNA-protein, DNA-DNA hybridisation, carbohydrate-protein and even particulate interactions like cell-protein interactions (IAsys, 1995b; BIAcore, 2001).

Lipid-protein interactions such as MA-antibody, and glycolipid-protein interactions such as ganglioside-antibody interactions, are much less characterised. Using liposomes as carriers for lipids and membrane bound glycolipids, these molecules can be immobilised on a cuvette surface as the ligands (Kalb *et al.*, 1992; Nikolelis *et al.*, 1999; Puu, 2001). Adding test sera from patients, antibodies against these structures can act as the ligates, thereby allowing the interaction between lipid/glycolipid antibodies and their antigens to be monitored and characterised.

2.1.4 Mycolic acid lipid antigens in tuberculosis

A peptidoglycan layer permeable to most microbicidals covers plasma membranes of Gram-positive bacteria. Gram-negative bacteria are covered by two lipid bilayers, peptidoglycan and lipopolysaccharides (LPS). The latter are major antigenic molecules. Compared to these organisms, mycobacteria have an even better protective barrier against host immune responses (Figure 2.6).

Besides peptidoglycan and arabinogalactan layers, mycobacteria also have a dense layer of acyl lipids, lipoarabinomannan (LAM) and mycolates (MA). The cell envelope of *Mycobacterium* species consists of an outer capsule, a cell wall and a plasma membrane (Daffé & Draper, 1998). The cell wall, composed of MA arranged along with the acyl lipids in a bilayer, serves as a permeability barrier separate of the plasma membrane and is extremely low in fluidity (Liu *et al.*, 1996). Mycolic acids are α-alkyl, β-hydroxyl fatty acids of high molecular weight (C_{60}-C_{90}) and constitute 40-60% (mass %) of the complex cell envelope (Minnikin, 1982).

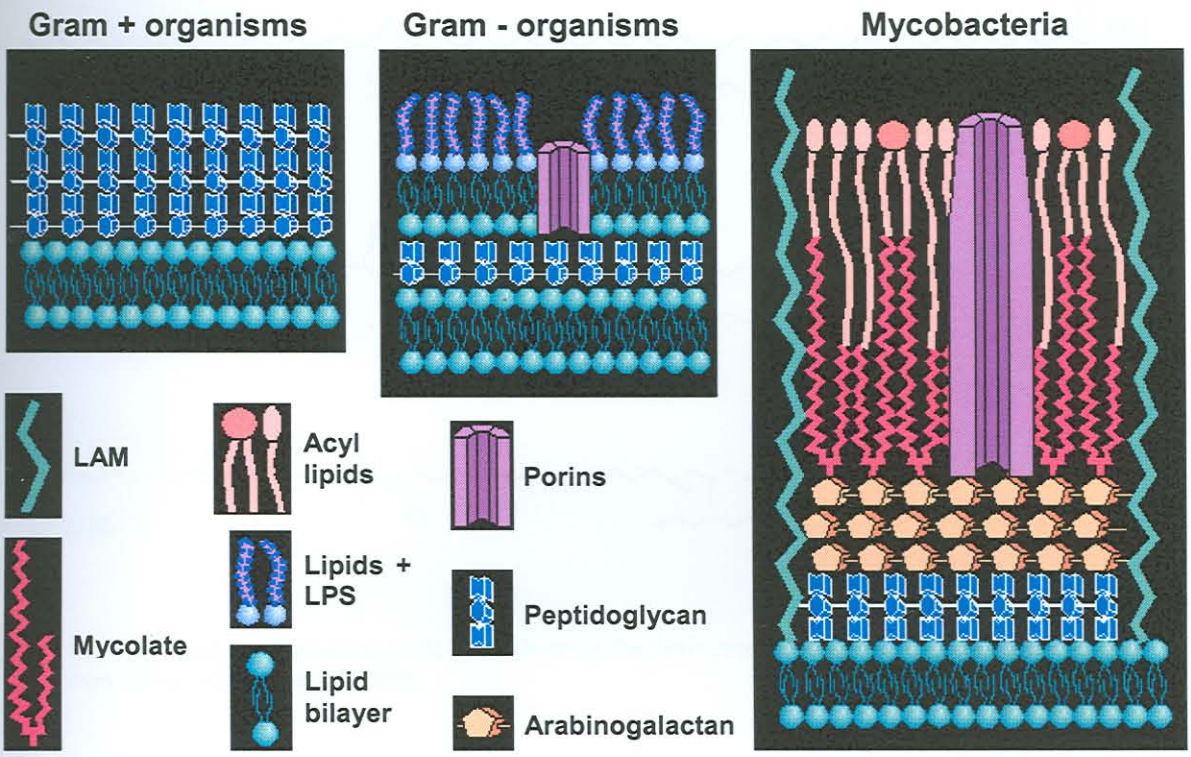

Figure 2.6: A comparison of bacterial cell barrier structures. Gram+ bacteria have only peptidoglycan besides a plasma membrane and Gram- bacteria have a double membrane with peptidoglycan and LPS. Mycobacteria have peptidoglycan and arabinogalactan layers that are covered by a bilayer consisting of MA and acyl lipids. LAM - lipoarabinomannan, LPS – lipopolysaccharides. (Source: Stannard, 1996)

Mycolic acids consist of mainly three subclasses: α-, keto- and methoxy-MA (Figure 2.7). In *Mycobacterium tuberculosis*, α-MA comprises almost half the total amount while the other two subclasses share the remainder almost equally (Barry *et al.*, 1998). It has been shown that only certain subclasses are responsible for MA's biological activity: one laboratory describes that antibodies against cord factor (trehalose 6,6'-dimycolate) recognises methoxy-MA stronger than the other subclasses (Pan *et al.*, 1999), while another shows that specifically the oxygenated MA (methoxy- and keto-) are responsible for *M. tuberculosis*' virulence in mice (Dubnau *et al.*, 2000).

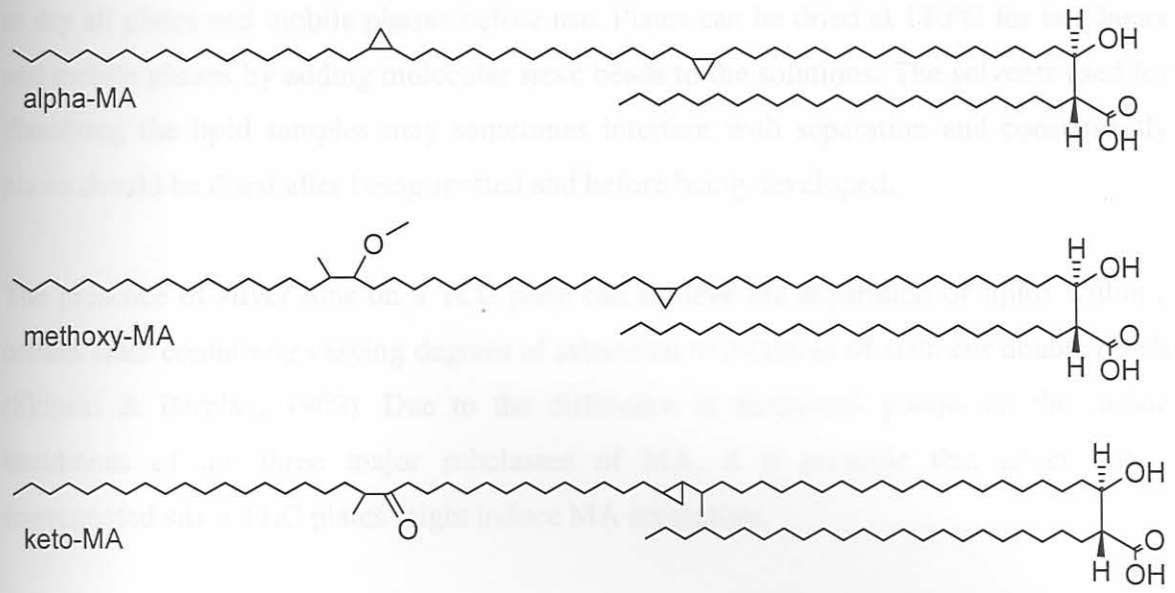

Figure 2.7: General structure of mycolic acids showing the distinction between the α-, keto- and methoxy-subclasses. (Source: Barry *et al.*, 1998)

As described in Chapter 1, an optical biosensor is well suited to characterise the interaction between antibodies and MA. Because the MA subclasses are not equally antigenic, it is preferable that the subclasses be characterised separately in the biosensor in terms of their antigenicity. Mycolic acid separation was achieved on preparative scale by Kaneda *et al.* (1986) using a silica column and on an analytical scale by Watanabe *et al.* (2001) using thin layer chromatography (TLC). Silica columns separate molecules on the same principle as silica TLC.

The separation of various lipids using TLC has been described in several articles (Dasgupta & Hogan, 2001; Kishimoto *et al.*, 2001; Wilson & Sargent, 2001) and reviewed in others (Skipski & Barclay, 1969; Olsson, 1992). The principle involves the application of small spots of lipid to a polar adsorbent immobilised onto a rigid support structure like aluminium or glass. The plates are placed upright in a tank containing a mobile phase usually consisting of organic solvents. Through capillary action, the mobile phase moves up through the adsorbent layer, dissolving the lipids in the spots along the way. The relative mobility of individual lipids is determined by the chemical groups, carbon chain length and isomerisation, thereby effecting a separation

A few aspects about lipid TLC are important to note: separation is affected by the presence of water both on the silica plate and in the organic mobile phase. Therefore it is important

to dry all plates and mobile phases before use. Plates can be dried at 110°C for two hours and mobile phases by adding molecular sieve beads to the solutions. The solvents used for dissolving the lipid samples may sometimes interfere with separation and consequently plates should be dried after being spotted and before being developed.

The presence of silver ions on a TLC plate can achieve the separation of lipids within a certain class containing varying degrees of saturation or mixtures of *cis*/*trans* double bonds (Skipski & Barclay, 1969). Due to the difference in functional groups on the carbon backbones of the three major subclasses of MA, it is possible that silver nitrate impregnated silica TLC plates might induce MA separation.

Lipids are not so easily detected, due to their lack of natural chromophores. Different detection methods are available: some specific for certain lipids or lipid classes, and some general for detecting most lipids. Mycolic acids are waxes and no specific detection method exists for visualising MA on developed TLC plates. One of the most sensitive general detection methods is sulphuric acid charring but others include spraying with water or immersion in sublimised iodine vapours. Another general detection method is to use silica plates containing a background fluorophore. After development, the plates are placed under UV light and the whole plate will fluoresce except where separated spots occur. Background fluorescence, water or iodine vapours are all less sensitive than sulphuric acid charring, but have the advantage of not altering the chemical composition of the lipids.

2.1.5 Ganglioside lipid antigens in the Guillain-Barré syndrome

Gangliosides are membrane glycolipids that are very abundant in the nervous system. They consist of two main parts: a ceramide tail that is inserted in the lipid membrane and a highly variable oligosaccharide part that protrudes externally. Sialic acid (N-acetyl neuraminic acid) has to be present for the glycolipid to be defined as a ganglioside but certain asialo-gangliosides have also been defined. Their nomenclature has been outlined by Svennerholm *et al.* (1994) and is based on the type of hexoses in the backbone, the number of sialic acids, TLC migration and isomer forms. Gangliosides are involved directly or indirectly in a range of functions including cell-growth, differentiation and recognition. They may play a role in signal transduction and can also act as receptors for bacterial toxins (Kurzchalia & Parton, 1999). The main glycolipids of importance in immune-mediated neuropathies are diagrammed in Figure 2.8.

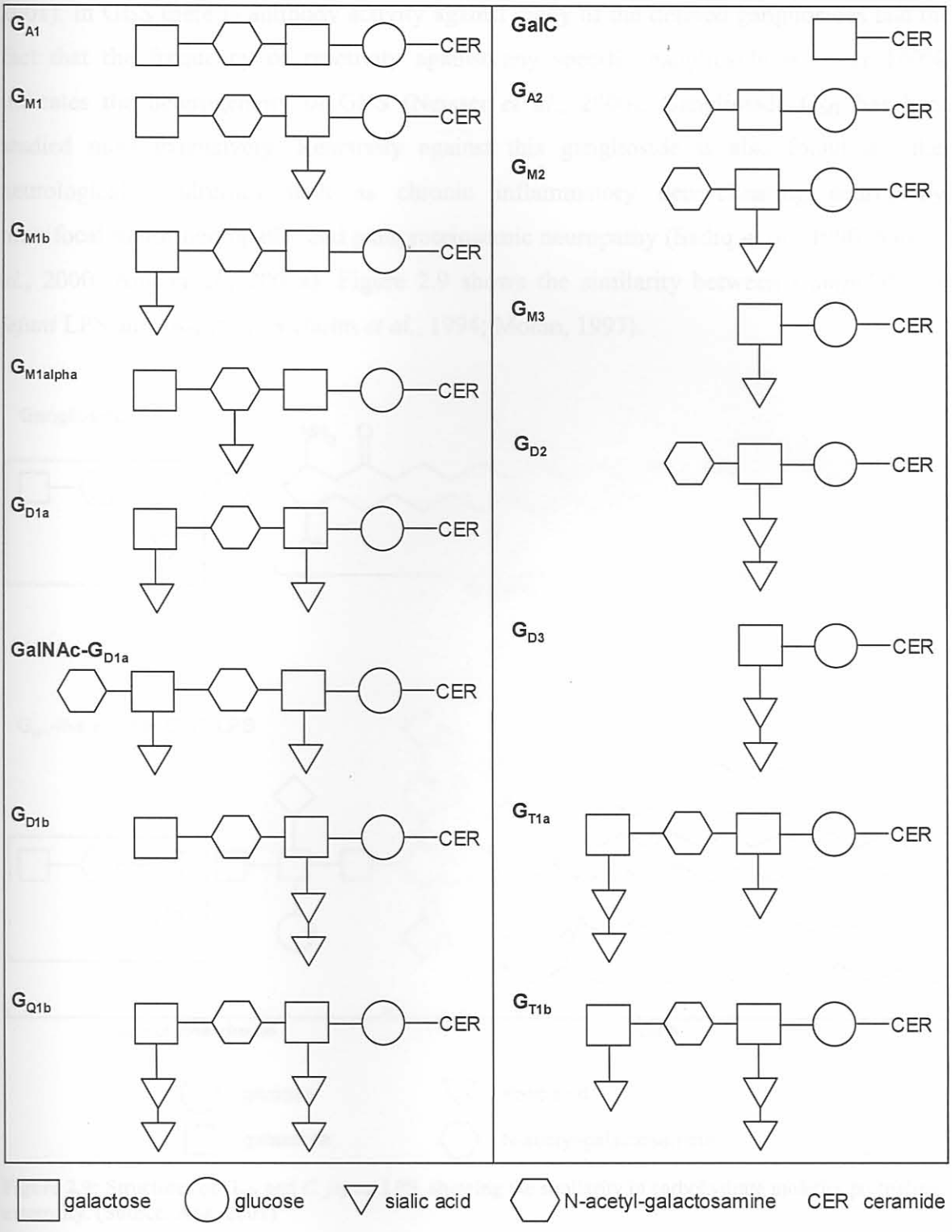

Figure 2.8: Structures of gangliosides and other glycolipids significant in GBS and other immune-mediated neuropathies. G: ganglioside, C: ceramide, Gal: galactose, GalNAc: N-acetyl-galactosamine. (Source: Ang, 2001)

Ganglioside composition differs not only between motor and sensory nerves but also between the axons and myelin of nerves. In axons, G_{M1} and G_{D1a} are the major glycolipids, and L_{M1}, G_{M3} and G_{D1b} predominates in myelin (Willison *et al.*, 1997; Aoyama *et al.*,

2001). In GBS there is antibody activity against many of the defined gangliosides and the fact that the frequency of reactivity against any specific ganglioside is never 100%, indicates the heterogeneity of GBS (Neisser *et al.*, 2000). Ganglioside G_{M1} has been studied most extensively. Reactivity against this ganglioside is also found in other neurological syndromes such as chronic inflammatory demyelinating neuropathy, multifocal motor neoropathy and paraproteinaemic neuropathy (Sadiq *et al.*, 1990, Yuki *et al.*, 2000; Ang *et al.*, 2001a). Figure 2.9 shows the similarity between *Campylobacter jejuni* LPS and G_{M1} (Svennerholm *et al.*, 1994; Moran, 1997).

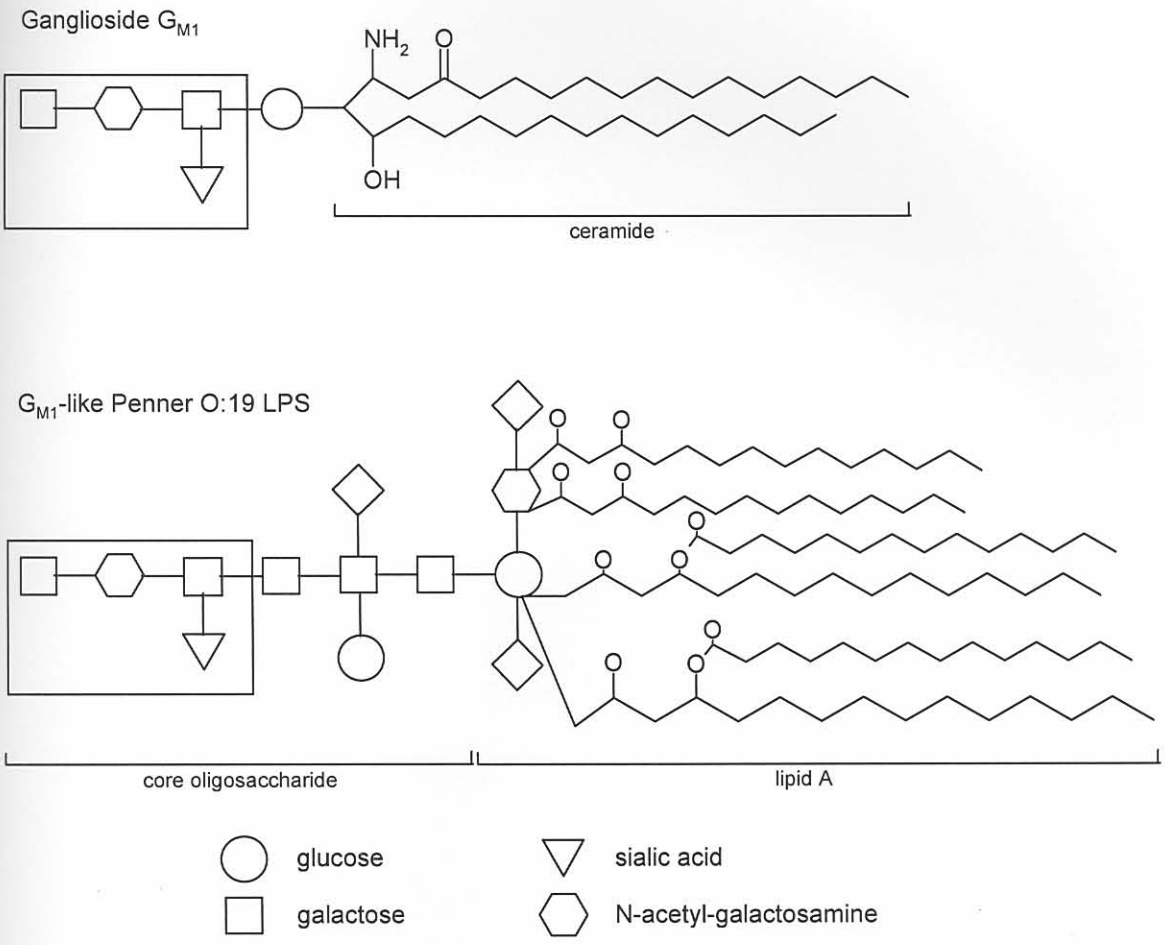

Figure 2.9: Structures of G_{M1} and *C. jejuni* LPS, showing the similarity in carbohydrate moieties protruding externally. (Source: Ang, 2001)

It has already been suggested that the onset of GBS is caused by a disturbance in the idiotype network of antibodies (Lundkvist *et al.*, 1993), triggered by the molecular mimicry between *C. jejuni* LPS and gangliosides (Ang, 2001). The biosensor method described here may be useful in supporting this hypothesis and also to quantify opposing antibody levels. Cholera toxin (CTx), a specific ligand for G_{M1} (Cuatrecasas, 1973), could

be useful as a reference for specific G_{M1} binding when determining kinetic parameters of the anti-G_{M1}, or cross-reactive GBS patient sera.

2.2 Aims

- Developing a thin layer chromatographic (TLC) system to separate mycolic acids into their subclasses
- Separation of mycolic acids (MA) on the developed TLC system
- Optimisation of a method for the immobilisation of mycolic acid-liposomes on a non-derivatised cuvette surface
- Optimisation of a method for the immobilisation of ganglioside-liposomes on a non-derivatised cuvette surface

2.3 Materials and Methods

2.3.1 Materials

Cholesterol, monosialoganglioside G_{M1} from bovine brain, L-α-phosphatidylcholine (PC) from lecithin and commercial MA from *Mycobacterium tuberculosis* were from Sigma. Sodium chloride (NaCl), anhydrous disodium hydrogen phosphate, potassium dihydrogen phosphate, iodine, general-purpose acetone and 3Å molecular sieve were supplied by Merck and analytical grade petroleum ether by Merck NT laboratories. The TLC plates (20 × 20cm with 20 × 2.5cm concentrating zone, glass support), and preparative thin layer chromato-graphy (PLC) plates (20 × 20cm with 20 × 4cm concentrating zone, glass support or 20 × 20cm without concentrating zone, glass support) were also from Merck. Analytical quality tris (hydroxymethyl) amino methane (Tris), ethylene diamine tetra-acetic acid (EDTA), chemically pure chloroform, *n*-hexane, diethyl ether, methanol, ethyl acetate and analytical grade sulphuric acid, hydrochloric acid (HCl), acetic acid, potassium bicarbonate ($KHCO_3$) and potassium hydroxide (KOH) were all from Saarchem and general purpose sodium azide (NaN_3) and sodium hydroxide (NaOH), as well as analytical grade benzene, ethanol and dichloromethane from BDH. Cetyl pyridinium chloride (CPC), saponin, guanidine thiocyanate (GSCN) and silver nitrate ($AgNO_3$) were from Sigma. For high-pressure liquid chromatography (HPLC) analyses, HPLC grade methanol and dichloromethane (BDH) were used. The C-100 internal standard was obtained from Ribi Immunochem Research Company (Hamilton, Montana, U.S.A.) and *p*-bromophenacyl-bromide (0.005mmol/ml crown ether in acetonitrile) from Pierce (Rockford, Illinois, U.S.A.). (Trimethylsilyl)-diazomethane (TMDM) was from Fluka. Double-distilled deionised water was used for all analytical experiments. Saarchem, BDH and Merck products (Darmstadt, Germany) were supplied by Merck NT Laboratories, Midrand, South Africa. Sigma and Fluka products were supplied by Sigma-Aldrich Corp., St. Louis, Missouri, U.S.A.

2.3.2 Calculations

Due to the heterogeneity of the crude self-prepared MA extract, relative MA concentrations are indicated as mass ratios. To determine molar ratios for use in G_{M1}-liposomes, it was assumed that PC contained two palmitoyl fatty acid chains and G_{M1} contained a 1:1 ratio of nervonoyl and stearoyl ceramides.

2.3.3 Analytical thin layer chromatography

Silica gel plates, with either glass or aluminium as support, were dried for two hours at 110°C and allowed to cool in a dessicator before use. Samples to be analysed were dissolved in chloroform and spotted onto the plates with a micropipette in volumes not exceeding 5µl at a time. Between 50 and 500µg of a test sample was spotted. To evaporate residual chloroform from the test samples, the plates were dried again briefly at 80°C. Mobile phases consisting of various ratios (v/v) of *n*-hexane and diethyl ether were prepared and dried overnight at 4°C with 3Å molecular sieves. Mobile phases containing ethyl acetate, petroleum ether, methanol, dichloromethane and/or acetic acid were treated similarly.

The developing tank was equilibrated with the mobile phase for at least 30 minutes prior to each experiment using paper towelling attached to the side of the tank so that the bottom just touched the mobile phase. During the experiment the mobile phase was kept dry with 3Å molecular sieve. The prepared TLC plates were lowered into the tank, the top of the tank sealed, and development allowed to take place until the eluent front reached 1-3cm from the top of the TLC plate. The plate was then removed, dried briefly at 80°C and the spots visualised.

Iodine vapours were used at first for visualisation. Iodine crystals were placed in a sealed tank at 80°C until the vapour/solid states reached equilibrium. The developed plates were placed in the tank until the spots were visible, removed and scanned using a Hewlett Packard 3200C flatbed scanner (Palo Alto, California, U.S.A.) and accompanying software. Iodine visualisation was later discontinued and replaced by sulphuric acid charring. A 65% (v/v) aqueous sulphuric acid solution was sprayed evenly onto the developed plate using an aerosol propellant (Sigma-Aldrich Corp., St. Louis, Missouri, U.S.A.). The plates were then placed at 110°C until visible spots appeared. Scanning of the plates was done as before.

2.3.4 Two-dimensional thin layer chromatography

For two-dimensional TLC, the plates were developed in the first mobile phase, dried for ten minutes at 80°C, turned through 90°, and developed in the second mobile phase. Visualisation was done with sulphuric acid charring.

2.3.5 Preparative thin layer chromatography

Preparative TLCs were either developed on plates with a 2mm or 5mm thick silica coat. The thinner plates had a concentrating zone of 2.5cm. Samples were striped at the bottom of the plates to a maximum of 10mg, dried and developed as for the analytical plates. After development, approximately 2cm of each side of the plate was removed so that a small amount of the developed sample was on each strip. The strips were visualised by sulphuric acid charring, compared to the rest of the plate and the bands identified accordingly. The silica containing the identified bands were scraped off the plate, powdered in a conical flask and extracted with chloroform using a vacuum filtration system and Whatman number 1 filter papers. The silica was washed thoroughly (five times) with chloroform to ensure a high yield. Samples were dried at 85°C under a steady stream of nitrogen gas, dissolved in small volumes of chloroform, transferred to amber vials and dried again under nitrogen gas for use in HPLC or HPLC-MS analysis.

Yuan *et al.* (1997) described the preparative separation of MA. This was attempted analytically by using dried analytical TLC plates as described (*see* par 3.4.2). After spotting the different MA samples, the plate was developed five times consecutively with 19:1 *n*-hexane:ethyl acetate (v/v), with drying at 80°C for five minutes in-between every development. Visualisation was done by sulphuric acid charring.

2.3.6 Complex argentation thin layer chromatography

A complex two-dimensional argentation TLC done by George *et al.* (1995) was attempted. An analytical TLC plate was submerged in a 10% (w/v) aqueous $AgNO_3$ solution so that 16cm of the plate was impregnated with $AgNO_3$ and a strip free of $AgNO_3$ would be left at one side. The plate was dried for an hour at room temperature and thereafter activated at 50°C, 80°C and 110°C for 20, 20 and 40 minutes respectively. The plate was allowed to cool in a dessicator, re-activated for 30 minutes at 110°C and used immediately. After MA was spotted on a corner outside the $AgNO_3$, the plate was developed twice into the strip without $AgNO_3$ with 19:1 (v/v) *n*-hexane:ethyl acetate. Thereafter, the plate was turned through 90° and developed three times into the $AgNO_3$ impregnated part with 17:3 (v/v) petroleum ether:diethyl ether. Between developments, the plate was dried for five minutes at 80°C. Both mobile phases were dried with 3Å molecular sieve overnight. Visualisation was done by sulphuric acid charring.

2.3.7 Preparation of *Mycobacterium tuberculosis* mycolic acids

Mycobacterium tuberculosis H37Rv, a virulent strain originally isolated from an infected human lung, was used for isolation of MA. The lyophilised culture was purchased from the American Type Culture Collection (ATCC 27294), Maryland, U.S.A. The bacteria were cultured, harvested, saponified and crudely extracted as described elsewhere (Goodrum *et al.*, 2001). The crude extract of MA was subjected to a preliminary purification step and then purified further on a countercurrent apparatus using a triphase solvent system comprising 42:39:19 chloroform:methanol:water (v/v) as described elsewhere (Goodrum *et al.*, 2001).

2.3.8 Preparation of *Mycobacterium avium* mycolic acids

Mycolic acids from *M. avium* were isolated similarly to that of *M. tuberculosis* but the method arrested after the addition of Reagent C (*see* par 2.3.8.1) during the crude extract preparation. Countercurrent purification was not performed on *M. avium* MA. The method used by Kaneda *et al.* (1986) was then applied as follows:

Crystalline, crude *M. avium* MA (after Reagent C) was dissolved in the two phases of a 42:39:19 (v/v) chloroform:methanol:water mixture. Two hundred millilitres of the bottom phase was added to the MA, the mixture shaken well, and 200ml upper phase added. After agitation, the bottom chloroformic phase was removed and extracted again with 200ml aqueous upper phase. The chloroformic phase was evaporated in a Buchi Roto-evaporator RE 120. Twenty millilitres of a 10:20:1 (v/v) benzene:methanol:sulphuric acid mixture was added to the MA and shaken vigorously. To this, 10ml *n*-hexane was added. The *n*-hexane partitioned mainly to the top benzenic layer. The bottom layer was removed, re-extracted with 10ml *n*-hexane, and the two *n*-hexane fractions combined. The hexanic fraction was extracted with 20ml water and evaporated on a Buchi evaporator. The concentrated MA in the flask after evaporation was dissolved in chloroform, evaporated again, washed with methanol, evaporated again and dissolved a second time in chloroform and evaporated as above to remove traces of benzene. The dry MA was finally dissolved in a small volume of chloroform, transferred to an amber vial and evaporated at 85°C under a steady stream of nitrogen gas.

2.3.9 High pressure liquid chromatography

2.3.9.1 Reagents

A: 25% (w/v) KOH in 1:1 (v/v) water:methanol

B: 1:1 (v/v) HCl:water

C: 2% (w/v) $KHCO_3$ in 1:1 water:methanol

D *p*-bromophenacylbromide in Crown ether

E: 1:1 (v/v) Reagent B:methanol

High molecular weight (C-100) internal standard

2.3.9.2 Derivatisation of mycolic acids

When the sample (eluted from TLC) was still in chloroform, it was added to a vial containing an aliquoted amount of internal standard (5µg). To derivatise the MA, 1.9ml Reagent A was added to each sample and heated to 85°C for 15 minutes in a heat block. Samples were allowed to cool to room temperature before adding 1.5ml Reagent B. Five hundred microlitres chloroform was added to each sample, vortexed for 30 seconds and the chloroformic (lower) phase removed with a glass Pasteur pipette and transferred to a clean vial. The chloroform extraction step was repeated once more and then the combined chloroformic extracts were evaporated under a steady stream of nitrogen gas to dryness at 85°C in a heat block. One hundred microlitres Reagent C was added and again evaporated to dryness as before. The samples were allowed to cool to room temperature and 1ml chloroform was added. One hundred microlitres Reagent D was added, vortexed for 30 seconds and incubated at 85°C in a heat block for 20 minutes. Samples were allowed to cool to room temperature, 1ml Reagent E added, vortexed for 30 seconds and the phases allowed to separate. The chloroform (lower) phase was transferred to a clean vial as before and dried under a steady stream of nitrogen gas at 85°C in a heat block.

2.3.9.3 Reverse phase HPLC

Samples were dissolved in 220µl dichloromethane, vortexed at 100% for 30 seconds and filtered through 0.22µm Teflon filters into pre-prepared inserts placed in 1.8ml vials. The vials were loaded in an AS-2000 autosampler (Hitachi Ltd., Tokyo, Japan)and 15µl volume of each sample was injected. The HPLC system was fitted with a Waters prefilter and a Luna 5µm C18 column (4.6mm x 250mm) obtained from Phenomenex (Torrance, California, U.S.A.) packed with 5µm spherical particles with a pore size of 10nm. An L-

6200A pump (Hitachi Ltd., Tokyo, Japan) was used to generate a flow rate of 1ml/min and the column was equilibrated with 98:2 (v/v) methanol:dichloromethane before use. The solvents were HPLC grade methanol and dichloromethane, run at the following methanol gradient (time indicated in minutes):

t = 0	100%
t = 2	98%
t = 15	55%
t = 25	35%
t = 30	35%
t = 35	98%
t = 50	98%

Detection was done at 260nm with an L-4500 UV detector (Hitachi Ltd., Tokyo, Japan). Peaks were quantified by area and those smaller than 30 000 units rejected. Mycolic acid yield was calculated as a ratio of the mycolic acid peak area and the internal standard peak area:

$$MA\ (\mu g) = \frac{MA\ peak\ area \times 5\mu g}{Internal\ std\ peak\ area} \qquad (2.1)$$

2.3.10 Methylation of mycolic acids

(Trimethylsilyl)diazomethane (TMDM) was purchased as a 2M solution in *n*-hexane. The solution was aliquoted in 1ml volumes and one aliquot was dried under a stream of nitrogen at 85°C and redissolved in 1ml diethyl ether. Twenty microlitres of the MA samples (10mg/ml for commercial and self-prepared *M. tuberculosis* MA and undetermined concentration for *M. avium* MA) were incubated with 5µl of either diethyl ether- or *n*-hexane-dissolved 2M TMDM at room temperature for one hour.

2.3.11 Thin layer chromatography of methylated mycolic acids

The total volume of the TMDM incubated samples was loaded onto a silica plate that had been dried for two hours at 110°C. After loading, the plate was dried briefly at 80°C and then developed five times consecutively in a mobile phase containing 9:1 (v/v) petroleum

ether:diethyl ether. Between developments, the plate was dried at 80°C for ten minutes. Visualisation was done by sulphuric acid charring.

For the determination of the number of developments necessary to resolve the MA subgroups, a new sample was spotted next to the previous spot onto the plate after each development so that five spots subjected to different numbers of development could be observed.

For the preparative TLC of the methylated MA, a total of 10mg (ten times 10µl of a 100mg/ml chloroform solution) self-prepared *M. tuberculosis* MA that had been methylated (*see* par 2.3.10) was striped on a preparative TLC plate. The plate was developed as described, the sides removed and visualised by sulphuric acid charring before compared with the remainder of the plate to identify the spots to be eluted.

2.3.12 Electron-impact mass spectrometry

Samples dissolved in chloroform were subjected to gas chromatography mass spectrometry (GC-MS) using a Varian 3400 gas chromatograph equipped with a Finnigan TSQ-700 triple quadrupole mass spectrometer (San Jose, California, USA), a Waters 600-MS system controller, Waters 490-MS programmable multi-wavelength detector (Milford, Massachusetts, USA) and a split/splitless injection port. The ZB624 column used was 30m long and had an internal diameter of 0.25mm with a 1.4µm thick film coating. The carrier gas was helium at a backpressure of 14psi. The injection port and transfer line temperatures were both set at 250°C while the split vent flow was set at 60-70ml per minute and the septum purge at 3-5ml per minute. Samples were dissolved in a 1:4 isopropyl alcohol:acetonitrile solution saturated with ammonium acetate as proton source and 1µl volumes were injected. The oven temperature was started at 40°C, ramped to 240°C with 10°C per minute increments and held for 15 minutes. The ionisation mode was electron impact (70eV) with the ion source temperature set at 200°C. The filament current was 200µA, the electron multiplier voltage 1kV and the lens voltage –10V.

2.3.13 Biosensors

Three different IAsys biosensors were used at the following localities:

1. Department of Immunology, Erasmus University Rotterdam, Rotterdam, Netherlands
2. R&D department, IAsys Affinity Sensors, Cambridge, U.K.
3. Department of Biochemistry, University of Pretoria, Pretoria, South Africa

Non-derivatised cuvettes were supplied by the biosensor manufacturer, IAsys Affinity Sensors, Cambridge, U.K.

2.3.14 Mycolic acid-liposome preparation

Mycolic acids were dissolved in chloroform and 100µg quantities aliquoted into amber vials and stored at 4°C. Phosphatidylcholine and cholesterol stock solutions were freshly prepared in chloroform at concentrations of 10mg/ml. Sixty microlitres PC and 30µl cholesterol were added to vials containing 0.1mg MA. The vials were dried in a heat block at 85°C under a steady stream of nitrogen gas. These vials were stored at 4°C until the day of use. Two millilitres phosphate buffered saline (PBS) with 0.025% (w/v) sodium azide and 1mM EDTA (PBS/AE), were added to a vial containing the dried lipids, the lipids melted at 85°C in a heat block for ten minutes, vortexed at 100% for one minute and then sonified in a Branson sonifier with a microtip set at a pulsed energy transfer at 20 duty cycles, output level 2, for 20 strokes or one minute. The melting step is crucial as MAs are waxes with higher melting points than PC and cholesterol and do not solvate easily. This was followed by another minute of vortexing at 100%. This resulted in a 0.5mg/ml liposome suspension containing PC, cholesterol and MA in a 6:3:1 mass ratio respectively.

2.3.15 Mycolic acid-liposome immobilisation on biosensor cuvettes

Cuvettes were washed with PBS/AE until a stable baseline could be maintained for at least five minutes. The cells were aspirated and 50µl of a 20µg/ml CPC in PBS/AE solution was added. After ten minutes the cells were washed five times with 60µl PBS/AE, then 25µl PBS/AE was added until a stable baseline was achieved. Twenty-five microlitres of the desired liposome solution was added and the response monitored for ten minutes. Cells were then washed five times with 60µl PBS/AE and immediately after that, treated five times with 60µl 1mg/ml saponin in PBS/AE. The cells were incubated with saponin for at

least ten minutes and until a stable baseline was achieved before a final five times wash with 60µl PBS/AE. Interaction analysis could be continued from this point.

Due to a response difference among saponin batches, it was necessary to titrate the amount of saponin required each time a new batch of saponin was used.

2.3.16 Mycolic acid-liposome cuvette regeneration

Unlike other surfaces where proteins and other molecules are immobilised covalently, regeneration of liposome coats on a non-derivatised surface partly removes the liposome coat. Subsequent liposome immobilisations or interaction analyses cannot be carried out on this partial coat. Accordingly, it is important that everything be stripped from the cell surface during a regeneration step and that a new liposome coat is prepared for a subsequent interaction analysis. Regeneration was initially performed with several steps including 95% ethanol to remove all fatty deposits and 3.5M GSCN to regain sharp resonance scan peaks. This was later changed to a three times wash step with 60µl 12.5M KOH, and later optimised to three times 50µl 95% ethanol for 30 seconds, followed by three times 80µl PBS/AE for one minute and five times 60µl PBS/AE. Following this was a five times wash step with 60µl 12.5M KOH for two minutes and again three times 80µl PBS/AE for one minute and five times 60µl PBS/AE. The buffer wash steps were included to ensure that both the ethanol and KOH are washed away thoroughly as both would severely affect liposome immobilisation. After the last PBS/AE step, the cuvette would be ready for another round of CPC activation, liposome immobilisation and interaction analysis.

2.3.17 Ganglioside-liposome preparation

Ganglioside G_{M1} was dissolved in chloroform and 100µg quantities aliquoted into amber vials and stored at 4°C. Phosphatidylcholine and cholesterol stock solutions were freshly made in chloroform at concentrations of 1mg/ml. Varying quantities of PC and cholesterol were added to the vials containing 100µg G_{M1} to make either mass or molar ratios of the different lipids as desired. For optimised G_{M1}-liposomes, 878µl PC was added to one vial containing 100µg G_{M1}. PBS/AE or a Tris based buffer (50mM Tris, 200mM NaCl, 3mM NaN_3, 1mM Na_2EDTA) was added to a liposome concentration of 0.5mg/ml, the solution

vortexed for one minute at 100%, sonified as above, and vortexed again for one minute at 100%. The G_{M1}-liposomes did not need to be melted since they did not contain MA.

2.3.18 Ganglioside-liposome immobilisation on biosensor cuvettes

After using the same method for MA-liposome immobilisation initially, the method was optimised as described elsewhere (*see* 2.5 Results). Fifty microlitres G_{M1}-liposomes were added directly to aspirated cells containing residual 20mM HCl (~15µl) after regeneration. After incubating the liposomes for ten minutes, the cells were washed four times with 60µl PBS/AE or Tris buffer, four times with 60µl 10mM NaOH and five times with 60µl PBS/AE or Tris buffer. Thereafter the cells were aspirated and 25µl of PBS/AE or Tris buffer was added and a stable baseline was obtained for at least five minutes before interaction analyses could proceed.

2.3.19 Ganglioside-liposome cuvette regeneration

The same regeneration protocol as for MA-liposomes was used initially but changed later to a modified method of Altin *et al.* (2001). After dissociation events, cells were washed four times with 60µl absolute ethanol, seven times with 100µl water, five times with 60µl 12.5M KOH and incubated at this step for two minutes. The cells were washed again seven times with 100µl water and then three times with 2M HCl and four times with 20mM HCl. After the 20mM HCl step, a stable baseline would be obtained for at least five minutes before the cells could be aspirated and liposomes added directly for the next round of immobilisation and interaction analysis.

2.4 Results

2.4.1 Separation of the mycolic acid subclasses with thin layer chromatography

2.4.1.1 Optimisation of detection method

Appropriate detection techniques for lipids or waxes include the use of iodine vapours, sulphuric acid charring and water vapour. Iodine vapour provides a general non-specific detection method and can be used to identify almost any lipid (Skipski & Barclay, 1969). Sulphuric acid oxidises all biological material to carbon dioxide and water as well as elemental carbon, which remains visible on TLC plates. Water vapour is adsorbed by the hygroscopic silica plates used, except where it is covered by a lipid spot or smear, thereby visualising the lipid. Although the water vapour technique is non-invasive and ideal for preparative purposes, it is limited in sensitivity. Iodine vapour is more sensitive and also non-invasive (iodine vapours sublimate after a while) but compared to sulphuric acid charring it is less sensitive (Figure 2.10). Throughout the TLC experiments, cholesterol was spotted as a control lipid because of its active mobility in diverse eluents. Also, to enable compensation for the effects of possible irregular eluent fronts, cholesterol samples were spotted on either side of the plates and/or in between test samples.

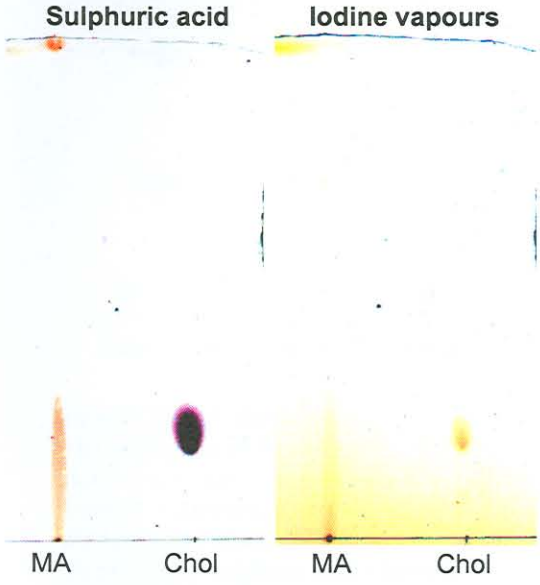

Figure 2.10: A comparison between the sensitivities of sulphuric acid charring and iodine vapours as visualisation techniques for MA and cholesterol on a silica TLC plate. The plates were developed with 50:50 diethyl ether:*n*-hexane as eluent. MA - *M. tuberculosis* mycolic acids, Chol - cholesterol

2.4.1.2 Thin layer chromatographic comparison of different mycolic acid sources

It has been reported that MA from *M. avium* separate into three distinct species (α-, keto- and methoxy-MA) on TLC (Kaneda *et al.*, 1986) using 20:80 diethyl ether:*n*-hexane. Using a crude extract of *M. avium* MA as a positive control as well as commercially available *M. tuberculosis* MA, a TLC was run with 20:80 diethyl ether:*n*-hexane (Figure 2.11). Pure commercial *M. tuberculosis* MA was used to compare it with the purity of the crude *M. avium* and self-prepared *M. tuberculosis* MA samples. Neither the commercial nor the self-prepared *M. tuberculosis* MA moved much from the origin. Most of the MA of *M. avium* remained behind at the origin but three faint spots with R_f values of 0.28, 0.51 and 0.67 were obtained. Because little mobility was observed with the *M. tuberculosis* MA, it was expected that these spots represent non-MA components present in the crude *M. avium* MA extract.

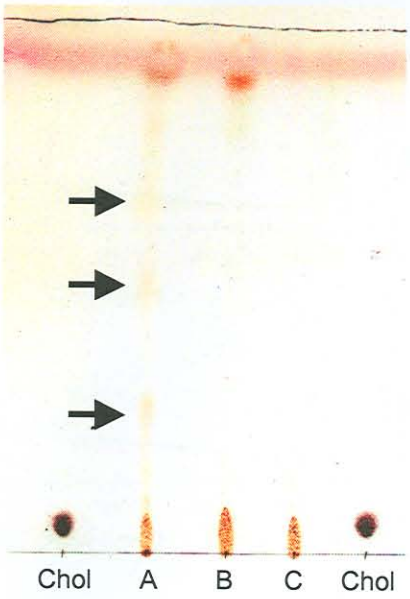

Figure 2.11: A thin layer chromatogram of *M. avium*, *M. tuberculosis* and commercial MA from *M. tuberculosis*, developed with 20:80 diethyl ether:*n*-hexane and visualised by sulphuric acid charring. Chol - cholesterol, A - *M. avium* MA, B - *M. tuberculosis* MA, C - commercial *M. tuberculosis* MA.

All the MA samples except the commercial MA showed a distinct spot at the very front of the mobile phase. It is not certain what this spot represents, but it may be a contaminant present in the solvents used for MA extraction. The next step was to analyse the different

fractions of *M. avium* as well as *M. tuberculosis* to confirm the localisation of the MA on the TLC chromatogram.

2.4.1.3 *High pressure liquid chromatography identification of mycolic acids in thin layer chromatography-separated samples*

Preparative TLCs were run separately on MA from both *M. avium* and *M. tuberculosis* using the same eluent as before, i.e. 20:80 diethyl ether:*n*-hexane. After the plates were developed, the sides were removed, visualised with sulphuric acid charring, compared with the remainder of the plate, and the strips of silica removed and eluted accordingly. The eluted samples were analysed by HPLC according to Goodrum *et al.* (2001). Figure 2.12 shows the TLC chromatogram as well as the HPLC analyses of pure MA from *M. tuberculosis* and the bands eluted from the TLC plate.

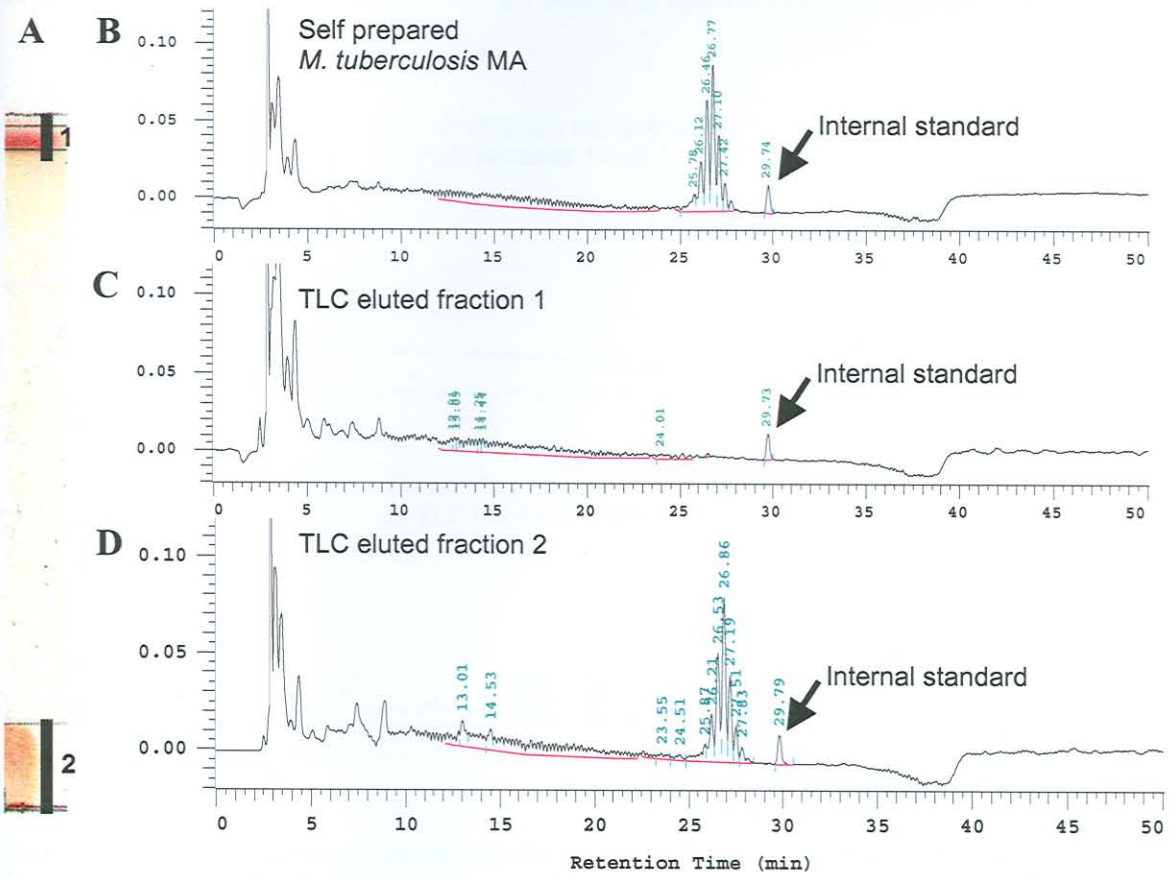

Figure 2.12: High-pressure liquid chromatography analysis of *M. tuberculosis* TLC bands. **(A)** The preparative TLC plate showing the bands isolated and extracted for analysis. **(B)** The HPLC chromatogram of an unseparated MA sample showing the typical retention time of the peak cluster of MA at a retention time of 26 minutes as well as the internal standard at a retention time of 30 minutes (indicated by arrows). **(C)** The HPLC chromatogram of the top eluted fraction of the TLC plate indicating the absence of MAs. **(D)** The HPLC chromatogram of the bottom eluted fraction of the TLC plate, confirming the presence of MA in the typical region of 25-8 minutes.

The cluster of nine peaks around a retention time of 26.8 minutes is characteristic of MA (Figure 2.12B). The nine peaks are due to the different chain lengths of MA species found. It is known that every peak representing a chain length contains all three subgroups (α-, keto- and methoxy-) in the same relative ratio. The second HPLC chromatogram shows that there are indeed no MA to be found in the band at the front of the TLC chromatogram (Figure 2.12C) and that all the *M. tuberculosis* MA remained at the origin (third HPLC chromatogram, Figure 2.12D).

Similarly, the HPLC analysis of the *M. avium* bands from the preparative TLC showed that the band at the elution front (Fraction 1) did not contain any MA (Figure 2.13B). Mycolic acids were found at the origin (Fraction 4) and the smear directly above (Fraction 3), similar to what was found with the *M. tuberculosis* sample, albeit at a much lower concentration due to the crudeness of the sample (Figure 2.13C).

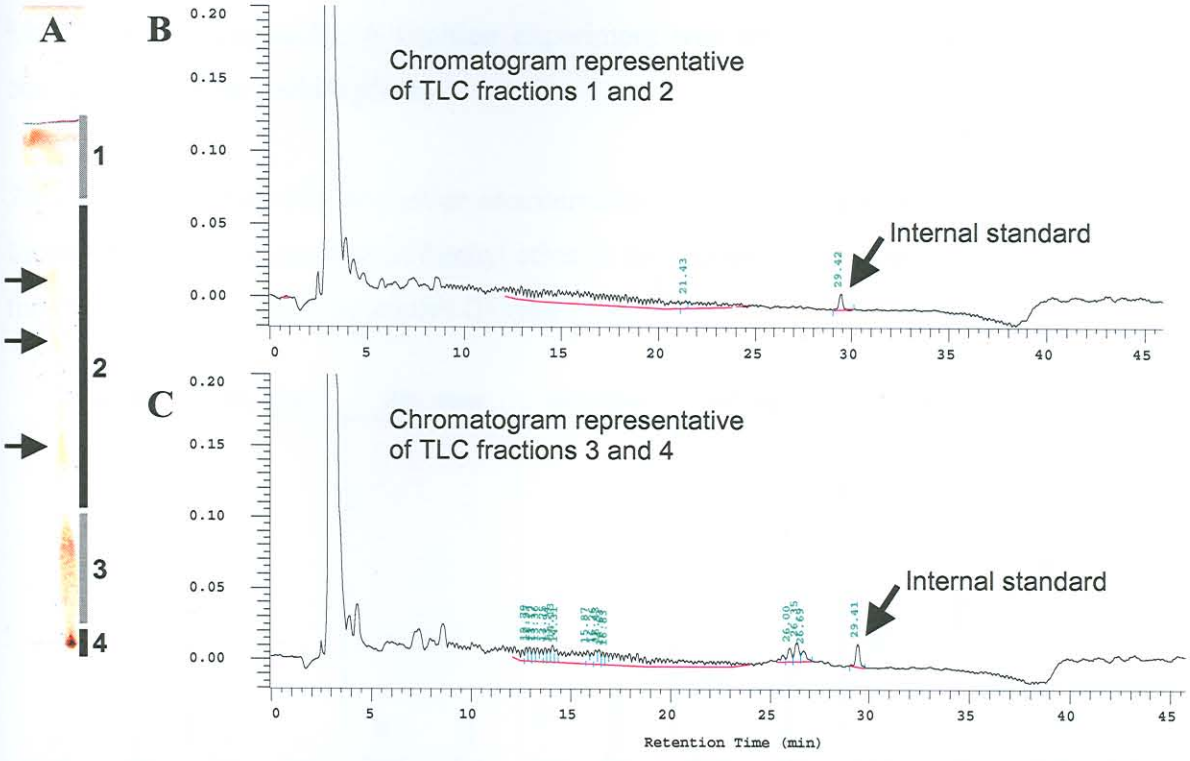

Figure 2.13: High-pressure liquid chromatography analysis of *M. avium* TLC bands. **(A)** The preparative TLC plate showing the bands isolated and extracted for analysis. Arrows indicate possible separated bands. **(B)** A representative HPLC chromatogram of eluted fractions 1 and 2 of the TLC plate indicating the lack of MAs. **(C)** A representative HPLC chromatogram of eluted fractions 3 and 4 of the TLC plate confirming the presence of MA in the typical region of 25-8 minutes.

The three spots that separated in the middle (indicated by arrows in Figure 2.13A) were pooled together for HPLC analysis (Fraction 2), and were shown not to contain any MA at

all (Figure 2.13B). This confirmed that the three faint separated spots of *M. avium* were not separate MA subgroups.

A curious observation was that in all the TLC experiments done, even though the experiments were faithfully followed as described in the literature, most of the MA remained largely immobile at the origin. This was in contrast to Kaneda *et al.* (1986) in which all the MA species had R_f values of at least 0.43 on similar TLC plates developed in this eluent. Comparing the initial experiments where the mobile phase contained 6:100 diethyl ether:*n*-hexane with later experiments where a ratio of 20:80 was used, it was noticed that the mobility of the MA correlate positively with the increase in diethyl ether concentration of the mobile phase. This trend was also noticed in the cholesterol samples that were spotted onto all plates as a control. The deduction that an increase in diethyl ether concentration would enhance MAs mobility seemed logical, since MA was found to be completely soluble in diethyl ether but much less so in *n*-hexane (personal communication, Mrs. S. van Wyngaardt). A titration experiment was set up to determine the optimum composition of the mobile phase.

2.4.1.4 Titration of diethyl ether concentration in the mobile phase

Increasing the concentration of diethyl ether in the mobile phase increased the R_f values of the cholesterol and the MA smears (Figure 2.14).

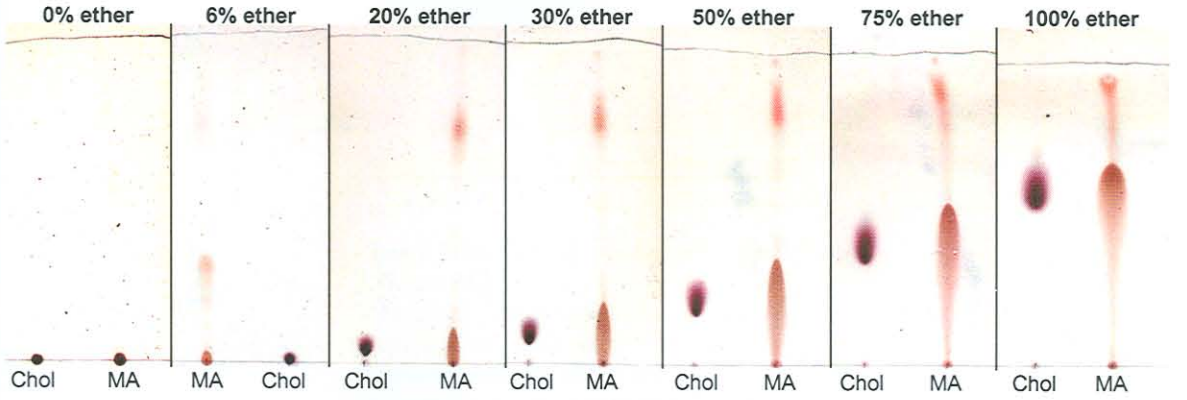

Figure 2.14: The effect of diethyl ether concentration in *n*-hexane as the eluent on the mobility of cholesterol and *M. tuberculosis* MA on TLC plates. Visualisation was done by sulphuric acid charring.

The much higher R_f values obtained with TLC using the high diethyl ether concentrations, suggested that a mistake was made in the article by Kaneda *et al.* (1986). It is much more likely that they have used 80:20 diethyl ether:*n*-hexane instead of 20:80. The R_f value of

0.51 obtained for MA with the 75% diethyl ether concentration, correlates well with the average R_f value of 0.52 obtained for the unresolved spot in the article by Kaneda *et al.* (1986) that was reportedly obtained with 20% diethyl ether in *n*-hexane. In subsequent experiments a ratio of 80:20 diethyl ether:*n*-hexane (v/v) was used instead of 20:80.

*2.4.1.5 Separation of mycolic acids with 80:20 diethyl ether:*n*-hexane*

Developing a TLC plate loaded with various MA species in 80:20 diethyl ether:*n*-hexane improved the mobility of the smears containing MA (*see* Figures 2.12 and 2.13) but did not effect any separation of the subgroups (Figure 2.15). All the MA smears had similar R_f values (0.88); much higher than those obtained with 20:80 diethyl ether:*n*-hexane (0.10). However, no distinct separate spots could be observed for the different subgroups of MA for any of the different MA species tested. No faint spots were observed above the smear for *M. avium* MA as was seen with the 20:80 diethyl ether:*n*-hexane development (*see* Figure 2.11), and it was assumed that the smear and origin both contained MA whereas the whole part above the smear did not, as indicated in Figure 2.13.

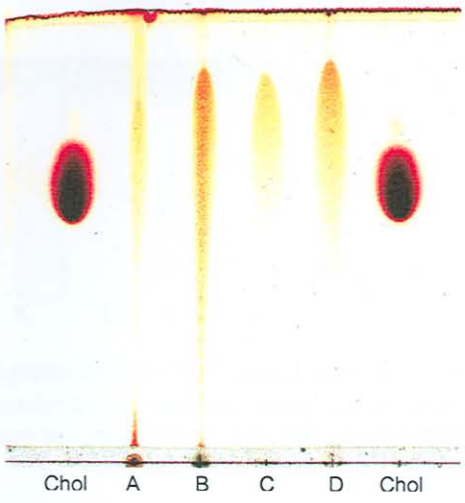

Figure 2.15: Comparing the mobilities of different MA samples on a TLC plate with 80:20 diethyl ether:*n*-hexane as mobile phase. Visualisation was done by sulphuric acid charring. Chol - cholesterol, A - *M. avium* MA, B - *M. tuberculosis* MA, C - 5µg commercial *M. tuberculosis* MA, D - 10µg commercial *M. tuberculosis* MA.

2.4.1.6 Effect of acetic acid in the mobile phase on mycolic acid mobility

It was suggested (personal communication, Dr. Chris Parkinson) that a lowering of pH of the mobile phase might facilitate the separation of the MAs. Since only a small amount of

acid could cause a pronounced drop of pH in the small volume of unbuffered mobile phase, it was necessary to use a weak acid like acetic acid and then only in small volumes. Adding a single drop of glacial acetic acid to 50ml of diethyl ether:*n*-hexane did not have any significant outcome in terms of the separation of the MA subgroups (not shown). The mobile phase composition was switched around to 20:80 diethyl ether:*n*-hexane as it was used before and a similar experiment carried out. No separation of MA could be visualised when the original eluent concentration was used (not shown).

Since such small volumes of acid and unbuffered mobile phase were involved it was possible that the amount of acetic acid could be crucial, maybe even a cause for the difference in R_f values between successive experiments. To test this, increasing amounts of acetic acid were added to 20ml of 80:20 diethyl ether:*n*-hexane. Appropriate volumes of the commercial and self prepared *M. tuberculosis* MA were spotted on separate plates and developed (Figure 2.16). No separation could be observed in any of the plates developed and it was concluded that acetic acid does not affect separation in a mobile phase of 80:20 diethyl ether:*n*-hexane.

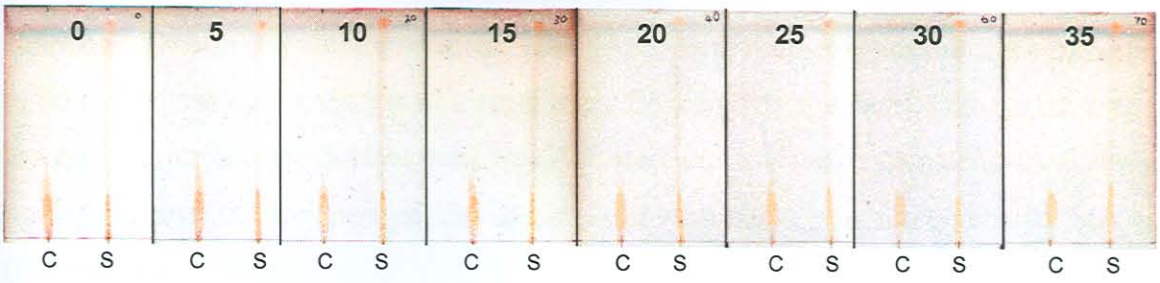

Figure 2.16: Thin layer chromatograms to titrate the optimal amount of acetic acid added to 20ml of the mobile phase (20:80 diethyl ether:*n*-hexane). Numbers indicate the volume (µl) of glacial acetic acid added. Visualisation was done by sulphuric acid charring. C - commercial *M. tuberculosis* MA, S - self-prepared *M. tuberculosis* MA.

2.4.1.7 Other methods of mycolic acid separation

According to Yuan *et al.* (1997), MA could be separated by developing a MA loaded plate five times with a 1:19 ethyl acetate:hexanes (v/v) mobile phase. The publication did not indicate the composition of the hexanes and the experiment was repeated using *n*-hexane as a substitute for hexanes. No separation could be observed for commercial- or self-prepared *M. tuberculosis* MA, and the smears observed had similar small R_f values (0.18). For *M. avium* MA very faint separated spots could be observed, similar to the spots observed with 20:80 diethyl ether:*n*-hexane developed plates. Because separated spots of

M. avium MA developed in diethyl ether:*n*-hexane did not contain MA (Figure 2.13), it was assumed that this also applied to the separated spots observed here. This method was therefore abandoned.

Another complex method described by George *et al.* (1995) was investigated. This method involves $AgNO_3$ impregnation of part of a TLC plate. The MA sample was developed twice with 19:1 hexanes:ethyl acetate into the strip not containing any $AgNO_3$ and three times into the $AgNO_3$ impregnated layer with 17:3 petroleum ether:diethyl ether. Once again the composition of the hexanes was not mentioned in the article and *n*-hexane was used as substitute in the same concentration. Sulphuric acid charring visualised a large spot with two much smaller spots at its edge, close to the origin (not shown). The MA migrated relatively little in the first dimension but not at all into $AgNO_3$ impregnated layer. This observation was contrary to what was expected and further experimentation with this method was abandoned.

2.4.1.8 Preparative isolation of mycolic acid subgroups

The separation of MA into different subgroups using TLC appeared to be quite a challenge. Drawn-out smears obtained with 80:20 diethyl ether:*n*-hexane were considered to be the closest one could get to a separation. Conceivably the part of the smear with the lowest R_f value (i.e. the bottom part) would contain more of the oxygenated MA (keto- and methoxy-) and the top part of the smear would contain the non-oxygenated MA (α-) (Kaneda *et al.*, 1986).

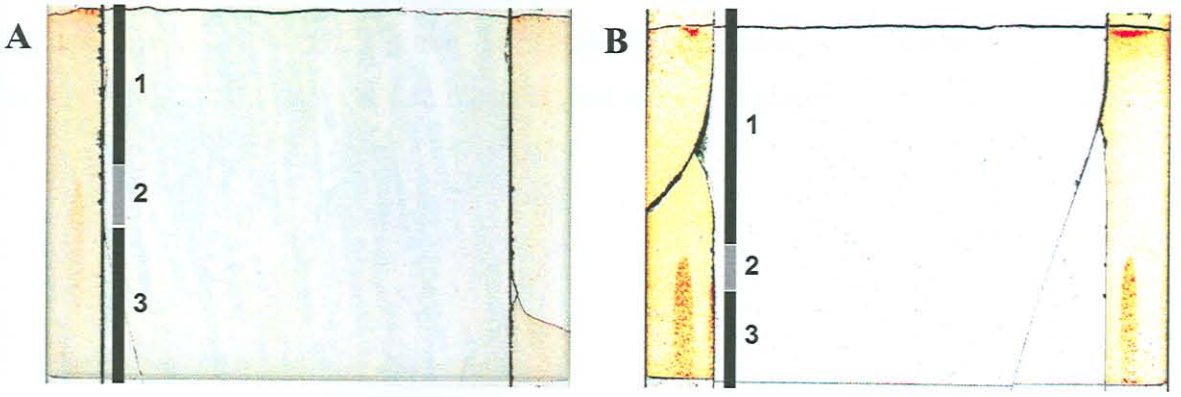

Figure 2.17: Preparative TLC plates developed with 80:20 diethyl ether:*n*-hexane and visualised by sulphuric acid charring. Fractions collected are numbered and the vertical bars indicate the extent of fraction collection. **(A)** Commercial *M. tuberculosis* MA. **(B)** Self-prepared *M. tuberculosis* MA.

To test this, commercial and self-prepared *M. tuberculosis* MA were striped on preparative TLC plates and developed in 80:20 diethyl ether:*n*-hexane. The fractions were defined as indicated (Figure 2.17), eluted and sent for electron-impact mass spectrometry (EI-MS) analysis at the Council for Scientific and Industrial Research (CSIR, Modderfontein, South Africa).

2.4.1.9 Electron-impact mass spectrometry

Electron-impact mass spectrometry done at the CSIR (Modderfontein, South Africa) showed very complex, virtually uninterpretable fragmentation patterns (Figure 2.18). However, analysis of the spectra of the different parts of the smears obtained with self-prepared *M. tuberculosis* MA (Figure 2.17B) indicated that the bottom part of the smear produced a larger number of small fragments than the top part. This may be indicative of oxygen-containing functional groups on the side chains of the MA. Such functional groups provide sites for pyrolysis and will lead to the fragmentation pattern seen. Since it is known that the oxygenated keto- and methoxy-MAs contain oxygenated functional groups, it was concluded that the bottom part of the smear does contain a higher percentage of oxygenated MA compared to the top part of the smear.

Due to the complex fragmentation patterns it was decided that the EI-MS data was inconclusive and together with the fact that the sizes of the MA were expected to be above 1000Da, it was decided that matrix-assisted laser desorption/ionisation time-of-flight mass spectrometry (MALDI-TOF MS) would be better suited to identify the different MA subclasses. Initial experimentation with MALDI-TOF MS was also inconclusive and it was suggested (personal communication: Dr. Caswell Hlongwane) to do a methylation step of the MA using TMDM even before it was loaded onto TLC plates.

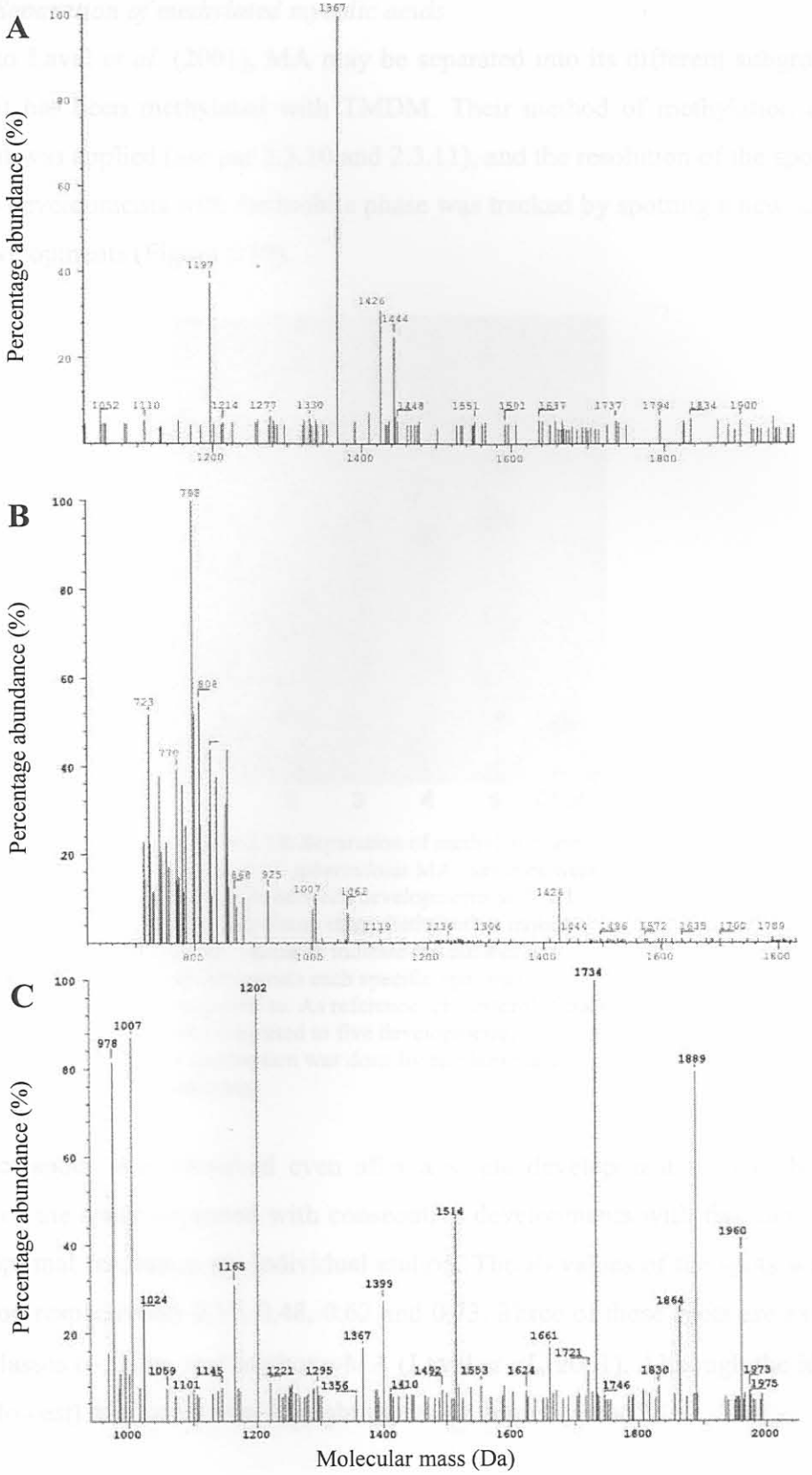

Figure 2.18: Electron-impact mass spectra of TLC separated self-prepared *M. tuberculosis* MA. **(A)** Mass spectrum of top part of the smear (Fraction 2 of Figure 2.17B). **(B)** Mass spectrum of bottom part of the smear (Fraction 3 of Figure 2.17B). **(C)** Mass spectrum of unseparated self-prepared *M. tuberculosis* MA.

2.4.1.10 Separation of methylated mycolic acids

According to Laval *et al.* (2001), MA may be separated into its different subgroups with TLC after it has been methylated with TMDM. Their method of methylation and TLC development was applied (*see* par 2.3.10 and 2.3.11), and the resolution of the spots during consecutive developments with the mobile phase was tracked by spotting a new sample in-between developments (Figure 2.19).

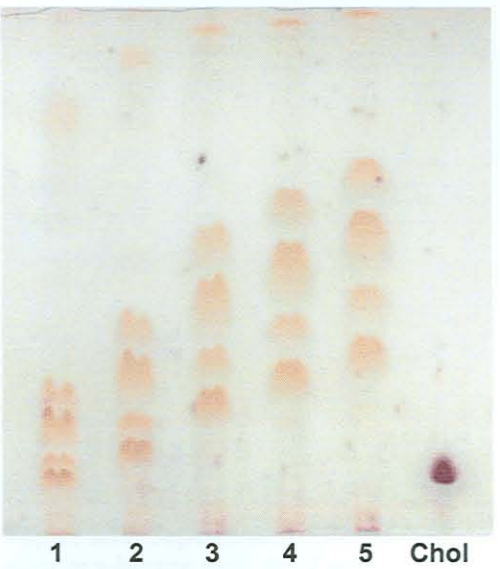

Figure 2.19: Separation of methylated self-prepared *M. tuberculosis* MA. Samples were spotted in-between developments with 9:1 (v/v) petroleum ether:diethyl ether mobile phase. Numbers indicate the number of developments each specific spot was subjected to. As reference, cholesterol (Chol) was subjected to five developments. Visualisation was done by sulphuric acid charring.

Four distinct spots were observed even after a single development with mobile phase. Resolution of the spots improved with consecutive developments with five developments providing optimal resolution for individual elution. The R_f values of the spots were (from bottom to top respectively) 0.37, 0.48, 0.62 and 0.73. Three of these spots are expected to be the subclasses α-, keto- and methoxy-MA (Laval *et al.*, 2001). Although the identity of the fourth (lowest) spot is unclear, it might represent unmethylated MA.

Laval *et al.* (2001) indicated that methylation was achieved with TMDM in an ethereal solution, but did not indicate the solvent composition of the solution. To analyse the effect of different solvent compositions of the methylation solutions as well as methylation's

effect on the mobility of other MA samples, a TLC was performed with self-prepared *M. tuberculosis* MA, commercial *M. tuberculosis* MA and *M. avium* MA methylated in either *n*-hexane or diethyl ether solutions of TMDM and compared to unmethylated samples (Figure 2.20).

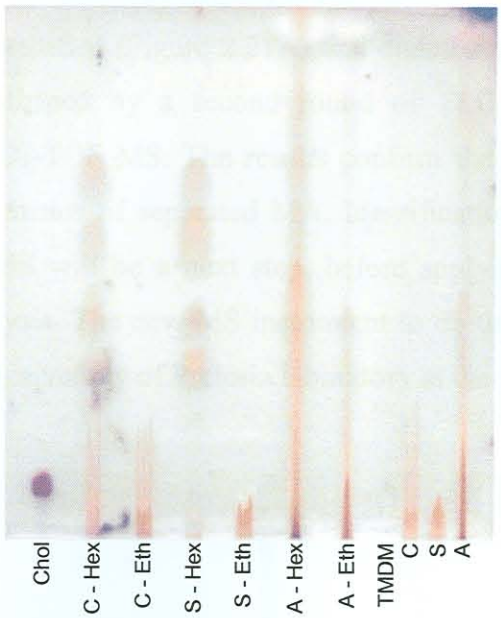

Figure 2.20: Separation of different diethyl ether or *n*-hexane methylated and unmethylated MA samples with five consecutive developments in 9:1 (v/v) petroleum ether:diethyl ether mobile phase. (Trimethylsilyl)diazomethane in *n*-hexane alone was spotted as a control along with cholesterol (Chol) as reference and visualisation was done by sulphuric acid charring. S – self-prepared *M. tuberculosis* MA, C – commercial *M. tuberculosis* MA, A – *M. avium* MA, Hex – *n*-hexane dissolved TMDM, Eth – diethyl ether dissolved TMDM.

Both the commercial and self-prepared *M. tuberculosis* MA methylated with the hexane dissolved TMDM showed resolved spots similar to those in Figure 2.19. *Mycobacterium avium* MA seemed to be too contaminated to be resolved. None of the unmethylated samples resolved beyond anything seen in previous experiments. All the MA samples incubated in the diethyl ether-dissolved solution of TMDM seemed to be unmethylated as no resolution of these samples occurred. No spot could be observed for TMDM alone indicating that all the spots observed were due to MA or contaminants remaining after isolation steps. As a result of this experiment it was determined that MA was successfully

separated into its different subclasses. Preparative separation of the MA followed by elution was now employed to prepare a source of separated MA subclasses.

2.4.1.11 Preparative thin layer chromatography of methylated mycolic acids

Self-prepared *M. tuberculosis* MA was striped, developed and visualised as described (*see* par 2.3.11). Spots were identified (Figure 2.21A) and eluted from the plate. Purity of the eluted fractions was confirmed by a second round of TLC (Figure 2.21B) and the remainder used for MALDI-TOF MS. The results confirm the success of the method to prepare pure samples by means of separated MA. Identification of the pure samples by means of MALDI-TOF MS will be a next step, before applying these pure samples as antigens in biosensor analysis. The new MS instrument to do this with was not, however, fully commisioned in the University of Pretoria laboratory at the time of going to print.

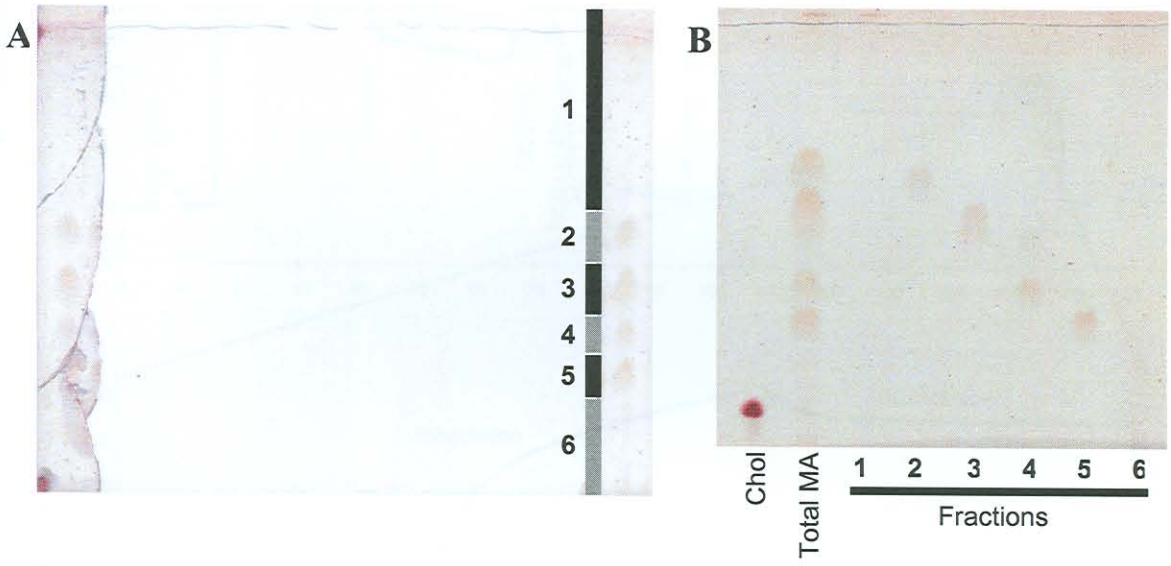

Figure 2.21A: Preparative TLC of methylated self-prepared *M. tuberculosis* MA. Fractions collected are numbered and vertical bars indicate the extent of collection. **(B)** Confirmation of purity of eluted methylated MA fractions. Visualisation was done by sulphuric acid charring.

2.4.2 Lipid antigen immobilisation on biosensor cuvette surfaces

2.4.2.1 Exploratory experiments with mycolic acid immobilisation on biosensor cuvette surfaces

A first experiment for the immobilisation of liposomes on non-derivatised IAsys cuvettes after activation with cationic detergent, performed according to the method innovated by G. Siko and J. Verschoor (Siko, 2002), gave a biosensorgram as shown in Figure 2.22A. The first peak and subsequent descent in signal was due to CPC activation of the surface.

The stable signal thereafter was obtained during a wash step with buffer. The response to liposomes being immobilised was variable and depended on the liposome concentration and constitution. The liposome immobilisation was followed by a brief wash step with buffer that stabilised the signal. A saponin 'blocking' step resulted in the sharp drop in signal that eventually stabilised. After another buffer wash step, the surface was ready for interaction analysis. Baseline was obtained in 25µl buffer, the test serum sample was added (25µl) and an association event was logged in the event log. Association was carried out over a predetermined time (here five minutes). The dissociation analysis was initiated with a wash step with buffer. Dissociation also continued over a predetermined time after which the cells were regenerated. In Figure 2.22B a typical interaction analysis is shown.

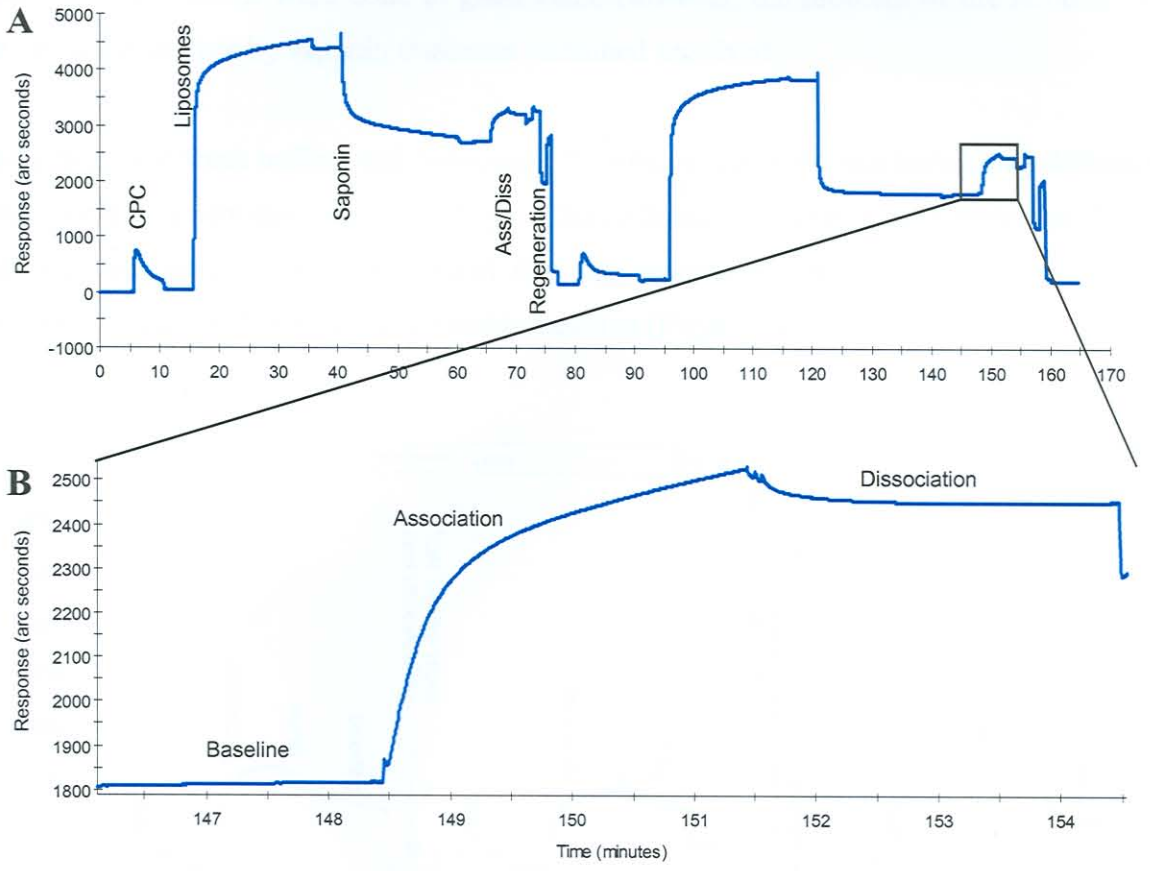

Figure 2.22: (A) A first IAsys biosensor interaction profile (biosensorgram) indicating the immobilisation of liposomes (10mg/ml) without MA, the association and dissociation of antibodies, and subsequent regeneration. **(B)** A magnification of the association/dissociation profile, showing the baseline, association and dissociation curves as recorded by the IAsys software.

Subsequent experiments were carried out with a liposome concentration of 10mg/ml or 500µg/ml not containing MA and a PC:cholesterol mass ratio of 2:1. Poor liposome binding followed by its removal during saponin wash steps were observed. Although MA-

liposomes showed a slightly better binding capacity than the empty liposomes (containing no MA), both liposome types were removed from the cuvette surface by the saponin treatment (not shown). Fresh stock solutions and new cuvettes could not improve the liposome binding capacity or prevent the immobilised layer from being removed by saponin.

It was suggested that plastic laboratory equipment used for liposome preparation might be responsible for poor results. Glass vials were used accordingly. Although liposomes prepared in glass vials had a better binding capacity, it still washed away with saponin treatment (not shown). Liposomes prepared in glass vials were tested on new cuvettes and reproducibly bound better than liposomes prepared in plastic tubes. All subsequent liposome preparations were done in glass vials. However, the problem of the removal of the liposome surface by saponin treatment remained unsolved.

Using the same fresh buffers and liposomes, the binding capacity was tested on a different biosensor and a new cuvette at the IAsys Affinity Sensors laboratory in Cambridge, U.K. Although successful, results suggested that the saponin treatment used to 'block' the liposome surface, still did not give a stable baseline (Figure 2.23).

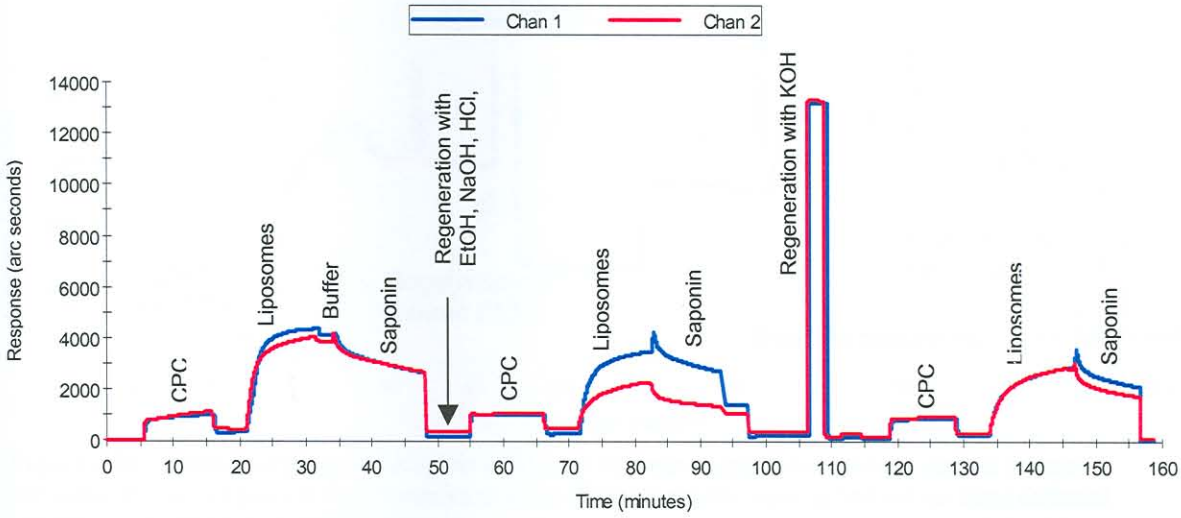

Figure 2.23: The biosensorgram obtained at the laboratories of IAsys Affinity Sensors, Cambridge, U.K. Uniform responses from both cells were achieved, baselines were stable, binding profiles were smooth and signals were high.

It was suggested that 12.5M KOH be used for regeneration instead of the complex steps used so far (personal communication, Paul Edwards, R&D Manager: IAsys, 2001) . The

extreme alkaline conditions created by the KOH wash step are believed to remove any excess fatty deposits and protein that might remain in a cuvette cell after interaction analysis. The KOH step showed promise as a regeneration method as the subsequent liposome immobilisation was stable and comparable between the two cells (Figure 2.23).

A third new biosensor was employed along with new cuvettes and 12.5M KOH as a standard regeneration method and gave comparable good results. The irreproducible results obtained on the three biosensor instruments using the identical reagents, buffers and solutions, suggested that the problem was to be found in the IAsys hardware of the first instrument. Although this was not followed up, possible problem areas could reside with oxidised stirrers or contaminated aspiration tubes. After several rounds of immobilisation and regeneration it was noticed that 12.5M KOH was not sufficient to remove everything from the surface of the cells. Ethanol was added to the protocol and Figure 2.24 shows that KOH alone does not regenerate the cell back to baseline but adding ethanol to the protocol does.

The sequence of first ethanol treatment and then KOH was subsequently found to be optimal (not shown).

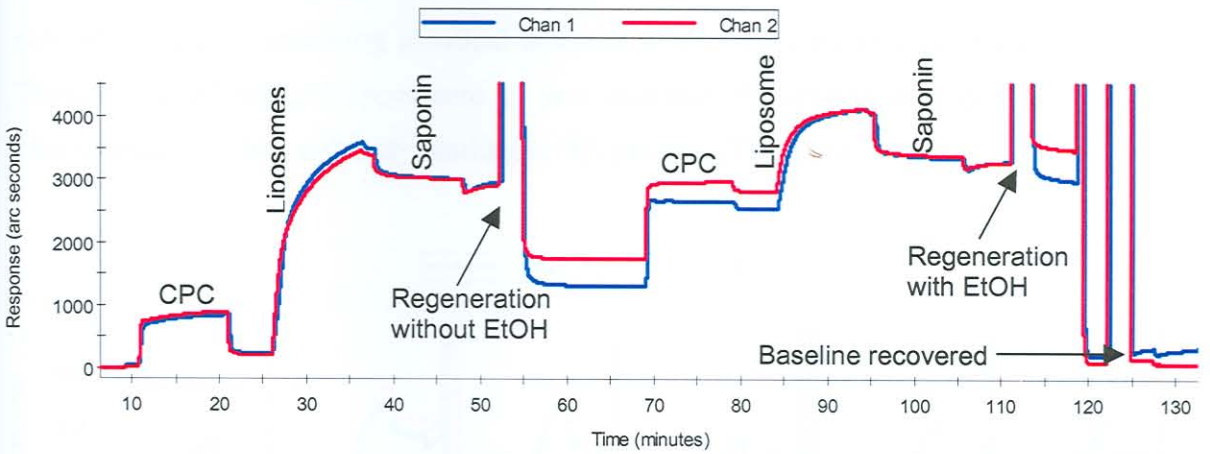

Figure 2.24: A biosensorgram showing the difference between regeneration with or without ethanol included. The sensorgram is representative of three identical experiments carried out on three different cuvettes, using liposomes at 500µg/ml.

2.4.2.2 Optimising mycolic acid-liposome concentration

With the regeneration method optimised, the MA-liposome concentration was titrated between 0.02mg/ml and 10mg/ml. The two channels, monitoring cell 1 and 2 respectively,

were taken as independent experiments and their extents of binding averaged in Figure 2.25. The MA-liposome concentration with the optimum binding capacity was found to be 500µg/ml and this concentration was used in all subsequent experiments.

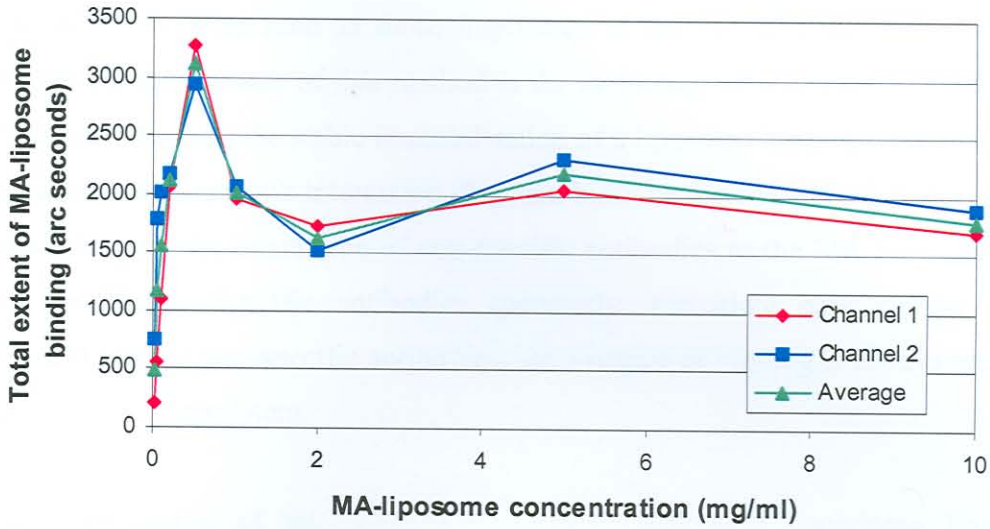

Figure 2.25: A titration of the optimal concentration of MA-liposomes for immobilisation on a non-derivatised biosensor cuvette. A concentration of 500µg/ml resulted in maximum liposome binding achieved in a biosensor measurement.

With the number of wash steps, incubation periods, CPC concentration, liposome concentration and saponin washing established, liposomes could be reproducibly immobilised on a non-derivatised surface, even when using liposomes prepared from separate aliquots containing identical amounts of PC, cholesterol and MA (Figure 2.26). This optimised method (Annexure 1) was successfully applied in a different study to characterise anti-MA antibody binding in TB patients (Thanyane, 2003).

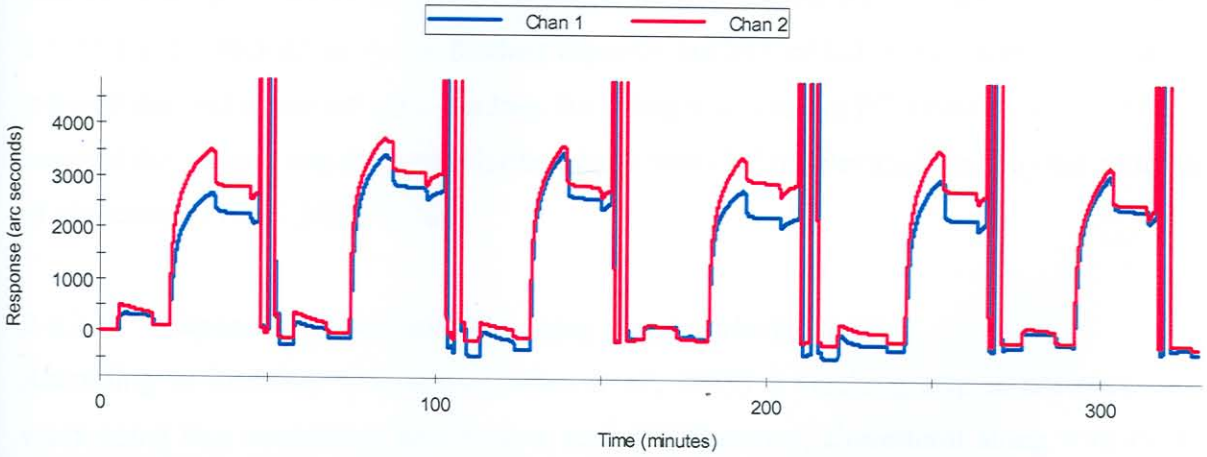

Figure 2.26: A biosensorgram to demonstrate reproducible immobilisation of separately prepared aliquots of MA-liposomes (500µg/ml) containing identical amounts of PC, cholesterol and MA in a non-derivatised IAsys biosensor cuvette.

2.4.2.3 *Application of method to ganglioside G_{M1}*

The method of immobilising MA-liposomes on a non-derivatised biosensor cuvette to analyse interactions of protein antibodies to lipid antigens is a novel application of the resonant mirror biosensor. The question arose whether this optimised method could be applied to other biolipids such as those implicated in the Guillain-Barré syndrome. As described above, the essence of this method is the activation of a non-derivatised surface with a cationic detergent, the stable immobilisation of a liposome layer and the blocking of this layer against non-specific interaction. Saponin binds to the cholesterol in the liposome membrane, blocking the interaction of non-specific antibodies to the MA imbedded in the liposome membrane. Specific antibodies apparently intercalate between the saponin molecules and replace non-specific antibodies, but a degree of binding is always seen when testing patient and control sera.

The wider application of this method was tested with G_{M1} containing liposomes, immobilised on a non-derivatised surface. Interaction analysis of G_{M1}-antibodies to G_{M1} was subsequently measured.

2.4.2.4 *Exploratory use of ganglioside-containing liposomes*

Based on initial trials with liposomes containing varying quantities of PC, cholesterol, MA and G_{M1}, it was observed that cholesterol generally added to the binding capacity of the liposomes (Table 2.1). The net binding capacities (calculated by subtracting the baseline response from the saponin treatment response) of different liposome compositions are listed separately for the two channels. Comparing the MA-liposomes (6PC:3Chol:1MA) to pure PC and empty liposomes (2PC:1Chol), it was concluded that MA and cholesterol had a synergistic effect on liposome binding capacity but MA added to PC alone (9PC:1MA), lowered the maximum possible binding. Including G_{M1} only in PC liposomes (9PC:1G_{M1}) lowered the binding capacity even further, but it was slightly elevated again by the addition of cholesterol (17PC:2G_{M1}:1Chol).

2.4.2.5 *Saponin is redundant when using ganglioside-liposomes*

According to literature (Athanassopoulou *et al.*, 1999) a blocking step is not necessary when using G_{M1} containing lipid bilayer surfaces. However, cholesterol along with PC in the liposome membrane appeared to enhance liposome immobilisation, and provide a target for saponin to stimulate blocking of non-specific ligand binding. Testing different

batches of saponin, it was found that batches are inconsistent in their activity. This could be due to the heterogeneity of saponin, a complex substance obtained from Quillaja bark, containing different sapogenins and monosaccharides. The age of the saponin could conceivably also make a difference due to different states of oxidation. The saponin did not contribute to attaining a stable baseline at 1mg/ml, as was observed in the MA-liposome coating, but instead washed away the G_{M1}-liposome coat. Experiments with G_{M1}-liposomes confirmed that even extensive washing with buffer only, after immobilisation, instead of 1mg/ml saponin, did not remove the liposome layer (Figure 2.27). It was decided to discontinue the use of saponin as a blocking agent. Cholesterol was employed at the start to have saponin bind to it for the purpose of blocking non-specific interaction. Since saponin was not being used anymore and blocking was shown to be redundant, it was decided to not include cholesterol in the liposomes anymore.

Table 2.1: Comparison of the net liposome binding capacities in an IAsys biosensor non-derivatised cuvette, using arbitrary compositions of PC, cholesterol, MA and G_{M1}.

Liposome composition	Channel 1 net liposome binding (arc seconds)	Channel 2 net liposome binding (arc seconds)	Average [(Chan1+Chan2)/2]
6PC:3Chol:1MA	2099	2073	2086
Pure PC	1493	1201	1347
2PC:1Chol	1290	1717	1504
9PC:1MA	1385	1097	1241
17PC:2G_{M1}:1Chol	1229	1215	1222
9PC:1G_{M1}	1143	883	1013

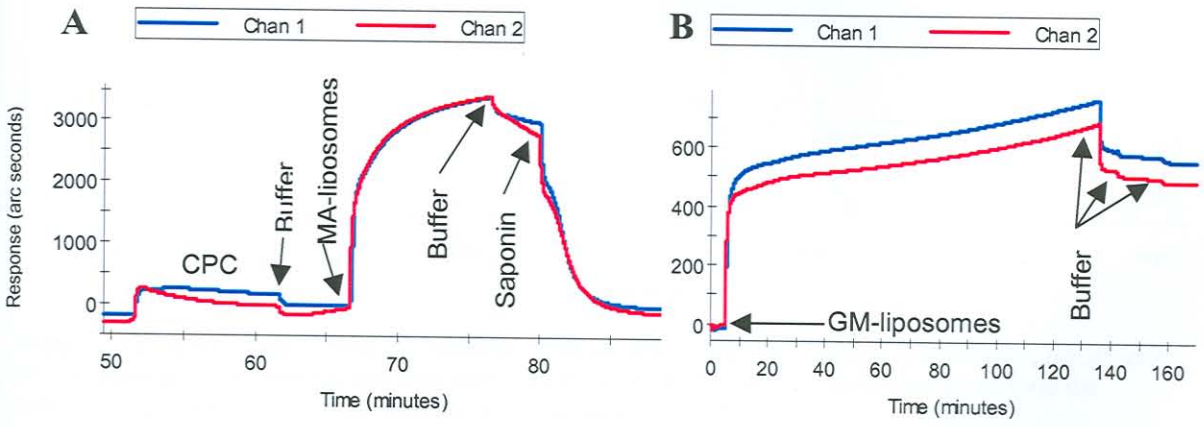

Figure 2.27: IAsys biosensorgrams demonstrating that successive wash steps with buffer do not remove an immobilised G_{M1}-liposome coat **(B)**, whereas a single treatment of saponin removes the MA-liposome coat **(A)**.

In the exploratory experiments a mass ratio of 6PC:3Chol:1G_{M1} was used following the optimised method for MA-liposome immobilisation (6PC:3Chol:1MA). This relates to PC,

cholesterol and G_{M1} molar percentages of 49.4%, 46.8% and 3.8% respectively. Molar ratios are the norm in publications and simplifies stoichiometric comparison.

2.4.2.6 Regeneration using ethanol/sodium hydroxide/hydrochloric acid

The continued regeneration of cuvettes after coating with G_{M1}-liposomes was found to be problematic. Progressively weaker binding of liposomes was observed, probably due to a cumulative etching effect of the surface during regeneration with 12.5M KOH during regenerations. As an alternative, NaOH and HCl were used in lower concentrations, as described by Altin *et al.* (2001). Briefly, three washes with 60µl 2M NaOH were performed after the ethanol washing step and followed by seven washes with 100µl water, three washes with 60µl 2M HCl and finally four washes with 60µl 20mM HCl. Besides being less harsh, improved liposome binding due to residual HCl remaining in the cuvettes before addition of subsequent liposomes was observed. Initial experiments with this method proved to be very successful in terms of the initial extent of liposome immobilisation, but the total binding capacity of G_{M1}-liposomes decreased with each re-coating (Figure 2.28).

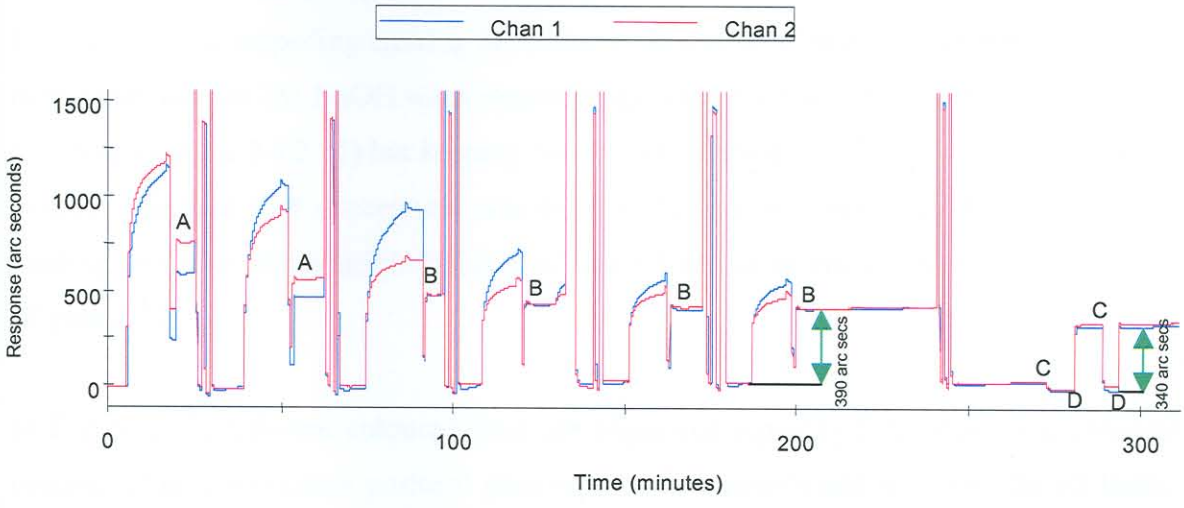

Figure 2.28: A biosensorgram of G_{M1}-liposome immobilisation and regeneration with ethanol, NaOH and HCl. Liposome coats were washed with either water or 10mM NaOH. The green arrows indicate the differences (arc seconds) in refraction indices between water and buffer.
A: Water wash step after G_{M1}-liposome immobilisation
B: 10mM NaOH wash step after G_{M1}-liposome immobilisation
C: Water wash step
D: Buffer (PBS/AE) wash step

After G_{M1}-liposome immobilisation, wash steps of either water (indicated by A in Figure 2.28) or 10mM NaOH (indicated by B in Figure 2.28) were included as was done by Altin *et al.* (2001). Cropped baseline levels were achieved with the 10mM NaOH wash steps, but not with the water wash steps. Subsequently, 10mM NaOH was used in all further experiments. The response (arc seconds) difference between buffer (PBS/AE) only (indicated by D in Figure 2.28), and water (indicated by C in Figure 2.28) was due to a difference in refractive indices of the two solutions. Comparing this difference (right green arrow), to the difference between baseline before and after liposome immobilisation (left green arrow), it was calculated that the net liposome binding was in fact only about 50 arc seconds (390-340 arc seconds). The response difference of 390 arc seconds is therefore not a true reflection of the G_{M1}-liposome binding capacity, as 340 of the 390 arc seconds can be ascribed to the difference in refractive indices of water and buffer.

2.4.2.7 Regeneration using ethanol/potassium hydroxide/hydrochloric acid

In a second experiment (not shown) good, reproducible liposome binding was attained using the method as described above, but subsequent binding of control serum to each new liposome coat, worsened progressively. It was thought that the 2M NaOH step in this new regeneration protocol (*see* par 2.4.2.6) was perhaps too weak to remove all of the protein from the surface, impeding ensuing experiments. It was decided to modify the regeneration method so that the 2M NaOH wash step be replaced by the harsher 12.5M KOH wash step as before (*see* par 2.4.2.11) but keeping the two HCl steps intact. This modification had the desired effect in that successive experiments showed not only reproducible liposome binding, but also reproducible binding of control serum to each new coat of liposomes (Figure 2.29).

In Figure 2.29, different coloured lines are sequential repeats of the same G_{M1}-liposome coating. This regeneration protocol gave reproducible results and was used for all further experiments.

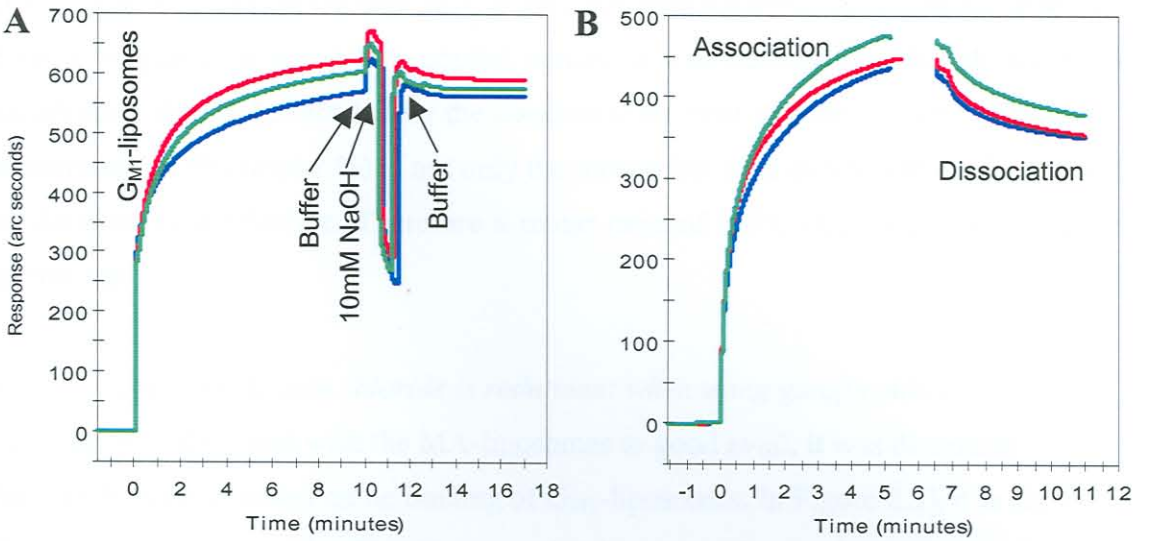

Figure 2.29: FASTplot overlays of sequential G_{M1}-liposome immobilisations and 10mM NaOH washing using ethanol, 12.5M KOH and HCl as regeneration solutions **(A)** and the subsequent association and dissociation of negative control serum **(B)**.

2.4.2.8 Ganglioside concentration optimisation

With other authors having used a range of 2-25% G_{M1} (molar percentage) for biosensor surface coating, it was deemed necessary to optimise the G_{M1} concentration. Three cholesterol-free liposome samples were used, containing respectively 5, 10 and 20% (molar) G_{M1}. The liposome binding capacities were fairly similar although a normal dose response was observed (Figure 2.30A). The association response of negative control serum to the three different surfaces were almost identical (Figure 2.30B).

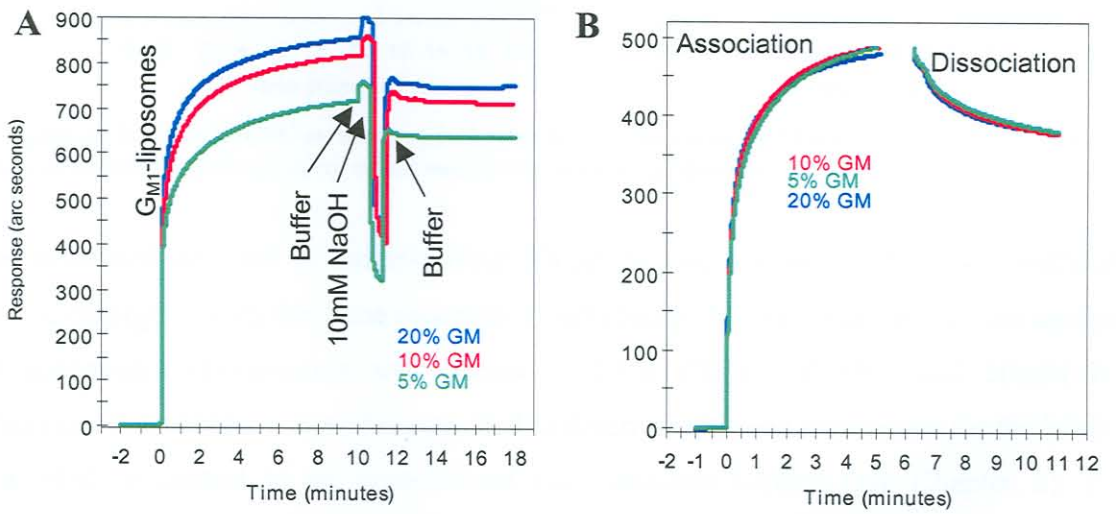

Figure 2.30: FASTplot overlays of G_{M1}-liposome immobilisations using three different G_{M1} concentrations (5, 10, 20%) and subsequent regeneration with ethanol, KOH and HCl **(A)**. The arrows indicate the different wash steps (Tris-buffer or 10mM NaOH) during liposome immobilisation. The negative control serum responses to the three different liposome coats were almost identical **(B)**.

With all three G_{M1} concentrations having the same binding capacity and more importantly the same response to a negative control serum, it was decided that the choice of G_{M1} concentration should be dictated by the concentration most popularly used in literature. A concentration of 5% (molar %) is not only the most often used in relevant publications, but also the most cost effective. Therefore a molar ratio of 19PC:1G_{M1} was used for further experiments.

2.4.2.9 Cetyl peridinium chloride is redundant when using ganglioside-liposomes

Since CPC was first used with the MA-liposomes to good avail, it was determined whether it had any beneficial effect on he binding of G_{M1}-liposomes. In Figure 2.31 it is shown that CPC does not enhance the G_{M1}-liposome binding capacity or the amount of negative control serum bound to the immobilised G_{M1}-liposomes. In fact, both are decreased by the presence of CPC.

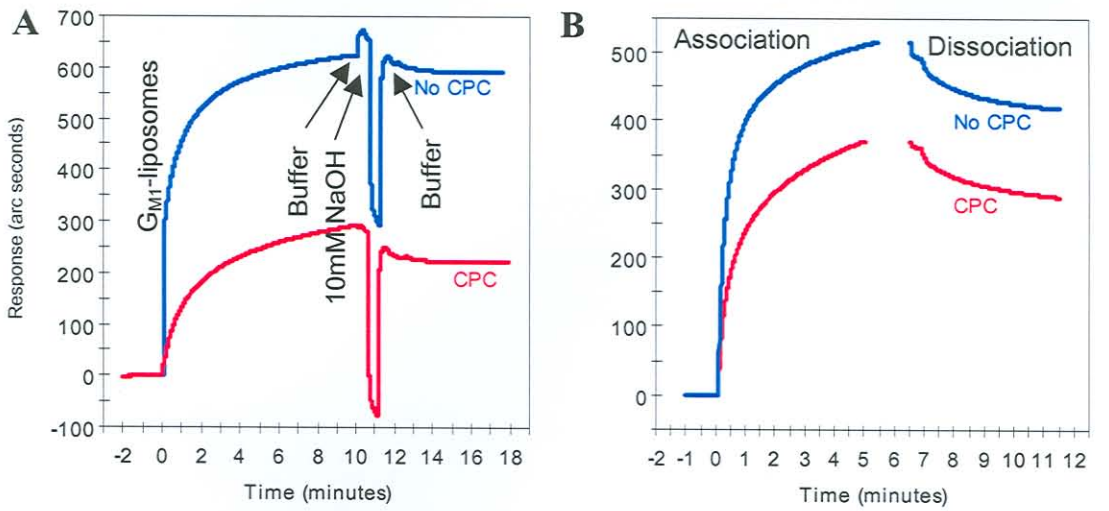

Figure 2.31: Effect of CPC on the immobilisation of G_{M1}-liposomes on IAsys biosensor cuvettes **(A)**, and subsequent negative control serum association to the G_{M1}-liposome coat **(B)**.

This optimised protocol of immobilising 500µg/ml G_{M1}-liposomes (5% G_{M1}) without a cationic detergent, stabilising the coat with 10mM NaOH before serum interaction analyses and subsequent regeneration with ethanol, 12.5M KOH, 2M HCl and 20mM HCl (Annexure 2) has been successfully applied to determine kinetic parameters for the binding of a positive control to an immobilised G_{M1}-liposome surface (*see* Chapter 3). It is expected that this method can be applied to obtain relevant kinetic data to discriminate between anti-G_{M1} antibody levels of different patients. This provides a tool to investigate

the role of such antibodies and their anti-idiotypic antibodies in the progression and recovery of GBS.

2.5 Discussion

2.5.1 The separation of mycolic acid subclasses with thin layer chromatography

In a study to determine the epitope specificity of IgG antibodies against cord factor (trehalose 6,6'-dimycolate, a monosaccharide containing two mycolic acids), it was shown that the antibodies distinguish between different subclasses of MA (Fujiwara *et al.*, 1999). This was confirmed in a follow-up study where a significant decrease in anti-cord factor IgG titre between *M. tuberculosis* cord factor and *M. avium* cord factor was observed (Pan *et al.*, 1999). The only difference between the two cord factors is the composition of the MA subclasses. This suggests that MAs are recognised as epitopes and that preferred subclasses are recognised by the antibodies in human TB patient sera.

The distribution of MA-subclasses in the cell wall determines the fluidity and therefore also the permeability of the cell wall (Liu *et al.*, 1996). Because MA-subclass composition has been linked to *M. tuberculosis*'s virulence in macrophages (Jackson *et al.*, 1999), it was suggested by these authors that the difference in virulence is not caused by different antibody profiles to different MA subclass compositions, but rather that the subclass composition determines the permeability of the cell wall and ultimately its virulence. Mycolic acids do, however, provide a unique footprint of *M. tuberculosis* and specific antibodies to one or more particular subclasses of MA may well turn out to be surrogate markers for tuberculosis infection (Pan *et al.*, 1999).

Moreover, the discovery of a structural mimicry between cholesterol and MA (Siko, 2002), first discovered as a cross-reactivity of tuberculosis patient antibodies to these compounds, emphasises the importance of determining the specificity of anti-MA antibodies against the various subclasses of MA. The biosensor is ideally suited to measure real-time affinities of ligates to ligands and subsequently to enable quantification of the antigenicities of the different subclasses of MA present in the cell walls of *M. tuberculosis*. This knowledge can be expected to contribute significantly to resolve the issue of the role of MA subclasses in the virulence of *M. tuberculosis*. The separation of MA into its subclasses for use in the biosensor would therefore be crucial to such research.

It is known that silver impregnated silica TLC plates can separate lipids in a single class differing only in the degree of saturation and the steric orientation of a double bond (Skipski & Barclay, 1969). This has been demonstrated by several laboratories (Kennerly,

1986; George *et al.*, 1995). In the publication by George *et al.* (1995), MA were radioactively labelled and applied to a TLC plate. The plate was developed twice into the $AgNO_3$-free strip with 19:1 hexanes:ethyl acetate, turned 90° and developed three times into the $AgNO_3$-impregnated part with 17:3 petroleum ether:diethyl ether. Plates were visualised and quantified with a Phosphor Imager to determine the quantities of each MA subclass. Initially, when applied in the current study, $AgNO_3$-impregnation was done by spraying a $AgNO_3$ solution onto a TLC plate and allowing it to dry. This method of $AgNO_3$-impregnation did not enhance separation, neither when TLC plates were submerged in $AgNO_3$ before separation as was done by George *et al* (1995). In fact, the MA did not move into the $AgNO_3$-impregnated region of the TLC plate at all. $AgNO_3$-impregnation of TLC plates was therefore abandoned.

All TLC analyses of the countercurrent purified MA samples showed a spot at the eluent front that did not contain MA. It is unclear what the nature of this contaminant is, but since all crude extracts went through the same initial purification steps, it is likely that the source of the contaminant originates from there. The mobile phases used here for all the experiments contained mostly hydrophobic organic solvents, so it is expected that the contaminant is also rather hydrophobic. It is likely that the spot may represent degradation products of fatty acids or alkanes formed during harsh saponification conditions or even countercurrent separation. Because it was shown that countercurrent purified MA preparations were pyrogen-free (Stoltz, 2002) and that the contaminant spot did not contain any MA, the matter was not investigated further.

Mycolic acids are considered to be neutral lipids as they don't contain any phosphorous or sugars in pure form (Skipski & Barclay, 1969). Due to this neutral character it was recognised that the introduction of a polar compound in the mobile phase, like acetic acid, might influence the separation. This increase in polarity of the mobile phase did not affect the mobility or the separation of the MA. Perhaps the non-polar nature of the MA is so overwhelming that polarity increase by adding an acid is irrelevant.

Mycobacterium avium, a slow grower like *M. tuberculosis*, has a slightly different MA TLC profile to *M. tuberculosis* (Kaneda *et al.*, 1986). Here it was shown to separate into three distinct spots, as opposed to *M. tuberculosis* MA that produces an unresolved smear. Unexpectedly, MA of *M. avium* did not separate into their different subclasses with the

20:80 diethyl ether:*n*-hexane mobile phase. Titration of the diethyl ether concentration demonstrated the possibility that a mistake was made by Kaneda *et al.* (1986) when they showed MA separation with 20:80 diethyl ether:*n*-hexane. Because MA is completely soluble in diethyl ether but only sparingly in *n*-hexane, it is to be expected that MA dissolves better in a higher diethyl ether concentration. Indeed, a mobile phase of 80:20 diethyl ether:*n*-hexane did increase the mobility of the MA even though it did not provide any resolution to the resultant smear.

In a different study, MA was methylated using TMDM after which separation on TLC was effected with five developments in a mobile phase consisting of 9:1 petroleum ether:diethyl ether (Laval *et al.*, 2001). The same method was successfully applied but the appearance of a fourth spot on the TLC profile was inconsistent with the results obtained by the authors. It is interesting that the R_f values obtained with the TMDM-methylated MA samples (between 0.37 and 0.73) correlate fairly well with the little resolved spots obtained by Kaneda *et al.* (1986) whose values ranged between 0.43 and 0.59. This suggests that the samples that Kaneda *et al.* (1986) separated must have been methylated as well. Inspection of their method indicates that they methylated their MA with methanol in the presence of sulphuric acid as an acid catalyst. Since it is not expected that the self-prepared MA used in this study are methylated at all, this observation explains the lack of mobility of MA during initial experiments. Similarly, the MA samples used in other publications were also methylated (George *et al.*, 1995; Yuan *et al.*, 1995; Yuan *et al.*, 1997). Methylation seem to be the only way to separate MA into their subclasses, but this might have implications for recognition by anti-MA antibodies in a biosensor set-up. If the methylated carboxylic acid group projects externally from the bacterial surface, methylation will decrease the affinity of antibodies to MA and biosensor experiments on TLC-separated MA will not reflect the true affinity differences. However, the separation on TLC of the methylated MA and its subsequent analysis in a biosensor is still a crucial step in determining the individual affinity constants of antibodies to the MA subclasses.

To analyse the identity of the different spots, mass spectrometry is employed. Electron-impact mass spectrometry has been successfully employed previously for the elucidation of MA structure (Dubnau *et al.*, 1997; Quémard *et al.*, 1997), but although this technique provides important information about MA structure, the fragmentation patterns caused by pyrolysis are complex due to the presence of homologues and the loss of water and

methanol from the native molecules (Laval *et al.*, 2001). Initial experimentation with EI-MS supported these findings. It was decided to attempt the more sensitive MALDI-TOF MS technique (Laval *et al.*, 2001) in future.

It was concluded that MA subclasses are separable with the methods described (George *et al.*, 1995; Yuan *et al.*, 1997; Watanabe *et al.*, 2001), but preparative isolation of the subgroups is expensive and very difficult. Pending the outcome of the analysis of the different bands of the separated MA, a decision can be made as to the useful testing of these fractions in the biosensor to determine the specificities of binding of TB patient antibodies. In the meantime the biosensor method for immobilising MA-liposomes was optimised and tested for application to the GBS disease model.

2.5.2 Immobilisation of lipid antigens on a biosensor cuvette surface

Protein-protein interactions are well defined and their interaction characteristics have been successfully determined with optical biosensors (Boulla *et al.*, 2000). These interactions were usually measured between proteins in solution and proteins on an immobilised surface. Broadening the application field, interactions between molecules in solution and their transmembrane protein receptors in their native environment have also been measured (Nikolelis *et al.*, 1999). This was done by creating artificial bilayer membranes on the surface of the biosensor with the transmembrane proteins imbedded in the bilayer. Expanding even further, studies have shown that it is possible to study interactions between the lipids of an artificial immobilised bilayer and ligands in solution (Altin *et al.*, 2001). Now a new field is emerging: characterisation of antibody binding properties to lipid and glycolipid antigens immobilised in liposomes on a biosensor surface.

The method for liposome immobilisation on a cationic detergent (CPC) activated sensor surface (Siko, 2002) worked well, but regeneration was optimised to include a concentrated KOH wash. Mycolic acids in the pure form consist of lipid only. Part of the waxy tail is imbedded in the membrane and the part that protrudes from the membrane is antigenic. This implies that the surface of the MA-liposomes probably retain some hydrophobic character, leading to the enhanced liposome binding possible with MA-liposomes on a CPC activated surface.

Perhaps due to an etching effect caused by the corrosiveness of the high KOH concentration, the cuvette surfaces deteriorated progressively throughout experiments. Maximally forty rounds of immobilisation, interaction analysis and regeneration could be achieved per cuvette.

Ganglioside G_{M1} had been immobilised in combination with PC before (Athanassopoulou *et al.*, 1999) and also as G_{M1}-liposomes (MacKenzie *et al.*, 1997). Athanassopoulou *et al.* (1999) utilised the standard hydrophobic cuvettes available to IAsys biosensor users. Although useful for certain studies, this method was found to be ineffective for MA immobilisation and abandoned (Siko, 2002). To our knowledge, a resonant mirror biosensor has never been used before for immobilising MA- or G_{M1}-liposomes on a non-derivatised surface.

There is a marked difference in the immobilisation protocols between MA-liposomes and G_{M1}-liposomes. It is shown here that CPC activation at the cuvette surface is not required for G_{M1}-liposome immobilisation. This is probably due to the polysaccharide moiety of G_{M1} gangliosides. Ganglioside-liposomes have a hydrophilic surface created by the glycosilated gangliosides. The hydrophilic liposome surface should be able to associate with a hydrophilic cuvette surface without the activation with cationic detergent.

Blocking of non-specific interactions has been shown to be redundant for G_{M1} (Athanassopoulou *et al.*, 1999). A matter that complicates the qualitative as well as quantitative determination of kinetic MA-antibody binding parameters, is the cross-reacting cholesterol antibodies found in varying levels in the sera of all humans (Alving & Wassef, 1999). With the antigenic properties of cholesterol, one would expect a certain degree of interaction with antibodies on liposome surfaces containing cholesterol. The stabilising effect of cholesterol on liposomes, especially when they contain MA, makes for a difficult choice whether to include cholesterol or not. If cholesterol could not be excluded, it would become necessary to block such surfaces from interactions not specific to MA. As saponin is specific to cholesterol, it would seem the ideal way of blocking MA-liposome surfaces.

Regenerations between the two surfaces also varied. It appeared to be necessary to neutralise the harsh alkaline conditions during regenerations when using G_{M1}-liposomes

but not MA-liposomes. It is possible that because G_{M1}-liposomes associate so much easier with the cuvette surface than MA-liposomes, they require less harsh conditions to remove. Even so, it has been shown that not having the harsh alkaline conditions, lessens the reproducibility of subsequent experiments in the same cuvette.

In the literature, concentrations of 2-25% G_{M1} have been used to determine cholera toxin (CTx) binding affinities (Masserini *et al.*, 1992; Kuziemko *et al.*, 1996; MacKenzie *et al.*, 1997; Athanassopoulou *et al.*, 1999). Although indicative of typical G_{M1} biomembrane concentrations, some of the experiments using 2% G_{M1} were unsuitable for the biosensor application. In one study it was shown that 25% G_{M1} reaches maximal binding capacity (Athanassopoulou *et al.*, 1999). However, this immobilisation was done on hydrophobic IAsys cuvettes with a different chemical immobilisation principle than used here. Kuziemko *et al.* (1996) determined that the lowest G_{M1} concentration that gave analysable kinetic data was 5% (molar %). Therefore the concentration of 5% G_{M1} seemed most logical and cost effective.

In a BIAcore biosensor, utilising surface plasmon resonance, *Salmonella* LPS imbedded into liposomes that contained different gangliosides, were captured with anti-LPS IgG immobilised on a CM5 sensor chip containing a CMD matrix similar to CMD surfaces of IAsys cuvettes (MacKenzie *et al.*, 1997). This complex set-up apparently created an artificial lipid bilayer of PC and gangliosides on the sensor chip surface and was used to determine kinetic parameters for cholera toxin B-subunit (CTxB) binding to gangliosides. It was determined that this set-up is too complex and not relevant for use in the IAsys biosensor. Kuziemko *et al.* (1992) also utilised a BIAcore biosensor, but successfully employed a method much similar to the optimised method used here for MA-liposome immobilisation. CM5 sensor chips were stripped completely of their CMD matrices to produce non-derivatised surfaces. Octadecylmercaptan (ODM) was used to activate the surface similar to CPC, after which a lipid solution (resembling liposomes) was added to create a self assembled bilayer.

Taken together, all these experiments indicate that there are different biosensor immobilisation methods available for different purposes and that they are not universally applicable. That has also been confirmed in this study with a different set-up needed for G_{M1}-liposome compared to MA-liposome immobilisation. The ultimate aim would be to

optimise a method for a specific purpose so that it is cost-effective, fast and optimal in terms of result output.

CHAPTER 3

APPLICATION OF THE BIOSENSOR TO MEASURE ANTI-GANGLIOSIDE ANTIBODIES IN GUILLAIN-BARRÉ SYNDROME PATIENTS

3.1 Introduction

3.1.1 The Guillain-Barré syndrome

When damage occurs to the myelin sheath that protects peripheral nerves, an affliction called neuropathy results. This damage can be caused by different mechanisms like toxic substances, metabolic instabilities, other degenerative processes and also one's own immune response components like macrophages, antibodies and T-cells. The latter is known as immune-mediated neuropathies and can be further divided into chronic and acute according to the manifestation of the symptoms (Ang, 2001).

The Guillain-Barré syndrome (GBS) is the most frequent acute immune-mediated neuropathy. In the Netherlands, it is responsible for 12 deaths in a million people annually (Van Koningsveld *et al.*, 2000). It is characterised by general muscle weakness that evolves rapidly, with varying distribution and severity. It may affect respiratory muscles, causing patients to become respirator dependent. The disease reaches its most severe stage two to three weeks after onset (Hughes & Rees, 1997; Van der Meché *et al.*, 1997). Most patients recover, although residual deficiencies may be disabling. Despite intensive care unit treatment, 3-7% of all patients die (Van Koningsveld *et al.*, 2000).

A number of factors may cause the onset of GBS. Bacterial and viral infections are the most common triggers and these include *Campylobacter jejuni*, cytomegalo virus, Epstein-Barr virus, *Mycoplasma pneumoniae* and *Haemophilus influenzae*. Events that may compromise an individual's immune response, such as vaccinations and surgery, have also been suggested to trigger the onset of GBS, but this has not yet been proven with case controlled studies (Hughes, 1990; Hughes & Rees, 1997; Ang *et al.*, 2000). In both a Dutch and a British study it was observed that *C. jejuni* was the most common antecedent infection to GBS and cytomegalo virus the second most common (Table 3.1) (Winer *et al.*, 1988; Jacobs *et al.*, 1998). Distribution and frequencies of each prior infection differ between countries but in Northern China and Çuracao, *C. jejuni* is responsible for 75% of GBS cases (Ho *et al.*, 1995).

Table 3.1: The frequency of infections noted prior to the onset of GBS. (Source: Ang, 2001)

Micro-organism	Frequency
Campylobacter jejuni	14-66%
Cytomegalo virus	5-15%
Epstein-Barr virus	0-10%
Mycoplasma pneumoniae	1-11%
Haemophilus influenzae	1-13%

3.1.2 *Campylobacter jejuni* as antecedent infection

Campylobacter jejuni infection usually causes bloody or watery diarrhoea in humans but sometimes the infection is overlooked. Carriers of the bacterium include chickens, other meats, contaminated water, raw milk and even pets (Hudson *et al.*, 1999). The genome of *C. jejuni* is known and it has been observed that regions encoding for surface structures are highly variable. Consequently one can expect a high diversity in presentable surface antigens. In South Africa the O:41 serotype is the most common, in Japan the O:19 serotype predominates. This serotype has also been found in patients from many Western European countries (Lastovica *et al.*, 1997; Ang *et al.*, 2001b).

3.1.3 Histopathology of Guillain-Barré syndrome

Two main forms of damage occur in the nerves of patients. In the first, demyelinating GBS, macrophages infiltrating the Schwann cells of the axon can be observed as well as the presence of complement activation products (Hughes 1990; Hughes & Rees, 1997). It is thought that the sequence of events that lead to demyelination is the binding of auto-antibodies to the Schwann cells, activation of complement that forms transmembranous pores and then the removal of myelin catabolic products by the observed macrophages. In the second type, primary axonal GBS, the degeneration is observed at the node of Ranvier where the axon is bare, rather than the myelin sheath of the Schwann cells. Binding of antibodies occurs along with the lengthening of the nodal gap and complement activation again takes place (Paparounas *et al.*, 1999). Macrophages cover these nodes and invade the axonal space itself, destroying it from the root to the nerve's most distal part (Figure 3.1)

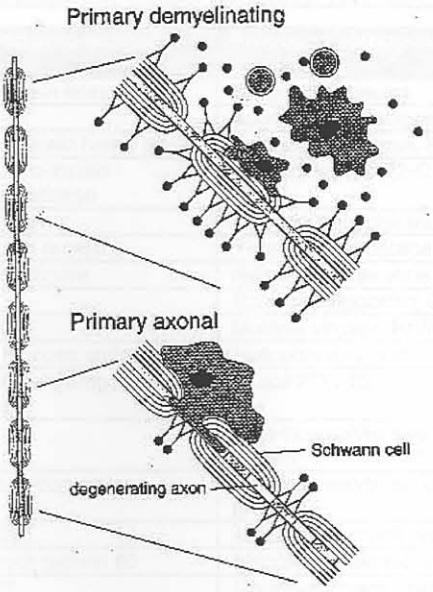

Figure 3.1: Histopathology of GBS showing macrophage invasion of the myelin sheath during demyelinating GBS and invasion of the axon during primary axonal GBS. (Source: Ang, 2001)

3.1.4 Molecular mimicry

Damian first used the term 'molecular mimicry' in 1964, when he referred to the antigens being similar between infectious agents and self-tissue (Damian, 1964). The mechanism can be explained as follow: antibodies are raised by the host against a certain infection. These antibodies are directed against structures on the surface of the bacterium or virus. A resemblance to surface structures of the host's own cells would allow the antibodies to recognise the host's own cells. This is called cross-reactivity and results in not only the infection to be destroyed but also the host's own tissue (Albert & Inman, 1999).

The explanation of cross-reactivity is simple. We now know that almost all B- and T-cell receptors are able to recognise more than one antigen, and that the strength of interaction depends on the quality or amount of resemblance between different antigens (Van Regenmortel, 1998). Due to the amount of knowledge available on protein structure, the study of molecular mimicry has focused on the similarity between amino acid sequences (Roudier *et al.*, 1996). In a number of cases similar protein structure were found between human self-antigens and bacterial and viral antigens (Table 3.2).

Table 3.2: Diseases associated with molecular mimicry. (Source: Ang, 2001)

Immune mediated disease	Proposed auto-antigen	Proposed pathogen/molecule	Antibody/T-cell mediated
Cardiovascular disease	Alpha-myosin heavy chain	*Chlamydia* species	Both
Celiac disease	Gliadin	Adenovirus/enteric microbes	Antibodies
Chagas' disease	Cardiac myosin heavy chain	*Trypanosoma cruzi*, B13 protein	T-cells
Diabetes mellitus type 1	GAD65, pro-insulin carboxypeptidase	Coxsackievirus P2-C	T-cells
Guillain-Barré/Miller Fisher	Gangliosides	*C. jejuni*, lipopolysaccharides	Antibodies
Graves disease	Thyrotropin receptor	*Yersinia enterocolica*	Antibodies
Herpes stromal keratitis	Corneal antigens	Herpes simplex virus type 1, UL6	T-cells
Lyme diseases	LFA-1	*Borrelia burgdorferi*, OSP-A	T-cells
Multiple sclerosis	MBP/MOG	Multiple viruses: HHV-6, Epstein-Barr	Both
Peptic ulcer	Gastric mucosa antigens	*Helicobacter pylori*	T-cells
Primary biliary cirrhosis	Pyruvate dehydrogenase complex	*E. coli* PDC-E2	Antibodies
Psoriasis	Keratin	Beta-haemolytic streptococcus, M-protein	T-cells
Rheumatic heart disease	Cardiac glycoproteins	Beta-haemolytic streptococcus, M-protein	Antibodies
Rheumatoid arthritis	HLA-DRB1	40kDa heat shock protein (dnaJ)	Both
Rheumatoid arthritis	Heat shock protein 60	*Mycobacterium tuberculosis* HSP 65	Both
Spondyloarthropathies	HLA-B27	*Chlamydia trachomatis*, Gram-negative enteric pathogens	Antibodies

In GBS, the focus has been on molecular mimicry involving non-protein antigens. Not much is known about the interactions of antibodies with glycolipids or glycopeptides, but it is clear that interaction depends on the three-dimensional structure and charge of the antigen. Since it is known that a large proportion of B- and T-cells react with non-protein antigens it can be stated that cross-reaction does not exclusively depend on amino acid sequence (Van Regenmortel, 1998; Deck *et al.*, 1999). Another observation that strengthens this theory is that monoclonal antibodies can also react with completely different peptides to those they have been raised against. These peptides are called mimotopes and have the same three-dimensional structures as the target peptide (Sparbier & Walden, 1999). Monoclonal antibodies against carbohydrate antigens that react with peptides are an even more extreme case of mimicry, where the peptides have the same conformational structure as the carbohydrates (Kieber-Emmons, 1998).

3.1.5 Cholera toxin: A specific probe for ganglioside binding

Cholera toxin, an enterotoxin secreted by *Vibrio cholerae*, is responsible for the gastrointestinal manifestation of cholera (Cuatrecasas, 1973). The disease causes watery diarrhoea leading to dehydration and metabolic acidosis that, untreated, may lead to death.

The mechanism of action of CTx involves receptor-mediated binding of CTx to mucosal cells and stimulation of adenylate cyclase activity (Holmgren, 1981). The resulting

increase in cyclic adenosine monophosphate (cAMP) inhibits mainly the uptake of sodium chloride subsequently causing fluid loss (Ouchterlony & Holmgren, 1980).

Cholera toxin is a member of the family of AB_5 toxins that consist of a cell-binding domain comprised by the pentameric B subunits and a toxic domain represented by the single catalytic A subunit (Cuatrecasas, 1973). Other toxins that belong to this family include heat-labile toxin produced by *Bordetella pertussis* that causes whooping cough, Shiga and Shiga-like toxins that cause bacillary dysentery, diphtheria toxin and *Pseudomonas aeruginosa* exotoxin A (Karlsson, 1995). Figure 3.2 shows the ribbon structures of some of these AB_5 toxin and also illustrates the so-called lunar lander structure of both CTx and heat-labile toxin.

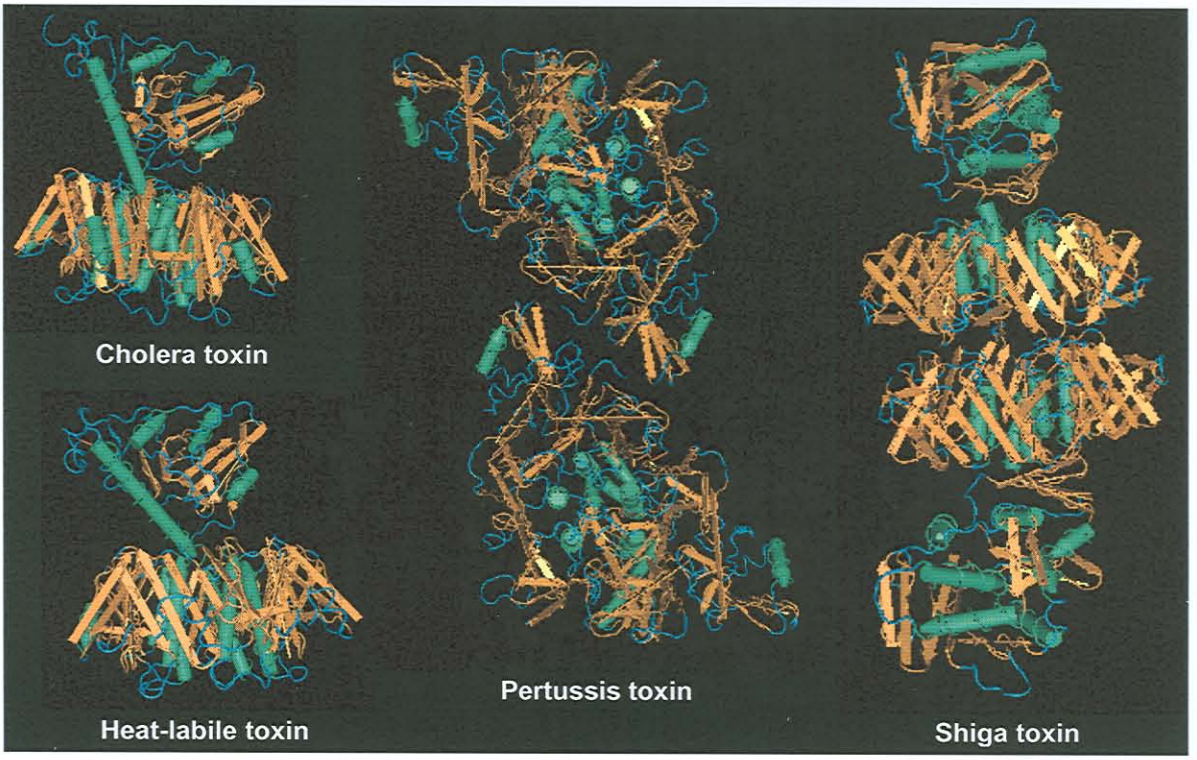

Figure 3.2: Members of the AB_5 family of toxins secreted by various bacteria. (Sources: Sixma *et al.*, 1991; Fraser *et al.*, 1994; Stein *et al.*, 1994; Zhang *et al.*, 1995)

All of these AB_5 toxins have a cell surface receptor. For CTx this is specifically G_{M1} (Cuatrecasas, 1973). Ganglioside G_{M1} binds to the B subunit of CTx in a 1:1 stoichiometry; therefore, a single CTx molecule containing five B subunits will bind to five G_{M1} molecules. Figure 3.3 illustrates the binding of the pentameric complex (choleragenoid or CTxB) to five G_{M1} molecules.

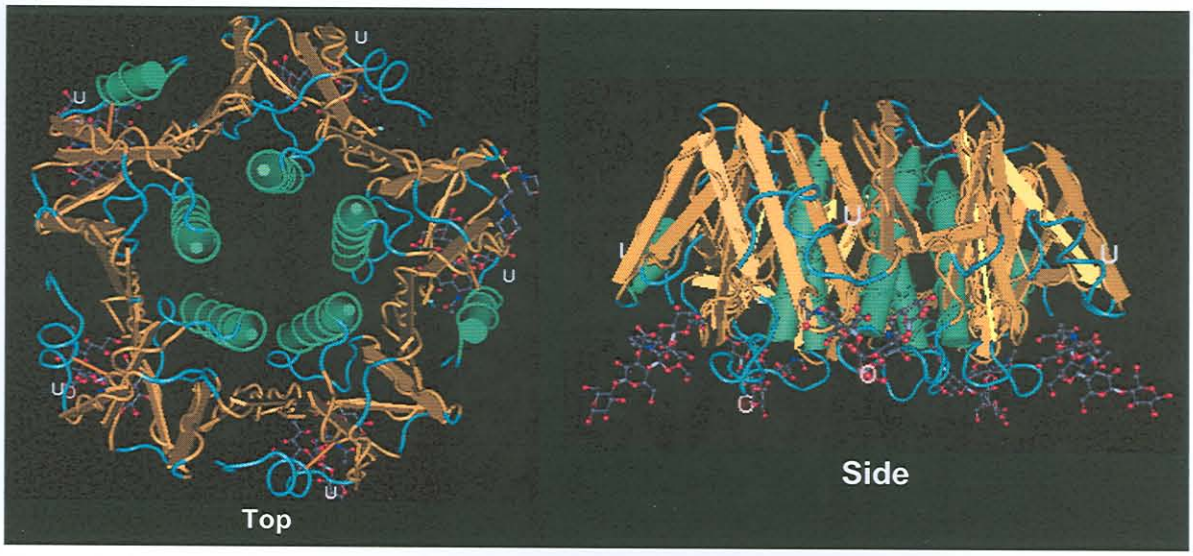

Figure 3.3: Binding of five G_{M1} molecules to the pentameric choleragenoid. (Source: Merritt *et al.*, 1994)

The G_{M1} gangliosides bind at the base of the pentamer and towards the side of the ring formed by the B subunits. The association of each ganglioside may be thought of as a two-fingered grip as a galactose-β1,3-N-acetyl galactosamine 'forefinger' inserts in a pocket of the binding site and a neuraminic acid 'thumb' in a shallow depression (Karlsson, 1995). The ceramide tail of the G_{M1} is buried in the membrane of the host, but the arrangement of G_{M1} binding puts the G_{M1} molecules relatively far from the pore of the pentameric complex. The C-terminal tail (18 residues) of the A2 chain of the catalytic A subunit fills the central pore formed by the pentameric complex, therefore lying on top of the pore (as illustrated in Figure 4.4) and aimed away from the membrane upon binding (Karlsson, 1995). The mechanism by which the A1 fragment of the catalytic A subunit eventually crosses the host membrane to exert its cytotoxic effects remains unknown, but mechanisms available for other AB_5 toxins may provide clues to CTx's mechanism (St Hilaire *et al.*, 1994). Nevertheless, the binding of G_{M1} to CTx and the choleragenoid is well defined, its stoichiometry known and kinetic parameters like the velocity of binding and affinity constants have been derived before (Masserini *et al.*, 1992; Kuziemko *et al.*, 1996; MacKenzie *et al.*, 1997; Athanassopoulou *et al.*, 1999). Therefore, CTx would be an ideal positive control in studies measuring the affinity of antibodies against G_{M1}.

3.1.6 Kinetics

Simple binding events like one molecule of ligand (G) binding to one molecule of ligate (L), can be illustrated as follows:

$$G + L \rightarrow GL \tag{3.1}$$

The dissociation of this complex to its original state can be illustrated by:

$$GL \rightarrow G + L \tag{3.2}$$

As a whole, this interaction can be numerically described by:

$$G + L \underset{k_{diss}}{\overset{k_{ass}}{\leftrightarrow}} GL \tag{3.3}$$

where the second order association rate constant, k_{ass}, describes the rate of complex formation and the first order dissociation constant, k_{diss}, describes the rate of complex dissociation (Pathak, 1995). The actual association rate is equal to the product of the association rate constant and the concentrations of the ligand and ligate. Similarly, the dissociation rate is equal to the product of the dissociation rate constant and the ligand-ligate complex concentration. Mixing ligand and ligate in solution will result in an initial fast rate of complex formation followed by a decrease as the rate of complex formation is opposed by the rate of complex dissociation. Eventually, an equilibrium is reached where the association and dissociation rates are equal. At this point, the equilibrium can be numerically described by the equal and opposing rates, therefore:

$$k_{ass}[G][L] = k_{diss}[GL] \tag{3.4}$$

which rearranges to:

$$\frac{[G][L]}{[GL]} = \frac{k_{diss}}{k_{ass}} = K_D \tag{3.5}$$

where K_D is termed the dissociation equilibrium constant and has units M.

The constant K_D is a measure of the affinity of the ligand for the ligate and is one of the prime kinetic parameters used to describe interactions. The lower the value of K_D, the higher the affinity of a ligand for its receptor. A K_D value of 10^{-6}M would mean that at this specific ligand concentration a state of equilibrium exists between the association and dissociation rates. If this value is lower, it means that a lower concentration of ligand is necessary to reach equilibrium and implies a higher affinity. The association equilibrium constant, K_A, is the inverse of K_D but is not used as often due to more complex calculations with its inverse unit of M^{-1} (IAsys, 1995b).

Typical ranges of the rate and equilibrium constants in biological samples are (IAsys, 1995b):

$$k_{ass} = 10^3 - 10^7 M^{-1}s^{-1}$$
$$k_{diss} = 10^{-5} - 10^{-1}\ s^{-1}$$
$$K_D = 10^{-11} - 10^{-4} M$$

The interaction of the immobilised ligand with the ligate present in the injected sample is recorded using the IAsys software and visualised as a standard association/dissociation curve. In order to accurately determine kinetic parameters with an interaction analysis, it is necessary to do a series of dilutions of a single test sample to generate multiple association and dissociation curves. A second program called FASTfit is then used to set the borders of the regions that should be used to calculate the kinetic parameters. Regions can be set manually or by the software, depending on the requirements of the experiment and/or user. For different concentrations the same time frame should be used for each baseline, association and dissociation region in order to calculate and compare parameters accurately (IAsys, 1995b, 1996).

All the above equations assume that the ligand and ligate are present free in solutions. However, the conditions under which ligate associates with ligand are different in the IAsys biosensor in a number of ways (IAsys, 1995b):

- Ligand is immobilised on the sensor surface
- There is a boundary layer present between the biosensor surface and the solution
- Ligand has a relatively high concentration (μM) but low absolute amounts

- Ligate has a relatively low concentration (nM) but is in excess to ligand due to the bulk volume of the solution
- Ligate concentration remains virtually unchanged during interaction analyses
- Ligate is replenished at the biosensor surface using stirring
- Dissociation can be directly observed by removing non-bound ligate

3.1.7 Association analysis

Association curves are in fact a net result of association and dissociation events. A time frame of several minutes is usually necessary for equilibrium to be reached due to the low concentrations of ligate present. When response to added ligate increases exponentially with only one phase distinguishable, it is termed monophasic association, and biphasic association if there are two distinguishable phases (Figure 3.4). Biphasic association usually occurs at high ligate concentrations and it is possible to select whether monophasic or biphasic theoretical curves are to be used for curve fitting. The choice should depend on the quality of the theoretical curve fit. There are various ways to determine this but most often it can be done by visually comparing the two curve fits or by comparing the residual errors of both fits (IAsys, 1995b).

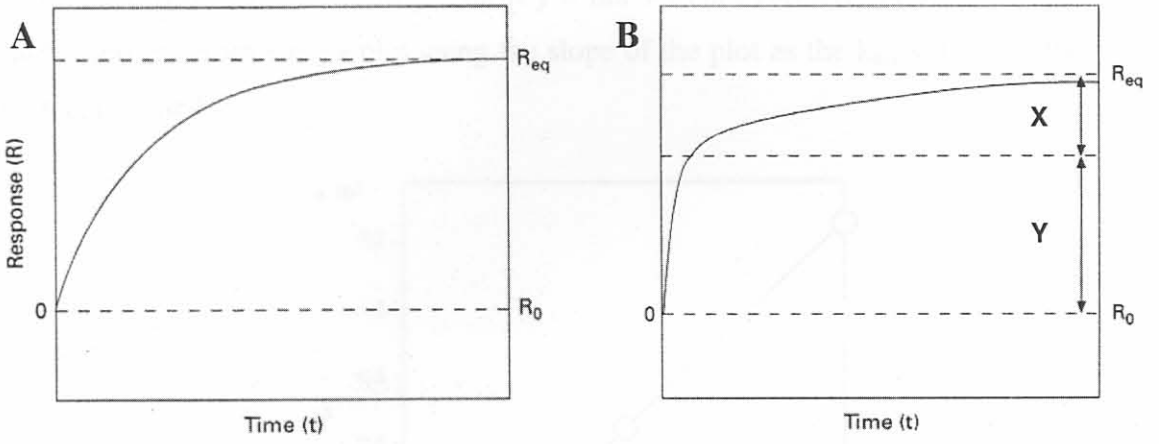

Figure 3.4: Theoretical association curves **(A)** Monophasic. **(B)** Biphasic. R_0 is the initial response, R_{eq} the equilibrium response and X and Y in graph B denotes the extents of the two phases. (Source: IAsys, 1995b)

A certain amount of complex ($[GL]_t$) is formed within time t, and is described by the equation:

$$[GL]_t = [GL]_{eq}\left(1 - e^{-k_{on}t}\right) \tag{3.6}$$

where $[GL]_{eq}$ is the complex concentration at equilibrium and k_{on} is the pseudo first-order rate where:

$$k_{on} = k_{ass}[L] + k_{diss} \tag{3.7}$$

The response of the biosensor (measured in arc seconds) is related to the mass of bound ligate and is given by the equation:

$$R_r = \left(R_{eq} - R_0\right)\left(1 - e^{-k_{on}t}\right) + R_0 \tag{3.8}$$

where R_t is the response at time t, R_0 is the initial response and R_{eq} the response at equilibrium (maximum). The responses in Equation 3.8 are determined experimentally and leave the k_{on} value to be derived for a single concentration. Multiple associations carried out at different concentrations, allow the generation of a plot of k_{on} versus ligate concentration (Figure 3.5). Since k_{on} is dependent on ligate concentration and a linear relationship (Equation 3.7 is in the form y = mx + c) is expected, the k_{ass} and k_{diss} values can be derived from such a plot using the slope of the plot as the k_{ass} value and the y-axis intercept as the k_{diss} value.

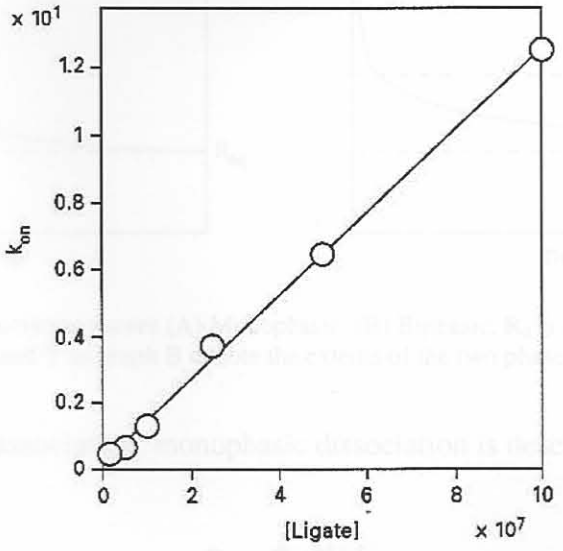

Figure 3.5: Sample plot of k_{on} versus ligate concentration. (Source: IAsys, 1995b)

In biphasic association, the total association is the sum of two individual association processes, each with its own association rate constant:

$$R_t = X\left(1-e^{-k_{on(1)}t}\right)+Y\left(1-e^{-k_{on(2)}t}\right)+R_0 \qquad (3.9)$$

where X and Y are the extents, and $k_{on(1)}$ and $k_{on(2)}$ the apparent on-rates of the two individual and separate phases (*see* Figure 3.4).The slower phase, described by $k_{on(2)}$, contains no easily interpretable data; therefore $k_{on(1)}$ is used to determine k_{ass}. This faster rate constant describes binding events best when dealing with biphasic association.

The K_D value can now be calculated using the derived k_{ass} and k_{diss} constants. However, k_{diss} derived from such a plot (k_{on} vs. [ligate]), is often very close to zero and the error around the value considerable. An improvement of the k_{diss} value can be found by analysing the dissociation data.

3.1.8 Dissociation analysis

Dissociation events can also exhibit monophasic or biphasic characteristics (Figure 3.6).

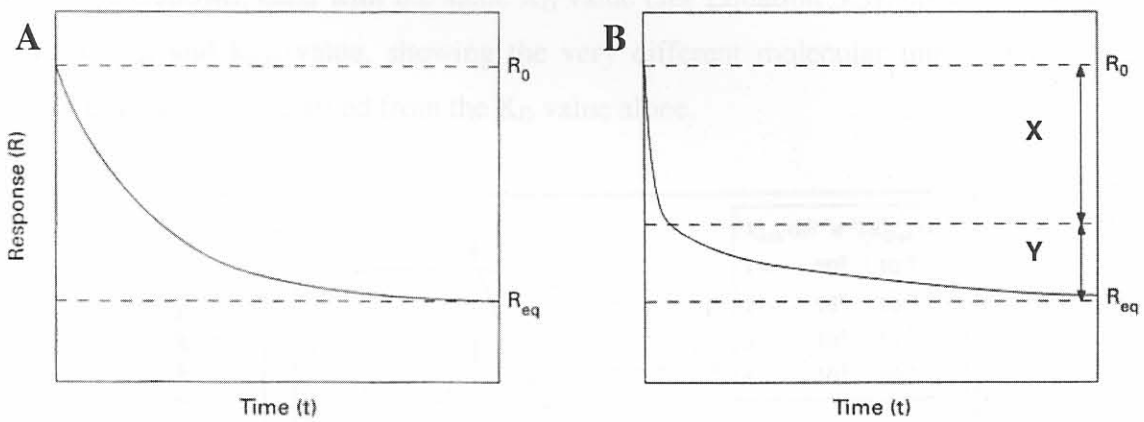

Figure 3.6: Theoretical dissociation curves **(A)** Monophasic. **(B)** Biphasic. R_0 is the initial response, R_{eq} the equilibrium response and X and Y in graph B denote the extents of the two phases. (Source: IAsys, 1995b)

Similar to monophasic association, monophasic dissociation is described by the equation:

$$R_t = R_0 e^{-k_{diss}t} \qquad (3.10)$$

where R_t is the amount of complex at time t, R_0 the initial complex concentration and k_{diss} the dissociation rate constant. Since k_{diss} is independent from ligate concentration, a single dissociation event can be used to determine k_{diss}. However, in practice, several different dissociation curves are compared to determine k_{diss} values.

Like association, dissociation curves may also be biphasic (*see* Figure 3.6) and is then described by:

$$R_t = Xe^{-k_{diss(1)}t} + Ye^{-k_{diss(2)}t} \qquad (3.11)$$

where X and Y are the extents, and $k_{diss(1)}$ and $k_{diss(2)}$ the dissociation rate constants of the two individual and separate phases (*see* Figure 3.6). Once again, the second phase of dissociation most likely contain uninterpretable information; hence $k_{diss(1)}$ is used to determine a value for biphasic dissociations.

The big advantage of the IAsys biosensor method is that the rate constants are also determined as opposed to the equilibrium constants alone, as with other methods. This ability is very important as is illustrated in Figure 3.7. Four different theoretical interaction analyses are shown, each with the same K_D value (*see* Equation 3.5), but each also with a different k_{ass} and k_{diss} value, showing the very different molecular interactions of each system that cannot be derived from the K_D value alone.

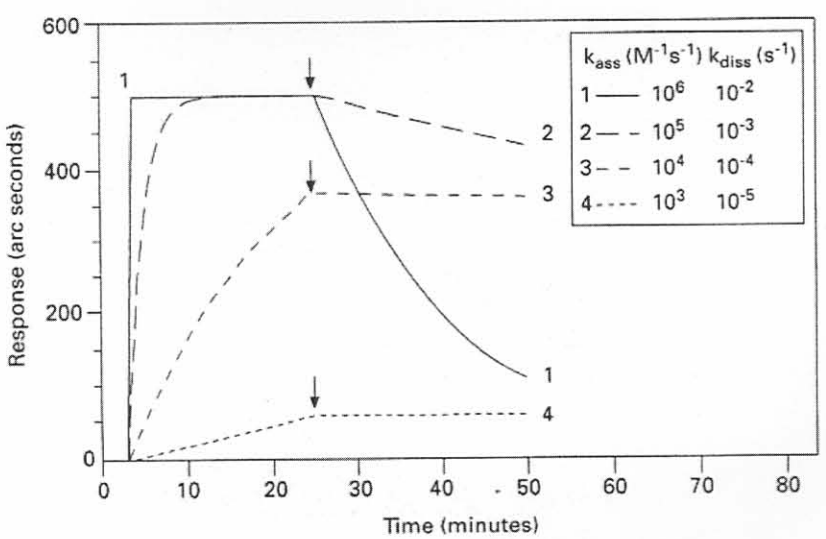

Figure 3.7: Association and dissociation curves of four theoretical molecular interactions. All four interactions have the same equilibrium constant (K_D = 10^{-8}M). The arrows indicate initiation of dissociation. (Source: IAsys, 1995b)

Therefore it can be assumed that the Interaction Analysis system (IAsys) is ideal for the purpose of direct comparisons of affinity of CTxB for G_{M1} as a positive control. Due to the complex composition of patient sera, kinetic parameters cannot be derived for such samples, as they inherently contain contamination by other serum proteins and other molecules that may bind non-specifically.

3.2 Hypothesis

The optimised method for G_{M1}-liposome immobilisation on a biosensor can be applied to determine affinity characteristics of auto-antibodies involved in the Guillain-Barré syndrome

3.3 Aims

- Determining statistically significant dissociation equilibrium constants (K_D) for choleragenoid binding to ganglioside G_{M1}
- Comparing acquired K_D values to published K_D values
- Optimising a method for relating patient serum reaction to G_{M1}-liposomes

3.4 Materials and Methods

3.4.1 Materials

Monosialoganglioside G_{M1} from bovine brain, L-α-phosphatidylcholine, cholera toxin B subunit (CTxB) from *Vibrio cholerae* and bovine serum albumin (BSA) (Fraction V) from lecithin were from Sigma. Sodium chloride, anhydrous disodium hydrogen phosphate and potassium dihydrogen phosphate were from Merck. Analytical quality Tris and EDTA were from Saarchem and general purpose NaN_3 from BDH. Chemically pure KOH and analytical grade HCl were from Saarchem while analytical grade ethanol, chemically pure chloroform and general purpose NaOH were from BDH. Double-distilled deionised water was used for all analytical experiments. Saarchem, BDH and Merck products were supplied by Merck NT Laboratories, Darmstadt, Germany. Sigma products were supplied by Sigma-Aldrich Corp., St. Louis, Missouri, U.S.A.

3.4.2 Biosensors

The IAsys biosensor that was used was situated at the Department of Biochemistry, University of Pretoria, South Africa

Non-derivatised cuvettes were supplied by the biosensor manufacturer, IAsys Affinity Sensors, Cambridge, U.K.

3.4.3 Sera

Guillain-Barré syndrome patient sera (five patients) were a kind gift of Dr. Bart Jacobs, Department of Neurology, Erasmus University Rotterdam, Rotterdam, Netherlands. The sera were all ELISA positive for IgG antibodies and some of them were also IgM positive. All patients provided sera before commencement of treatment of the disease (F102A, F152A, F183A, F226A, F292A) and three of the patients provided sera six months after onset of the disease (F102E, F226F, F292E). Negative control serum was obtained from the investigator. All sera were aliquoted and stored at -70°C in cryovials. For interaction analyses, sera were diluted between 50× and 1000× with the running buffer (*see* par 3.4.4), prior to injection into the cuvette chamber.

To overcome discrepancies between different cuvette cells, the cells were 'calibrated' by injecting 25µl 1000× diluted control serum and allowing it to bind for five minutes in both

cells. Only if the responses in both cells were the same, was the experiment continued, upon which another 25µl serum, either GBS or control, was injected at lower dilutions (100×) into the cells without aspirating.

3.4.4 Modification of running buffer

Cholera toxin B subunit was stored in a Tris-based buffer that could affect calculations due to its difference in refractive index in relation to PBS/AE. Accordingly, G_{M1}-liposomes and CTxB dilutions were carried out with a Tris-based buffer corresponding to the same concentrations as already contained in the CTxB. The Tris buffer contained 50mM Tris, 200mM NaCl, 3mM NaN_3, and 1mM Na_2EDTA (pH=7.5).

3.4.5 Ganglioside-liposome surfaces

Ganglioside-liposomes were prepared and immobilised as described (*see* Chapter 2, par 2.3.17 & 2.3.18). Throughout the experiments 5% G_{M1} (molar %) liposomes were used except where the effect of different concentrations of G_{M1} was tested on CTxB when 2, 5, 10, 14.3 and 20% were used. Regeneration was done as described (*see* Chapter 2, par 2.3.19).

3.4.6 Choleragenoid preparation and dilutions

Due to the biohazardous danger of working with a toxin, it was decided to use the non-toxic pentameric B subunit of CTx or choleragenoid (CTxB), the subunit responsible for binding to G_{M1}.

Five hundred micrograms of CTxB was dissolved in 500µl water, aliquoted into 50µl aliquots and stored at 4°C as prescribed by the suppliers. Upon use, an aliquot was diluted ten times with Tris buffer and then diluted again with Tris buffer to the desired concentrations. For statistical analysis, concentrations of 100-400nM with 50nM increments were prepared and used. This resulted in final CTxB concentrations of 50-200nM with 25nM increments.

3.4.7 Bovine serum albumin preparation and dilutions

It was assumed that BSA had an average molecular mass of 67 000Da. It was dissolved in Tris buffer and diluted to 20, 50, 100, 150 and 200nM with Tris buffer.

3.4.8 Interaction analysis

For the interaction analyses, baseline was maintained with 25µl Tris buffer for at least five minutes while a baseline event was entered in the event log. An association event was initiated upon the addition of 25µl of CTxB, BSA, control or patient serum dilutions. Association continued for five minutes, after which dissociation was initiated by washing five times with 60µl Tris buffer. Due to the high affinity of CTxB for G_{M1}-liposome surfaces, almost no dissociation occurred and derived dissociation rate constants were uninterpretable. Dissociation rate constants were therefore derived from the association data. Accordingly, no dissociations were done with CTxB and regeneration was done directly after associations.

3.4.9 FASTfit analysis

Kinetic parameters were determined using FASTfit software (IAsys, 1996). Baseline, association and dissociation regions were selected so that all baseline, association and dissociation regions contained the same number of data points. At least 70% of association and dissociation curves were selected. Baselines were selected only during stable time frames. Every interaction analysis's parameters were calculated and fitted to theoretical mono- and biphasic kinetic curves and the best curve fit selected. Plots of $k_{on(1)}$ versus ligate concentration were obtained and used to derive the association and dissociation rate constants (k_{ass} and k_{diss}). The dissociation equilibrium constant, K_D, was accordingly calculated from these two rate constants.

3.4.10 Statistical analysis

To determine the best average kinetic parameters, three different sets of CTxB associations were done with the concentrations indicated (*see* par 3.4.6). The three sets were done on three different cuvettes. The experiment was duplicated in each cell and each cell represented a separate experiment. Consequently six different sets of data were used to determine the average $k_{on(1)}$ values. These were plotted against the final ligate (CTxB) concentration. Standard deviations of the average values were calculated and indicated. The slope and y-axis intercept were determined from a linear fit through the data points and these were used to derive the rate constants that were, in turn, used to determine a dissociation equilibrium constant.

3.5 Results

3.5.1 Suitability of cholera toxin as positive control

An important modification to the method when using CTxB was tested: CTxB is stored with a ready buffer mixture containing Tris, NaCl, NaN_3 and EDTA. Reconstituting the CTxB as prescribed by the manufacturers would result in a different buffer concentration as used for patient serum interaction analyses. As already mentioned (*see* Chapter 2 par 2.1.2.6), it is important that the buffer used for obtaining baselines in the biosensor be the same buffer used for preparing and diluting serum samples. The effect of the CTxB Tris-based buffer was tested and it was found that there are no significant effects on G_{M1}-liposome immobilisations, washings or regenerations (not shown).

In a preliminary experiment, four different concentrations of CTxB were used for interaction analysis on a surface created with liposomes containing 9PC:1G_{M1} (molar ratio) as described in Chapter 2 (*see* par 2.3.18), following the method as described in Annexure 2. The responses due to the different CTxB concentrations are shown in Figure 3.8.

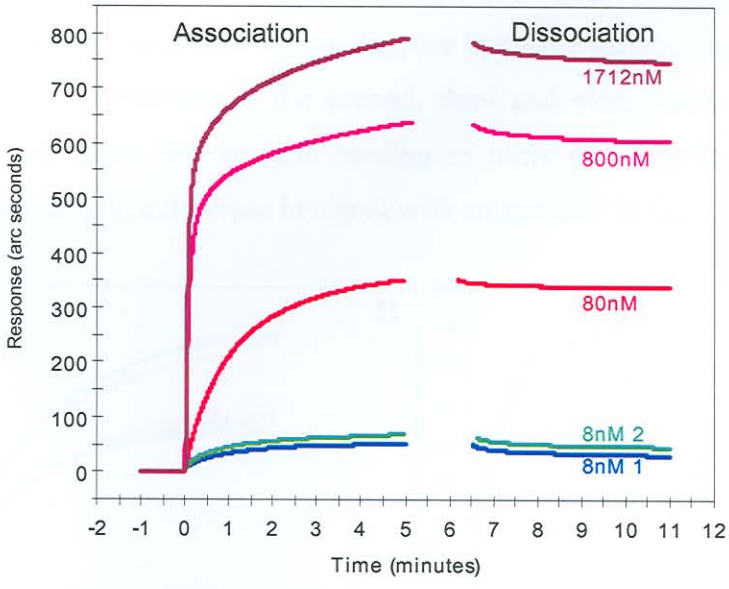

Figure 3.8: A FASTplot overlay showing the association and dissociation of different concentrations of CTxB (final concentrations) on an immobilised G_{M1}-liposome surface as obtained with an IAsys biosensor. The responses of the two interactions carried out with 8nM CTxB were almost identical and the other responses correlated with the CTxB concentration.

Two separate interaction analyses were done with the 8nM CTxB concentration (final concentration) to determine the reproducibility of the experiment. Both analyses gave the same low response as expected. Therefore, the use of CTxB as a positive control for GBS

patient serum antibodies against a G_{M1}-liposome biosensor surface was considered suitable.

3.5.2 Effect of ganglioside concentration in ganglioside-liposomes on choleragenoid binding kinetics

To confirm the best concentration of G_{M1} to be used in G_{M1}-liposomes, a fixed concentration of CTxB (171nM) was injected over immobilised G_{M1}-liposome layers containing different amounts of G_{M1} ranging from 0-20% (molar percentage). As shown in Figure 3.8, it was observed that there was very little dissociation of CTxB from the surface and even some increase in signal, possibly due to re-association (not shown). Re-association of CTxB with G_{M1} on the surface is likely when loosely bound CTxB dissociates, thereby freeing G_{M1} molecules for association with other CTxB molecules with higher avidity. The result is a net increase in the signal during dissociation analyses.

Interestingly, a higher G_{M1} concentration did not correlate to the better binding of CTxB (Figure 3.9A). This could be explained by the avidity effect of the pentameric CTxB subunit. Having more G_{M1} available for binding, the liposome surface might bend a little to allow binding of G_{M1} molecules to the second, third and even fourth monomer of the subunit. This would allow less specific binding of other CTxB subunits due to steric hindrance and accordingly, a decrease in signal with an increase in G_{M1} concentration.

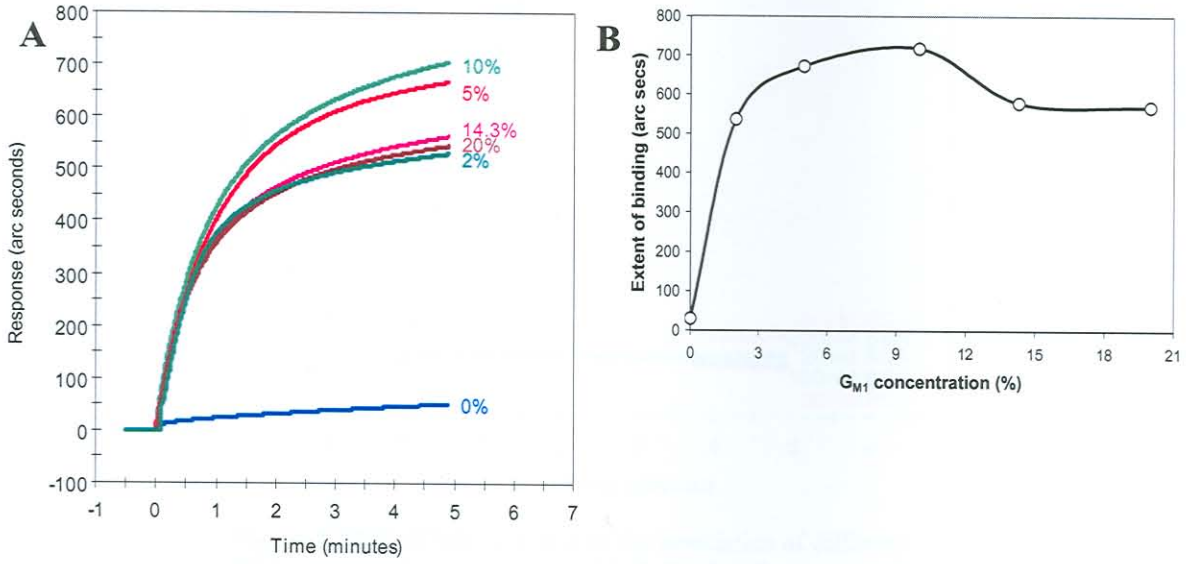

Figure 3.9: Association of 171nM CTxB to different G_{M1} concentrations on immobilised G_{M1}-liposomes. **(A)** FASTplot overlays. **(B)** Graph of G_{M1} percentage versus the total response. Percentages indicate the G_{M1} mole percentage in the immobilised liposomes.

At G_{M1} concentrations of 2%, the least binding of CTxB took place. The amount of CTxB that bound to the G_{M1}-liposome surface, appeared to be directly proportional to the G_{M1} concentration (Figure 3.9B), but reached a peak at about 10% before decreasing again to a lower plateau region. As expected, virtually no binding of CTxB to empty liposomes (pure PC) was observed. It was therefore concluded that molar concentrations higher than 5% G_{M1} in the liposomes had no significant advantage on CTxB binding, while G_{M1} concentrations at lower than 5%, evoked suboptinal binding of CTxB. Further experiments were continued with 5% G_{M1}-liposomes only.

3.5.3 Specificity of choleragenoid for ganglioside G_{M1}

It was necessary to test the possibility that non-specific association might create artefacts during interaction analyses of CTxB binding to G_{M1}-liposomes. Therefore, a 5% G_{M1}-liposome surface was immobilised and different concentrations of a non-specific protein (BSA) were injected as well as 100nM CTxB. As expected, very little BSA bound to the G_{M1}-liposome surface, even at twice the molar concentration of CTxB (Figure 3.10).

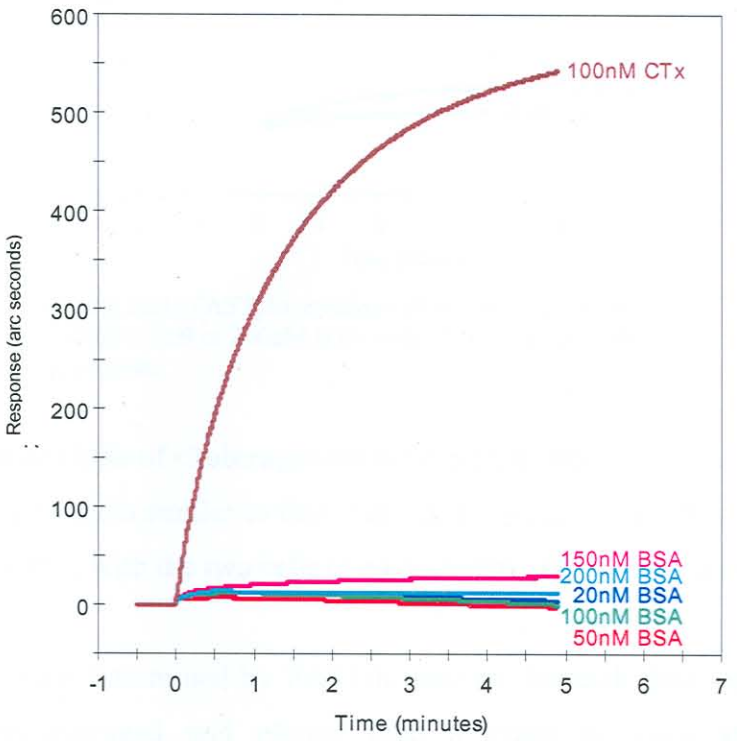

Figure 3.10: FASTplot overlays of the association of different BSA concentrations and 100nM CTxB to a G_{M1}-liposome surface measured with an IAsys biosensor.

Consequently, it was expected that non-specific interactions would have a negligible effect on the interaction analysis profiles.

To confirm the specificity of CTxB for G_{M1}, identical concentrations (200nM) of both CTxB and BSA were prepared and injected separately over a 5% G_{M1}-liposome or PC-liposome surface (Figure 3.11). Results indicated that the only high response was when CTxB was injected over the G_{M1}-liposome surface. When CTxB was injected over a PC-liposome surface, a negligible amount bound and BSA associated only negligibly to either surfaces, indicating that the specific binding of CTxB to G_{M1} can be measured quantitatively on the IAsys biosensor using immobilised G_{M1}-liposomes.

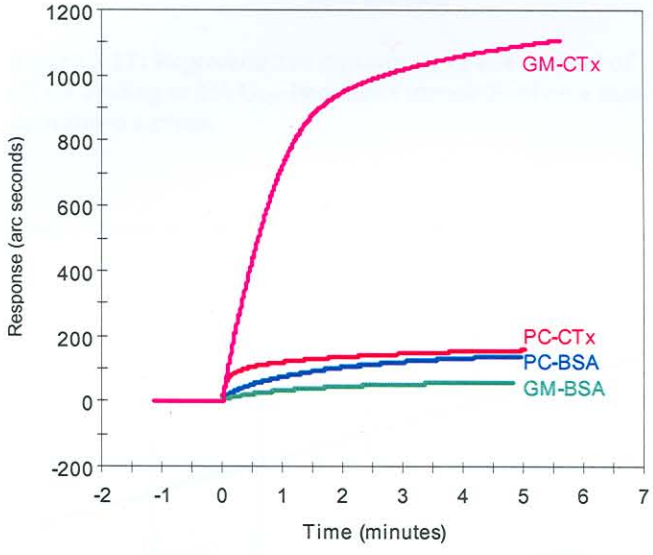

Figure 3.11: FASTplot overlays of the associations of 200nM CTxB or 200nM BSA with 5% G_{M1}- or pure PC-liposomes.

3.5.4 Statistical analysis of choleragenoid binding kinetics

Six sets of binding kinetics similar to that illustrated in Figure 3.12, were generated using three different cuvettes, with the two cells of each cuvette representing a separate data set.

The $k_{on(1)}$ values were determined by FASTfit analysis for each data set separately. The values were then averaged and plotted onto a graph of $k_{on(1)}$ versus the ligate concentrations (Figure 3.13).

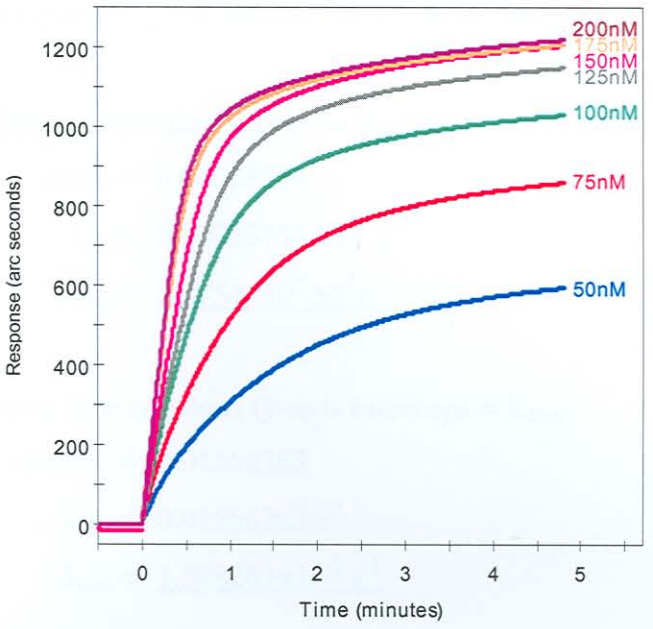

Figure 3.12: Representative sensorgram of one data set of CTxB binding to 5% G_{M1}-liposomes immobilised on a non-derivatised surface.

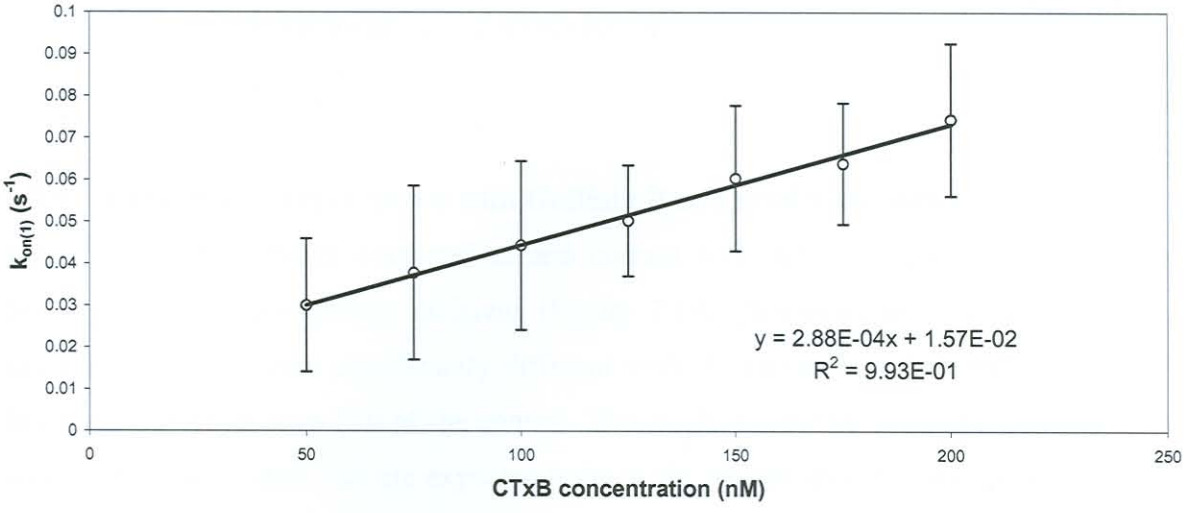

Figure 3.13: Plot of the first order apparent on-rate ($k_{on(1)}$) versus ligate concentration for the binding of CTxB to a 5% G_{M1}-liposome surface. The linear fit through the data points is illustrated and the slope, intercept and quality of the fit, expressed as an R^2 value, is shown.

The slope and y-axis intercept of the linear fit were used to calculate the association and dissociation rate constants respectively (*see* Equation 3.7):

Linear fit equation: $y = 0.00028754x + 0.01568263$

Association rate constant (slope = k_{ass})

slope = 0.00028754

$\therefore k_{ass} = 0.00028754\ nM^{-1}s^{-1}$

$\therefore k_{ass} = \underline{2.8754\times10^{5}\ M^{-1}s^{-1}}$

Dissociation rate constant (y-axis intercept = k_{diss})

y-axis intercept = 0.01568263

$\therefore k_{diss} = 0.01568263\ s^{-1}$

$\therefore k_{diss} = \underline{1.568263\times10^{-2}\ s^{-1}}$

Using Equation 3.5, these rate constants can be used to determine the K_D value:

$K_D = k_{diss} / k_{ass}$

$= 1.568263\times10^{-2}\ s^{-1} / 2.8754\times10^{5}\ M^{-1}s^{-1}$

$= \underline{5.45\times10^{-8}\ M}$

3.5.5 Exploratory experiments with Guillain-Barré syndrome patient sera

Initial serial experiments with patient and control sera indicated that the capacities of binding are not significantly different (Figure 3.14). However, the slopes of the two association events were significantly different with the patient's initial association curve being much steeper than that of the control. This might be due to the higher percentage of specific G_{M1} antibodies that are expected to be in the patient sera. Serial experiments were carried out in preference to parallel experiments with the patient and control sera in either of the two cuvette cells, due to earlier observations that the two cells of one cuvette sometimes do not provide the same response to the same solutions (*see* Chapter 2, Table 2.1) and cannot be compared directly.

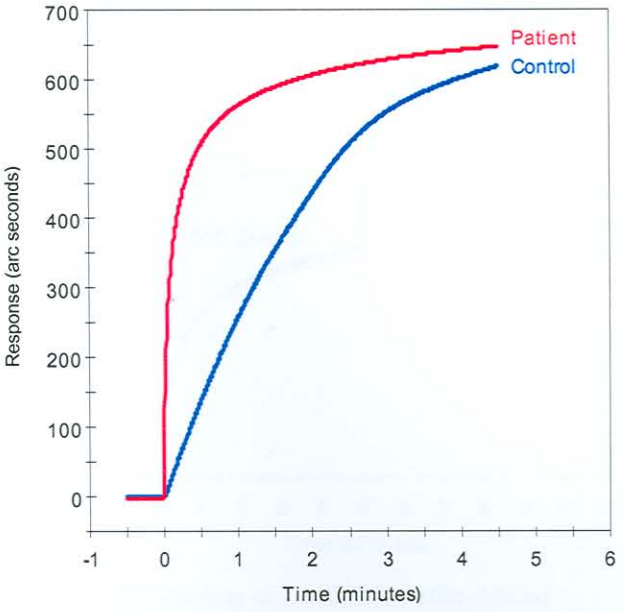

Figure 3.14: Binding of 1:50 Tris-buffer-diluted control and patient (F102A) sera to a 5% G_{M1}-liposome surface. The sensorgram is representative of two serial experiments in the same cell.

An improvement on this method was suggested where control serum is used at a very low concentration to calibrate the two cells. Typically, a sample volume of 1000× diluted control serum is added to both cells after liposome immobilisation and only if the response to this addition is identical in the two cells, a further addition is made with less diluted patient and control sera in the respective control and test cells.

In Figure 3.15 it is shown that initial non-specific binding of control serum was identical in both cells but the difference between the subsequent patient and control sera added on top of the 'calibration binding' was significantly different. The control and test cells were also alternated to determine if the higher binding of the patient serum was not artefactual. Even in alternated cells the patient sera showed significantly higher binding compared to the control serum (not shown). Due to the heterogeneity of sera and the required calibration step on the biosensor, it may prove difficult to quantify specific antibody binding directly from serum using the biosensor. However, the biosensor technique might be employed to semi-quantitatively distinguish among patients using the calibration bindings to determine a ratio of binding that may be compared among patient and control sera.

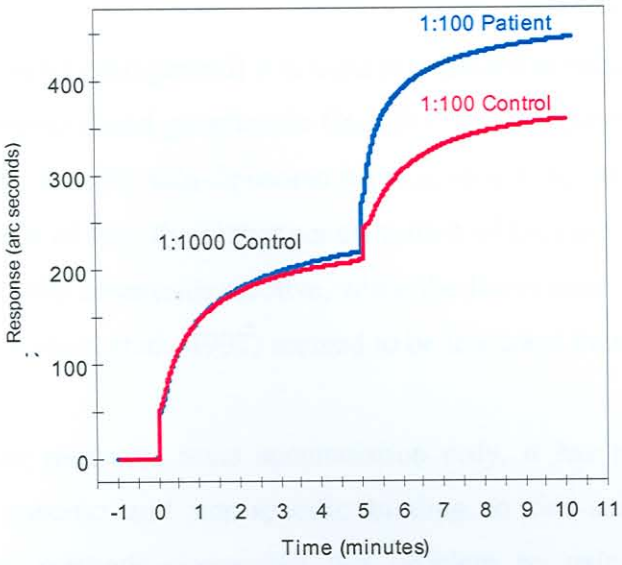

Figure 3.15: Binding of 1:100 Tris-buffer-diluted control and patient sera (F102A) after calibration with 1:1000 Tris-buffer-diluted control serum to a 5% G_{M1}-liposome surface.

It was not yet possible to calculate absolute K_D values for the binding of patient and control sera to immobilised G_{M1}-liposome surfaces, as was done with the CTxB (positive control) binding to the same surfaces. This is primarily due to the fact that the absolute antibody concentrations in the sera were unknown and variable among patients. Furthermore, there are antibodies against other types of gangliosides like G_{A1} and G_{D1a} that would result in complex cross-reactivity patterns.There is also the different avidities to consider between the different antibody isotypes present in all human sera.

For further characterisation it would be necessary to isolate specific isotypes with singular specificities as Ab1, before they can be immobilised and Ab2 antibodies against the Ab1 antibodies characterised. It would also be necessary to increase the number of control sera to produce a statistically significant background against which the different antibody sets could be measured.

3.6 Discussion

Cholera toxin B subunit (choleragenoid) was used to standardise conditions for the specific binding of ligate to immobilised ganglioside G_{M1}. Preliminary experiments indicated that CTxB bound optimally to a 5% G_{M1}-liposome surface, similar to other studies (Kuziemko *et al.*, 1996). In the light of this, the higher concentration of G_{M1} used by Athanassopoulou *et al.* (1999) was probably counter-productive, while the lower concentrations of G_{M1} used by other studies (MacKenzie *et al.*, 1997) seemed to be less ideal than 5%.

Because the biosensor measures mass accumulation only, it has no way of telling the difference between specific and non-specific binding to the surface. Enzyme-linked immunosorbent assay methods circumvent this problem by using a specific reporter antibody that recognises bound antibody specifically. A disadvantage of ELISA is that it is unable to measure low affinity antibodies. In addition, it cannot determine rate constants as it measures only end-point equilibrium data, compared to real-time measurements with the biosensor. Results presented here conclusively show that CTxB binds specifically to G_{M1} and that it is not necessary to confirm this with ELISA techniques, as may have been desirable with antibody binding.

The K_D value for binding of CTxB to G_{M1} under the optimised conditions was determined to be 5.45×10^{-8}M. Other laboratories have also determined K_D values for the binding of CTxB to G_{M1} using various biosensors or isothermal titration calorimetry (ITC). Their results are summarised in Table 3.3:

Table 3.3: Comparison of K_D values obtained by different laboratories

Method	G_{M1} molar %	k_{ass} ($M^{-1}s^{-1}$)	K_D (M)	Reference
IAsys biosensor, lipid monolayer on hydrophobic cuvettes	25	N.A.	3.00×10^{-8}	(Athanassopoulou *et al.*, 1999)
BIAcore biosensor, lipid bilayers on non-derivatised chips	5	1.27×10^{6}	4.61×10^{-12}	(Kuziemko *et al.*, 1996)
BIAcore biosensor, LPS containing lipid bilayer captured by IgG immobilised on CMD chip	2	6.2×10^{5}	7.3×10^{-10}	(MacKenzie *et al.*, 1997)
Isothermal titration calorimetry	2	N.A.	1.37×10^{-8}	(Masserini *et al.*, 1992)
IAsys biosensor, lipid bilayers on non-derivatised cuvettes	5	2.88×10^{5}	5.45×10^{-8}	This study

N.A. – Not available

The K_D value determined in this study, correlates very well with the two published values that were also determined using an IAsys biosensor. Two of the values in Table 3.3 do not correlate well with IAsys results. In the first instance by Kuziemko *et al.*, (1996), who determined a K_D of 4.61×10^{-12}M using the BIAcore biosensor, the authors used $k_{diss(2)}$ instead of $k_{diss(1)}$ to determine the K_D which they claim to be a result of non-specific interactions. However, they have determined $k_{diss(1)}$ as well, and when this value is used instead of the $k_{diss(2)}$, a K_D value of 7.03×10^{-9} M is obtained, much closer to the published values of Athanassopoulou *et al.* (1999) and Masserini *et al.* (1992). In the second instance (MacKenzie *et al.*, 1997) the authors used a 2% molar concentration of G_{M1} in their lipid bilayer on the BIAcore instrument as well as smaller concentrations of CTxB. At these lower concentrations the pentavalent binding capability of CTxB is probably better determined. As a consequence, CTxB will dissociate slower, leading to a higher k_{diss} value and, in turn, a lower calculated K_D value.

The ITC of Masserini *et al.* (1992) is probably the best technique to determine kinetic parameters because it measures these parameters in free solution while ligand-ligate pairs are in their native states. This is opposed to the biosensor technique that measures binding to immobilised ligand under very different concentration ranges. This is in contrast to ITC where the molecules are in similar concentration ranges and parameters determined from interactions in free solutions (Masserini *et al.*, 1992; Jelesarov & Bosshard, 1999; Menze *et al.*, 2001). Therefore it can be considered to be the standard against which to measure values obtained by other methods. A possible disadvantage is that affinity constants are calculated from the measured heat that is released during a molecular recognition reaction. Unless the recognition mechanism between the ligand-ligate pair is very simple and defined, the total measured heat is a global heat – that includes the energy of chemical transformation following the recognition interactions, should this be a result of the interaction. The K_D determined in this study, where no chemical transformation during recognition is anticipated, does not compare badly to the ITC results of Masserini *et al.* (1992).

The K_D value obtained by Athanassopoulou *et al.* (1999), also using the IAsys biosensor, is in very good agreement with the value obtained here. The authors used a much higher G_{M1} concentration and also used a different method of immobilising the G_{M1} molecules. Exploratory experiments using the same method employed by these authors were

problematic as it was impossible to maintain stable baselines when working with hydrophobic cuvettes (not shown). The method of immobilising G_{M1}-liposomes on a non-derivatised surface used in the current study is not only more reliable, but also mirrors the normal molecular and physiological environments of G_{M1} better than when G_{M1} is immobilised on a hydrophobic cuvette. During such an immobilisation, G_{M1} is subjected to relatively harsh conditions with iso-propanol.

The method employed by Mackenzie *et al.* (1997) on the BIAcore biosensor may provide a more interesting perspective on CTxB binding kinetics and subsequent affinity and avidity measurements, as a much slower dissociation rate is observed with the lower concentrations of both CTxB and G_{M1} employed by them. Inspection of the association rate constants of two of these studies (Kuziemko *et al.* (1996): 1.27×10^{6} $M^{-1}s^{-1}$ and Mackenzie *et al.* (1997): 6.2×10^{5} $M^{-1}s^{-1}$) indicate that the association rate constant, k_{ass}, calculated by our method (2.88×10^{5} $M^{-1}s^{-1}$) is within one logarithmic unit of the published BIAcore values (Table 3.3). The other two studies (Masserini *et al.*, 1992; Athanassopoulou *et al.*, 1999) did not indicate their k_{ass} values for comparison. In the Introduction of this Chapter the desirability to consider not only the equilibrium constant on its own, but also the rate constants was emphasised, as is evident from the results obtained here when comparing patient and healthy control sera. It was determined that both sera bound with the same capacity, but not the same vigour.

Standard deviations for the apparent on-rate versus ligate concentration plot determined here, are relatively large despite the linear regression fit being very accurate. The main reason for this might be that three different cuvettes were used to get a value closer to the average.

In conclusion, the method for measuring and comparing the anti-G_{M1}-antibody binding kinetics of GBS patient sera at different stages of the disease and especially after recovery, using the method described here, seems to be entirely feasible. This should corroborate the studies by Lundkvist *et al.* (1993) and provide better insight for studying the idiotype network's role in GBS.

CHAPTER 4
CONCLUDING DISCUSSION

Diseases are characterised by the interaction of molecules in one way or another, whether the disease occurs in humans, animals or plants. At least one of these molecules will be a macromolecule like protein or DNA. During poisoning, the responsible toxin usually resembles the normal substrate or ligand and subsequently binds and inactivates the macromolecular target. Infectious diseases are normally precipitated by the expression of a macromolecule on the surface of a pathogen that binds to a host macromolecular target. In auto-immune diseases the body produces anti-self immunoglobulins that recognize and bind to macromolecules on normal cells and subsequently cause damage. This dissertation concerns the sophisticated biomolecular interaction analysis (BIA) biosensor technology with which the interaction of molecules with one another can be measured if and when they take place. The dissertation demonstrates the particular advantages of this technique to better our understanding of the interactions that take place in the pathogenesis of two diseases, an infectious disease (tuberculosis) and an auto-immune disease (Guillain-Barré syndrome)

One of the key molecular interactions that take place during the pathogenesis of tuberculosis (TB) is the recognition of *Mycobacterium tuberculosis* surface antigens by the host's immune cells and immunoglobulins. Vaccinating new-born individuals with *M. bovis* Bacillus Calmette Guerrin (BCG) effectively prevents infection, but complicates diagnosis of TB, since antibodies against BCG cross-react with purified protein derivative (PPD) used world-wide in skin-tests for TB diagnosis (Mustafa, 2002). Human immune deficiency virus (HIV) co-infection also hampers TB diagnosis as HIV patients have almost immeasurably low titres for antibodies against these protein antigens. However, antibodies against waxes (mycolic acids) on the surface of *Mycobacterium* species are still produced in measurable quantities, even in immunocompromised HIV positive patients (Schleicher *et al.*, 2002). The interaction of these mycolic acids (MA) with anti-MA antibodies may be exploited for a more reliable diagnostic technique. Unfortunately these antibodies are of low affinity and are easily washed away during enzyme-linked immunosorbent assay wash steps. Lacking wash steps, a biosensor is able to measure such low affinity antibodies in real-time. J.A. Verschoor and D.G.R. Siko

adopted this technique for TB serodiagnosis by immobilizing MA contained in liposomes on non-derivatised surfaces of a cuvette for measurement in a resonant mirror biosensor (Siko, 2002). This dissertation shows how this technique was optimised so that interactions between closely related structures can be measured and used to discriminate between them. This resolution is essential since MA of *M. tuberculosis* consist of three closely related subclasses that have significantly different binding properties to antibodies (Pan *et al.*, 1999). The interactions of these individual MA subclasses with host immunoglobulins can be particularly helpful to determine the specific mechanism of infection. It has been suggested that one of these subclasses (methoxy-MA) mimics the structure of cholesterol, abundantly found in all animal cell membranes. The most important evidence to support this hypothesis was obtained with direct interaction analysis of cholesterol-containing liposomes with MA-containing liposomes on the biosensor (Siko, 2002). Since the presence of the oxygenated MA (keto- and methoxy-MA) are associated with virulence (Pan *et al.*, 1999), the understanding of how these molecules interact, may be crucial for understanding virulence of, and immunity to TB.

Before the individual subclasses of MA can be compared, they must be separated. In this study it was shown how this separation could be achieved using thin layer chromatography. For proper separation the MA had to have its carboxylic acid group methylated. This methylation might influence its immunogenicity and has consequences for molecular recognition by antibodies in the biosensor method. Structures of the methylated and separated compounds wait to be determined by matrix-assisted laser desorption/ionisation time-of-flight mass spectrometry (MALDI-TOF MS), a better technology than EI-MS for this purpose (Laval *et al.*, 2001). It is expected that if preparatively separated MA are immobilized using the novel biosensor method, a difference in affinity of binding between antibodies and the different subclasses of MA will be demonstrated much more clearly than was demonstrated by Pan *et al.*, (1999), who used ELISA for this purpose.

It was shown here that the novel method of immobilizing liposomes on a non-derivatised cuvette surface is problematic due to two main shortcomings. The first is that the two cells of the binary cuvette are often not equally responsive to mass accumulation from identical solutions. Calibrating the cells with a dilute serum solution prior to the actual measurement has been shown to overcome this problem (Thanyane, 2003), but it is expected that

automated pipetting may solve the problem to a large extent. The second is that, despite the cuvette surfaces being made of hafnium-oxide, a corrosion resistant compound, the surface of these cuvettes deteriorate during serial cycles of liposome immobilization, interaction analysis and regeneration. Cuvettes may last for up to forty regenerations but usually last for less than twenty (not shown). The integrity of cuvette surfaces is measured by the quality of the resonance scan, which was monitored throughout experiments, and was used to determine when a cuvette has become defect or exhausted. Since similar studies reported that up to fifty regenerations are possible with similar cuvettes (Altin *et al.*, 2001), the current number of regenerations possible is less than ideal and adds to the expensiveness of the technique. The harsh potassium hydroxide regeneration step has been blamed for this deterioration but was found to be a crucial step in the regeneration of the cuvette surface. It is expected that the re-design of the biosensor configuration to especially suit TB serodiagnosis may result in cuvettes that are either cheaper or less prone to deterioration.

Future work aims at using the biosensor to measure and calculate the quantitative binding properties of TB patient antibodies to the MA subclasses and the binding properties of the MA subclasses with cholesterol. The importance of cholesterol in the uptake of *M. tuberculosis* by macrophages has been illustrated by Gatfield & Pieters (2000). They indicated that cholesterol depleted macrophages were inhibited from infection by *M. tuberculosis* and also that *M. tuberculosis* binds cholesterol directly. Since complement receptor type 3 (CR-3) is responsible for receptor-mediated uptake of *M. tuberculosis* (Cywes *et al.*, 1997) and its activity mediated by the presence or absence of cholesterol, it was further suggested that the accumulation of cholesterol into cholesterol-rich microdomains, or lipid rafts, may be crucial to *M. tuberculosis*'s infectivity (Gatfield & Pieters, 2000). Many protein receptors are located in lipid rafts (Stulnig *et al.*, 2001) and their co-localisation with the lipid rafts is crucial for function (Simons & Toomre, 2000). Lipid rafts have been implicated in immune cell activation (Cherukuri *et al.*, 2001) and it is known that they play a role in the infectivity of HIV-1 (Campbell *et al.*, 2001). The importance of determining the molecular interaction affinities and mechanisms of the different MA-subclasses with cholesterol and their different antibodies, can therefore not be overstated.

Auto-immune diseases like the Guillain-Barré syndrome (GBS) are triggered by a specific kind of molecular interaction manifested by molecular mimicry (Moran, 1997). Guillain-

Barré syndrome is most commonly triggered by prior infections with *Campylobacter jejuni* (Winer *et al.*, 1988; Jacobs *et al.*, 1998) because the bacterial surface lipopolysaccharides (LPS) closely resemble gangliosides in the membranes of the host's peripheral nerves. This leads to cross-reaction of anti-LPS antibodies with the gangliosides, triggering the onset of GBS. In this study it was shown that the interaction of the antibodies with these gangliosides (glycolipids) could be followed with a biosensor method very similar to that used for determining the interactions of anti-MA antibodies with MA in TB patients. Although both gangliosides and MAs are lipids, gangliosides have a carbohydrate moiety that necessitated a different biosensor technique to measure the interaction between gangliosides and antibodies. It was discovered that the surface activation with a cationic detergent, cetyl pyridinium chloride, used for immobilisation of MA-liposomes, is not required when coating with G_{M1}-liposomes. This was explained by the absence of the long hydrophobic MA tails protruding from the MA-liposomes as opposed to the presence of the hydrophilic sugars coating the surfaces of G_{M1}-liposomes. Ganglioside-liposomes could spontaneously associate with the polar surface of non-derivatised cuvettes. Blocking of hydrophobic sites with saponin to prevent non-specific interactions was determined to be redundant as well. This was based on the following: the cationic detergent enables MA-liposomes to build up in layers on the cuvette surface, probably by insertion of the hydrophobic detergent tail in the liposome membrane. These non-uniform, unblocked surfaces are vulnerable to non-specific associations. If the surfaces are blocked, more specific binding can be measured. In G_{M1}-liposomes however, it is expected that the liposomes form a uniform bilayer on the surface. This theory is supported by observations with atomic force microscopy where it was shown that liposomes spontaneously flatten on a smooth glass surface, break open, slide over the bottom layer and fill available space until a uniform bilayer is created (Fisher & Tjärnhage, 2000; Deleu *et al.*, 2001). Excess liposomes are washed away. It is further supported by observations by Altin *et al.* (2001) who included a dilute sodium hydroxide washing step to lyse unbound liposomes for easy aspiration. Athanassopoulou *et al.* (1999) also noted that blocking of heterogeneous lipid bilayers containing G_{M1} and PC, formed on a hydrophobic surface, is unnecessary.

Infections other than that of *C. jejuni* or immunocompromising events like surgery or vaccinations may also trigger GBS (Ang, 2001). If the onset of GBS is so well explained by molecular mimicry between LPS and gangliosides, how can other infections or events trigger the disease? It is believed that the adaptive immune system constitutes a delicate

equilibrium of idiotypes (Bona, 1987). A disturbance in this so-called idiotype network causes an imbalance, which the body will try to correct. Failure to do so may have significant effects on the entire immune system. The disturbed idiotype network may then provide the pathway towards susceptibility to various infections and to immune compromise, triggering the onset of GBS or other auto-immune diseases. Idiotypes of complementary and opposing sets of antibodies in the idiotype network will be closely related and affinities for the same idiotype or antigen may be very similar. Although attempts have been made to give structure to the idiotype network concept (Perelson, 1989; Rossi *et al.*, 1989; Kazatchkine & Coutinho, 1993), it is not easily generalised and remains poorly understood. The biosensor technique developed and optimised in this study may be ideally suited to distinguish between closely related antibodies and provide crucial detail of how the idiotype network functions. To distinguish between idiotypes it is necessary that differences in affinity between antibodies can be measured. Using cholera toxin B subunit, a natural ligand for G_{M1} as a receptor, it was demonstrated that the affinity constant derived from the IAsys biosensor method performed here, correlated well with affinity constants generated by other biosensor methods (Athanassopoulou *et al.*, 1999) as well as isothermal calorimetry studies (Masserini *et al.*, 1992).

Initial studies with control and GBS patient sera showed sensorgrams for binding to G_{M1}. Prior calibration of the two cells in the IAsys cuvette by association analysis of diluted control serum to the immobilized G_{M1}-liposome coat allowed the semi-quantitative characterization of the sera. The technique was shown to be amenable to determine the anti-G_{M1} antibody activity in GBS patients at the peak of the disease and after their recovery. Comparing antibody levels during different stages of the disease may allow the elucidation of some of the complexities of the regulation of the idiotype network. If these idiotype antibodies (Ab1) can be isolated and immobilised on the biosensor cuvette surface and then used to assess affinities of the anti-Id antibodies (Ab2), even more of the idiotype network may be understood. The biosensor is currently the only technique that can be applied to elucidate Id-anti-Id interactions without the need for labelling one of the ligands.

It has already been shown that idiotypes can be immobilized on biosensor surfaces and the affinities of anti-Id antibodies against this accurately determined (Haimovich *et al.*, 1998). Understanding the idiotype network better should enable us to understand how seemingly unrelated infections and events can precipitate an auto-immune disease like GBS. It might

also be the explanation for observations that anti-HIV-1 antibodies increase HIV-1 infection of monocytes and lymphocytes (Robinson *et al.*, 1988) and that cross-reactivity exists between lymphocyte antigens and Id-anti-Id immune complexes (Root-Bernstein, 1995). Süsal *et al.* (1996) has already hinted at the auto-immune characteristics of acquired immune deficiency syndrome (AIDS) by demonstrating how different opposing sets of idiotypes or mimics of idiotypes can disturb the idiotype network. This has serious consequences for current Phase III clinical trials on vaccines based on a surface antigen like gp120 (Johnston, 2003). Introducing a self-antigen to generate antibody proliferation, the standard aim of a vaccination, may disturb the sensitive idiotype network equilibrium of immunocompromised individuals in such a way that it cannot recover. In the case of AIDS vaccines, where the antigen mimics MHC-structure of the host, this may lead to the progression to full-blown AIDS. Using GBS as a model, a better understanding of HIV/AIDS and other auto-immune diseases, in the context of the idiotype network, may lead to novel therapies to substitute or supplement existing drugs.

The expectation of the discovery of fine-specificity between antibodies and lipid antigens in auto-immune aspects of infectious diseases has been brought close to realisation with this study. Cross reactivity of antibodies between MA and cholesterol in TB, and ganglioside specificity of auto-antibodies in GBS can be characterised by biomolecular interaction analysis with biosensor technology. Immobilisation methods for lipid antigens and characterisation of antibody binding to these ligands have been amply demonstrated. The next focus level will be the characterisation of anti-MA antibodies to the individual members of MA subclasses and relating the binding properties of anti-G_{M1} and anti-anti-G_{M1} antibodies at different stages of GBS. This has all the potential of extending the current naive understanding of auto-immunity in infectious diseases to a universal comprehension of Id-anti-Id relationships. This may launch a new appreciation of the value of idiotype vaccination in seemingly incurable diseases – even a cure for AIDS.

SUMMARY

Biomolecular interactions form the basis of virtually all disease mechanisms in one way or another. Some of these interactions, especially protein-protein interactions are well characterised. Lipid-ligand protein-receptor interactions are far less understood, but this study shows how a resonant mirror biosensor can be employed to analyse such interactions using two examples. These lipid-protein interactions are also characterised by the manifestation of molecular mimicry between certain molecules.

In the first example, tuberculosis lipid antigens (mycolic acids) were immobilised on the biosensor surface using a cationic detergent. It is shown how these mycolic acids, or ligands, can be separated into their different subclasses using thin layer chromatography so that individual subclasses may be immobilised on the biosensor surface. The biosensor technique then allows discriminating between the different binding affinities of the subclasses with their relevant serum antibodies. In addition, it allows the characterisation of the relationship of the mycolic acids and their auto-antibodies with a very important structural mimic of keto-mycolic acid, namely cholesterol.

For the second example it is shown that the method optimised for the tuberculosis antigens is not generic and how this method had to be adapted for the use of Guillain-Barré syndrome glycolipid antigens: gangliosides. In this disease, the biomolecular antibody-auto-antigen interactions are characterised by molecular mimicry between gangliosides and lipopolysaccharides of *Campylobacter jejuni* infections. The measurement of binding of antibodies to auto-antigen G_{M1}-liposomes in a biosensor is shown to be a good model for studies of the idiotype network disturbances as gangliosides could be reproducibly coated on biosensor surfaces to report the specific binding of antibodies. A good positive control exists in the cholera toxin B subunit that binds with high affinity to ganglioside G_{M1}. Analysis of affinity constants reveals a good correlation with literature values. Lastly, it is shown that the immobilised G_{M1}-liposomes can be used to distinguish qualitatively and semi-quantitatively between Guillain-Barré syndrome patient and control sera. Besides providing the possibility of being a new diagnostic technique, it opens the possibility of studying the idiotype network and its role in auto-immunity much closer.

The idiotype network is a complex, tightly regulated network of antibodies, T- and B-cells. Disturbance of this equilibrium triggers auto-immune diseases like the Guillain-Barré syndrome. Molecular mimicry between self and foreign antigens is one mechanism by which auto-immunity may be triggered. In this study it is shown how a novel method of immobilising liposomes containing a glycolipid self-antigen on a resonant mirror biosensor may be used in unravelling the complexities of the idiotype network.

OPSOMMING

Biomolekulêre interaksies vorm die basis van byna alle siekte-meganismes op een of ander manier. Sommige van hierdie interaksies, veral proteïen-proteïn interaksies, is goed gekarakteriseer. Lipied-ligand proteïen reseptor interaksies word heelwat swakker verstaan, maar in hierdie studie word aangetoon hoe 'n resonans-spieël-biosensor aangewend kan word om sulke interaksies te analiseer deur gebruik te maak van twee voorbeelde. Hierdie lipied-proteïen interaksies word ook gekarakteriseer deur die manifestering van molekulêre nabootsing tussen sekere molekules.

In die eerste voorbeeld word tuberkulose lipied antigene (mikoolsure) gïmmobiliseer op die biosensor oppervlak deur van 'n kationiese detergens gebruik te maak. Dit word aangetoon hoe hierdie mikoolsure, of ligande, geskei kan word in hulle individuele subklasse deur gebruik te maak van dunlaag chromatografie sodat individuele subklasse geïmmobiliseer kan word op die biosensor oppervlak. Die biosensor tegniek laat dan die diskriminasie tussen verskillende bindings affinitieite van die subklasse met hul tersaaklike serum teenliggame toe. Verder laat dit die karakterisasie van die verhouding tussen mikoolsure en hul outo-teenliggame met 'n baie belangrike strukturele mimiek van keto-mikoolsuur, naamlik cholesterol, toe.

Vir die tweede voorbeeld word aangetoon dat die metode wat geoptimiseer was vir tuberkulose lipied antigene nie generies is nie en aangepas moes word vir die gebruik van Guillain-Barré sindroom glikolipied antigene: gangliosiede. In hierdie siekte word biomolekulêre teenliggam-outo-antigeen interaksies gekarakteriseer deur molekulêre nabootsing tussen gangliosiede en lipopolisakkariede van *Campylobacter jejuni* infeksies. Daar word aangetoon dat die meet van teenliggaam outo-antigeen binding aan gangliosied-liposome in 'n biosensor 'n goeie model is vir die bestudering van die idiotiepnetwerk-versteurings aangesien gangliosied betroubaar die biosensor oppervlak dek en teenliggaam binding rapporteer. 'n Goeie positiewe kontrole daarvoor bestaan in die cholera toksien B subeenheid wat bind aan gangliosied G_{M1} met hoë affiniteit. Analise van die affiniteits-konstantes toon goeie korrelasie met literatuur waardes. Laaste word getoon dat die geïmmobiliseerde G_{M1}-liposome gebruik kan word om kwalitatief en semi-kwantitatief te onderskei tussen Guillain-Barré sindroom pasiënt en kontrole sera. Behalwe die

verskaffing van 'n moontlike nuwe diagnostiese tegniek, skep dit die moontlikheid om die idiotiepnetwerk en sy rol in outo-immuniteit beter te bestudeer.

Die idiotiep netwerk is 'n komplekse, streng gereguleerde netwerk van teenliggame, T- en B-selle. Versteuring van hierdie ewewig sneller outoimmuun siektes soos die Guillain-Barré sindroom. Molekulêre nabootsing tussen self en vreemde antigene is een meganisme waardeur outoimmuniteit gesneller kan word. In hierdie studie word gewys hoe 'n nuwe metode van immobilisasie van liposome, wat 'n glikolipied self-antigeen bevat, op 'n resonans-spieël-biosensor gebruik kan word om die kompleksiteit van die idiotiep netwerk te ontrafel.

ANNEXURE 1

OPTIMISED METHOD FOR MYCOLIC ACID-LIPOSOME IMMOBILISATION

1.1 Liposome preparation

1. Aliquot MA in 100µg quantities
2. Make fresh PC and cholesterol stock solutions of 10mg/ml in cold chloroform
3. Add necessary quantities of PC and cholesterol stock solutions to one vial of MA (100µg)
4. Dry the mixture in a heat block at 85°C under a steady stream of nitrogen gas.
5. Add 2ml PBS containing 0.025% (w/v) sodium azide and 1mM EDTA (PBS/AE) to the dried lipids
6. Melt the lipids at 85°C in a heat block for ten minutes or until no residual flakes are visible
7. Vortex the solution at 100% for one minute
8. Sonify with a micro probe sonicator set at pulsed, 20 duty cycles, output level two for one minute
9. Vortex the solution at 100% for one minute

1.2 Liposome immobilisation

1. Achieve a stable baseline with PBS/AE for at least five minutes
2. Aspirate cells, add 50µl of 20µg/ml CPC in PBS/AE and incubate for ten minutes
3. Wash the cells five times each with 60µl PBS/AE and add 25µl of PBS/AE
4. Incubate for at least five minutes and until a stable baseline has been achieved.
5. Add 25µl of the liposome solution and incubate for ten minutes
6. Wash cells five times with 60µl PBS/AE, and immediately wash with five times 60µl 1mg/ml saponin in PBS/AE. Note: Saponin concentration should be titrated first to optimal blocking capacity concentration
7. Incubate for ten minutes and until a stable baseline has been achieved
8. Wash five times with 60µl PBS/AE and add a final 25µl PBS/AE

1.3 Interaction analysis and regeneration

1. Enter a baseline event as soon as a stable baseline has been achieved after the PBS/AE wash. Baseline should be monitored for at least five minutes
2. Add 25µl of the desired test sample at an appropriate dilution to the cells and enter an association event
3. Incubate for five to ten minutes depending on association velocity
4. Wash five times with 60µl PBS/AE to initiate dissociation and enter a dissociation event
5. Continue dissociation for five minutes before regenerating the cells as follow:
6. Wash three times with 50µl 95% ethanol
7. Follow immediately with three times 80µl PBS/AE and five times 60µl PBS/AE over one minute
8. Wash five times with 60µl 12.5M KOH and incubate for two minutes
9. Follow with three times 80µl PBS/AE and five times 60µl PBS/AE over one minute

ANNEXURE 2

OPTIMISED METHOD FOR GANGLIOSIDE-LIPOSOME IMMOBILISATION

2.1 Liposome preparation

1. Aliquot G_{M1} in 100µg quantities
2. Make fresh PC stock solution of 1mg/ml in cold chloroform
3. Add necessary quantity of PC stock solution to one vial of G_{M1} (100µg)
4. Dry the mixture in a heat block at 85°C under a steady stream of nitrogen gas.
5. Add Tris based buffer (50mM Tris, 200mM NaCl, 3mM NaN_3, 1mM Na_2EDTA) to the dried lipids to a concentration of 0.5mg/ml
6. Vortex the solution at 100% for one minute
7. Sonify with a micro probe sonicator set at pulsed, 20 duty cycles, output level two for one minute
8. Vortex the solution at 100% for one minute

2.2 Liposome immobilisation

Ganglioside-liposomes are immobilised with residual HCl remaining in the cells after regeneration. Therefore the regeneration protocol should be followed first and then immobilisation can be continued.

1. Aspirate the HCl solution remaining after regeneration and add 50µl of the liposome solution
2. Incubate for ten minutes before washing cells four times with 60µl Tris buffer, four times with 60µl 10mM NaOH and another five times with 60µl Tris buffer finishing with a 25µl Tris buffer addition
3. Incubate for five minutes and until a stable baseline has been achieved

2.3 Interaction analysis and regeneration

1. Enter a baseline event as soon as a stable baseline has been achieved after the Tris buffer wash. Baseline should be monitored for at least five minutes
2. Add 25µl of the desired test sample at an appropriate dilution to the cells and enter an association event.
3. Incubate for five to ten minutes depending on association velocity

4. Wash five times with 60µl Tris buffer to initiate dissociation and enter a dissociation event
5. Continue dissociation for five minutes before regenerating the cells as follow:
6. Wash four times with 60µl absolute ethanol
7. Follow immediately with seven times 100µl water, five times 60µl KOH and incubate for two minutes
8. Wash seven times with 100µl water and follow with three times 2M HCl and four times 20mM HCl
9. Achieve a stable baseline for at least five minutes before aspirating for the next round of immobilisation

REFERENCES

ABDOU N.I., WALL H., LINDSLEY H.B., HALSEY J.F. & SUZUKI T. (1981). Network theory in autoimmunity. In vitro suppression of serum anti-DNA antibody binding to DNA by anti-idiotypic antibody in systemic lupus erythematosus. *J Clin Invest* **67**(5): 1297-304

ABE T., TAKEUCHI T., KIYOTAKI M., KOIDE J., HOSONO O., HOMMA M., OTAKE T. & KANO S. (1984). Anti-idiotypic antibodies in a patient with monoclonal rheumatoid factor after pneumococcal bacteremia. *J Immunol* **132**(5): 2381-5

ADORINI L., BARNABA V., BONA C.A., CELADA F., LANZAVECCHIA A., SERCARZ E., SUCIU-FOCA N. & WEKERLE H. (1990). New perspective on immunointervention in autoimmune diseases. *Immunol Today* **11**(11): 383-6

ALBERT L.J. & INMAN R.D. (1999). Molecular mimicry and autoimmunity. *N Engl J Med* **341**(27): 2068-74

ALTIN J.G., WHITE F.A.J. & EASTON C.J. (2001). Synthesis of the chelator lipid nitrilotriacetic acid ditetradecylamine (NTA-DTDA) and its use with the IAsys biosensor to study receptor-ligand interactions on model membranes. *Biochim Biophys Acta* **1513**: 131-48

ALVING C.R. & SWARTZ JR G.M. (1991). Antibodies to cholesterol, cholesterol conjugates and liposomes: implications for atherosclerosis and autoimmunity. *Crit Rev Immunol* **10**(5): 441-53

ALVING C.R. & WASSEF N.M. (1999). Naturally occurring antibodies to cholesterol: a new theory of LDL cholesterol metabolism. *Immunol Today* **20**(8): 362-6

ANG C.W. (2001). Molecular mimicry in the Guillain-Barré syndrome. PhD. Departments of Immunology and Neurology, Erasmus University Rotterdam, Rotterdam

ANG C.W., DE KLERK M.A., ENDTZ H.P., JACOBS B.C., LAMAN J.D., VAN DER MECHE F.G.A. & VAN DOORN P.A. (2001a). Guillain-Barré syndrome- and Miller Fisher syndrome-associated *Campylobacter jejuni* lipopolysaccharides induce anti-GM_1 and anti-GQ_{1b} antibodies in rabbits. *Infect Immun* **69**(4): 2462-9

ANG C.W., KOGA M., JACOBS B.C., YUKI N., VAN DER MECHE F.G.A. & VAN DOORN P.A. (2001b). Differential immune response to gangliosides in Guillain-Barré syndrome patients from Japan and the Netherlands. *J Neuroimmunol* **121**: 83-7

ANG C.W., VAN DOORN P.A., ENDTZ H.P., MERKIES I.S.J., JACOBS B.C., DE KLERK M.A., VAN KONINGSVELD R. & VAN DER MECHÉ F.G.A. (2000). A case of Guillain-Barré syndrome following a family outbreak of *Campylobacter jejuni* enteritis. *J Neuroimmunol* **111**: 229-33

AOYAMA K., ISHIKURA H., MISHIMA S., MURAI M., TSUMURA H., KUMAKURA S. & KOBAYASHI S. (2001). Guillain-Barré syndrome complicated with hemolytic anemia in association with antiganglioside GM3 antibody. *Am J Med* **110**: 399-400

ATHANASSOPOULOU N., DAVIES R.J., EDWARDS P.R., YEUNG D. & MAULE C.H. (1999). Cholera toxin and G_{M1}: a model membrane study with IAsys. *Biochem Soc Trans* **27**(2): 340-3

BAMBAUER R., SCHWARZE U. & SCHIEL R. (2000). Cyclosporin A and therapeutic plasma exchange in the treatment of severe systemic lupus erythematosus. *Artif Organs* **24**(11): 852-6

BARIÉ N. & RAPP M. (2001). Covalent bound sensing layers on surface acoustic wave (SAW) biosensors. *Biosens Bioelectron* **16**(9-12): 979-87

BARRY C.E., LEE R.E., MDLULI K., SAMPSON A.E., SCHROEDER B.G., SLAYDEN R.A. & YUAN Y. (1998). Mycolic acids: structure, biosynthesis and physiological functions. *Prog Lipid Res* **37**(2/3): 143-79

BENNER R., VAN DONGEN J.J., VAN EWIJK W. & HAAIJMAN J.J. (1996). Medische immunologie. Utrecht, Wetenschappelijke uitgeverij Bunge

BIACORE (2001). BIAcore website. http://www.biacore.com: http://www.biacore.com

BINZ H. & WIGZELL H. (1975). Shared idiotypic determinants on B and T lymphocytes reactive against the same antigenic determinants. I. Demonstration of similar or identical idiotypes on IgG molecules and T-cell receptors with specificity for the same alloantigens. *J Exp Med* **142**(1): 197-211

BONA C.A. (1987). Regulatory idiotopes. New York, John Wiley & Sons

BONA C.A. & BONILLA F.A. (1990). Textbook of immunology. Amsterdam, Harwood Academic Publishers

BOULLA G., RANDRIAMAMPITA C., RAPOSO G. & TRAUTMANN A. (2000). Binding kinetics of soluble ligands to transmembrane proteins: comparing an optical biosensor and dynamic flow cytometry. *Cytometry* **40**(76-80)

CALVANICO N.J. (1993). The humoral immune response in autoimmunity. *Dermatol Clin* **11**(3): 379-89

CAMPBELL S.M., CROWE S.M. & MAK J. (2001). Lipid rafts and HIV-1: from viral entry to assembly of progeny virions. *J Clin Virol* **22**: 217-27

CAPRA J.D. & KEHOE J.M. (1975). Hypervariable regions, idiotypy, and the antigen-combining site. *Adv Immunol* **20**: 1-40

CHERUKURI A., DYKSTRA M.L. & PIERCE S.K. (2001). Floating the raft hypothesis: lipid rafts play a role in immune cell activation. *Immunity* **14**: 657-60

CLAFLIN J.L., LIEBERMAN R. & DAVIE J.M. (1974). Clonal nature of the immune response to phosphorylcholine. II. Idiotypic specificity and binding characteristics of anti-phosphorylcholine antibodies. *J Immunol* **112**(5): 1747-56

CLEM L.W. & LESLIE G.A. (1982). Phylogeny of immunoglobulin structure and fraction XV. Idiotypic analysis of shark antibodies. *Dev Comp Immunol* **6**(3): 463-72

COOKE A., LYDYARD P.M. & ROIIT I.M. (1984). Autoimmunity and idiotypes. *Lancet* **2**(8405): 723-5

COOPER M.D. (1986). B cell development in birds and mammals. *Prog Immunol* **6**: 18-32

CORNELL B.A., BRAACH-MAKSVYTIS V.L.B., KING L.G., OSMAN P.D.J., RAGUSE B., WIECZOREK L. & PACE R.J. (1997). A biosensor that uses ion-channel switches. *Nat* **387**: 580-583

COSENZA H. (1976). Detection of anti-idiotype reactive cells in the response to phosphorylcholine. *Eur J Immunol* **6**(2): 114-6

CUATRECASAS P. (1973). Gangliosides and membrane receptors for cholera toxin. *Biochemistry* **12**(18): 3558-66

CUSH R., CRONIN J.M. & STEWART W.J. (1993). The resonant mirror: a novel optical biosensor for direct sensing of biomolecular interactions Part I: Principle of operation and associated instrumentation. *Biosens Bioelectron* **8**(7-8): 347-54

CYWES C., HOPPE H.C., DAFFÉ M. & EHLERS M.R.W. (1997). Nonopsonic binding of *Mycobacterium tuberculosis* to complement receptor type 3 is mediated by capsular polysaccharides and is strain dependent. *Infect Immun* **65**(10): 4258-66

DAFFÉ M. & DRAPER P. (1998). The envelope layers of mycobacteria with reference to their pathogenicity. *Adv Microb Physiol* **39**: 131-203

DAMIAN R.T. (1964). Molecular mimicry: antigen sharing by parasite and host and its consequences. *Amer Nat* **98**: 129-49

DAR V.V. & SETH P. (1993). Monoclonal anti-idiotype antibody to HSV-1 neutralizing monoclonal antibody: production and characterization. *Disease Markers* **11**(2-3): 113-23

DASGUPTA S. & HOGAN E.L. (2001). Chromatographic resolution and quantitative assay of CNS tissue sphingoids and sphingolipids. *Lipid Research* **42**(2): 301-8

DECK M.B., SJÖLIN P., UNANUE E.R. & KIHLBERG J. (1999). MHC-restricted, glycopeptide-specific T cells show specificity for both carbohydrate and peptide residues. *J Immunol* **162**: 4740-4

DELEU M., NOTT K., BRASSEUR R., JACQUES P., THONART P. & DUFRÊNE Y.F. (2001). Imaging mixed lipid monolayers by dynamic atomic force microscopy. *Biochim Biophys Acta* **1513**: 55-62

DELFRAISSY J.F., TCHERNIA G., LAURIAN Y., WALLON C., GALANAUD P. & DORMONT J. (1985). Suppressor cell function after intravenous gammaglobulin treatment in adult chronic idiopathic thrombocytopenic purpura. *Br J Haematol* **60**(2): 315-22

DIAMANDIS E.P. & CHRISTOPOULOS T.K., Eds. (1996). Immunoassay. London, Academic Press Inc.

DIETRICH G., VARELA F., BOUANANI M. & KAZATCHKINE M.D. (1993). Selection of the expressed B cell repertoire by infusion of normal immunoglobulin G in a patient with autoimmune thyroiditis. *Eur J Immunol* **23**(11): 2945-50

DIJKSTRA J., SWARTZ JR G.M., RANEY J.J., ANIAGLU A., TORO L., NACY C.A. & GREEN S.J. (1996). Interaction of anti-cholesterol antibodies with human lipoproteins. *J Immunol* **157**: 2006-13

DUBNAU E., CHAN J., RAYNAUD C., MOHAN V.P., LANÉELLE M.-A., YU K., QUÉMARD A., SMITH I. & DAFFÉ M. (2000). Oxygenated mycolic acids are necessary for virulence of *Mycobacterium tuberculosis* in mice. *Mol Microbiol* **36**(3): 630-7

DUBNAU E., LANÉELE M.-A., SOARES S., BENICHOU A., VAZ T., PROME D., PROME J.C., DAFFÉ M. & QUÉMARD A. (1997). *Mycobacterium bovis* BCG genes involved in the biosynthesis of cyclopropyl keto- and hydroxy-myolic acids. *Mol Microbiol* **23**(2): 313-22

DWYER D.S., BRADLEY R.J., URQUHART C.K. & KEARNEY J.F. (1983). Naturally occurring anti-idiotypic antibodies in myasthenia gravis patients. *Nat* **301**(5901): 611-4

EICHMANN K. & RAJEWSKY K. (1975). Induction of T and B cell immunity by anti-idiotypic antibody. *Eur J Immunol* **5**(10): 661-6

FEHR J., HOFMANN V. & KAPPELER U. (1982). Transient reversal of thrombocytopenia in idiopathic thrombocytopenic purpura by high-dose intravenous gamma globulin. *N Engl J Med* **306**(21): 1254-8

FELDMAN R.G., BREUKELS M.A., DAVID S. & RIJKERS G.T. (1998). Properties of human anti-group B streptococcal type III capsular IgG antibody. *Clin Immunol Immunopathol* **86**(2): 161-9

FISHER M.I. & TJÄRNHAGE T. (2000). Structure and activity of lipid membrane biosensor surfaces studied with atomic force microscopy and a resonant mirror. *Biosens Bioelectron* **15**: 463-71

FRASER M.E., CHERNAIA M.M., KOZLOV Y.V. & JAMES M.N. (1994). Crystal structure of the holotoxin from *Shigella dysenteriae* at 2.5Å resolution. *Nat Struct Biol* **1**(1): 59-64

FUJIWARA N., PAN J., ENOMOTO K., TERANO Y., HONDA T. & YANO I. (1999). Production and partial characterization of anti-cord factor (trehalose-6,6'-dimycolate) IgG antibody in rabbits recognizing mycolic acid subclasses of *Mycobacterium tuberculosis* or *Mycobacterium avium*. *FEMS Immunol Mol Microbiol* **24**: 141-9

GATFIELD J. & PIETERS J. (2000). Essential role for cholesterol in entry of mycobacteria into macrophages. *Science* **298**: 1647-50

GEORGE K.M., YUAN Y., SHERMAN D.R. & BARRY III C.E. (1995). The biosynthesis of cyclopropenated mycolic acids in *Mycobacterium tuberculosis*. *J Biol Chem* **270**(45): 27292-8

GOODRUM M.A., SIKO D.G.R., NIEHUES T., EICHELBAUER D. & VERSCHOOR J.A. (2001). Mycolic acids from *Mycobacterium tuberculosis*: purification by countercurrent distribution and T-cell stimulation. *Microbios* **106**(413): 55-67

GUILLET J.G., CHAMAT S., HOEBEKE J. & STROSBERG A.D. (1984). Production and detection of monoclonal anti-idiotype antibodies directed against a monoclonal anti-beta-adrenergic ligand antibody. *J Immunol Methods* **74**(1): 163-71

HAIMOVICH J., CZERWINSKI D., WONG C.P. & LEVY R. (1998). Determination of anti-idiotype antibodies by surface plasmon resonance. *J Immunol Methods* **214**(1-2): 113-9

HALL P.D. (1993). Immunomodulation with intravenous immunoglobulin. *Pharmacotherapy* **13**(6): 564-73

HARVEY H.A., SWORDS W.E. & APICELLA M.A. (2001). The mimicry of human glycolipids and glycosphingolipids by the lipooligosaccharides of pathogenic neisseria and haemophilus. *J Autoimmun* **16**(3): 257-62

HASTINGS A., MORRISON S.L., KANDA S., SAXTON R.E. & IRIE R.F. (1992). Production and characterization of a murine/human chimeric anti-idiotype antibody that mimics ganglioside. *Cancer Res* **52**(7): 1681-6

HIERNAUX J. & BONA C.A. (1982). Shared idiotypes among monoclonal antibodies specific for different immunodominant sugars of lipopolysaccharide of different Gram-negative bacteria. *Proc Natl Acad Sci USA* **79**(5): 1616-20

HIRMO S., ARTURSSON E., PUU G., WADSTRÖM T. & NILSSON B. (1999). *Helicobacter pylori* interactions with human gastric mucin studied with a resonant mirror biosensor. *J Microbiol Methods* **37**: 177-82

HO T.W., MISHU B., LI C.Y., GAO C.Y., CORNBLATH D.R., GRIFFIN J.W., ASBURY A.K., BLASER M.J. & MCKHANN G.M. (1995). Guillain-Barré syndrome in northern China. Relationship to *Campylobacter jejuni* infection and anti-glycolipid antibodies. *Brain* **118**: 597-605

HOLMDAHL R., TARKOWSKI A., NORDLING C., RUBIN K. & KLARESKOG L. (1987). Connection between autoimmunity to cartilage type II collagen and rheumatoid factor production. *Monogr Allergy* **22**: 71-80

HOLMGREN J. (1981). Actions of cholera toxin and the prevention and treatment of cholera. *Nat* **292**: 413-7

HOOD L.E., KUMAR V., OSMAN G., BEALL S.S., GOMEZ C., FUNKHOUSER W., KONO D.H., NICKERSON D., ZALLER D.M. & URBAN J.L. (1989). Autoimmune disease and T-cell immunologic recognition. Cold Spring Harbor symposia on quantitative biology, Cold Spring Harbor Laboratory Press

HUDSON J.A., NICOL C., WRIGHT J., WHYTE R. & HASELL S.K. (1999). Seasonal variation of *Campylobacter jejuni* types from human cases, veterinary cases, raw chicken, milk and water. *J Appl Microbiol* **87**: 115-24

HUGHES R.A.C. (1990). The Guillain-Barré syndrome. London, Springer

HUGHES R.A.C. & REES J.H. (1997). Clinical and epidemiologic features of Guillain-Barré syndrome. *J Infect Dis* **176 (Suppl 2)**: S92-8

IASYS A.S. (1995a). IAsys plus user's guide. Cambridge, Human-Computer Interface Limited

IASYS A.S. (1995b). Methods guide. Cambridge, Human-Computer Interface Limited

IASYS A.S. (1996). FASTfit guide. Cambridge, Human-Computer Interface Limited

ILYAS A.A., QUARLES R.H., DALAKAS M.C., FISHMAN P.H. & BRADY R.O. (1985). Monoclonal IgM in a patient with paraproteinemic polyneuritus binds to gangliosides containing disialosyl groups. *Ann Neurol* **18**(6): 655-9

JACKSON M., RAYNAUD C., LANÉELLE M.-A., GUILHOT C., LAURENT-WINTER C., ENSERGUEIX D., GICQUEL B. & DAFFÉ M. (1999). Inactivation of the antigen 85C gene profoundly affects the mycolate content and alters the permeability of the *Mycobacterium tuberculosis* cell envelope. *Mol Microbiol* **31**(5): 1573-87

JACOBS B.C., ROTHBART P.H., VAN DER MECHÉ F.G.A., HERBRINK P., SCHMITZ P.I.M., DE KLERK M.A. & VAN DOORN P.A. (1998). The spectrum of antecedent infections in Guillain-Barré syndrome: a case-control study. *Neurology* **51**: 1110-5

JEAN-FRANCOIS M.J., POSKITT D.C., MACDONALD L.M., TURNBULL S.J. & YASMEEN D. (1993). Production of monoclonal anti-idiotype antibodies which mimic an M-like protein of *Streptococcus equi*. *Microbiol Immunol* **37**(9): 737-42

JELESAROV I. & BOSSHARD H.R. (1999). Isothermal titration calorimetry and differential scanning calorimetry as complementary tools to investigate the energetics of biomolecular recognition. *J Mol Recognit* **12**: 3-18

JERNE N.K. (1974). Towards a network theory of the immune system. *Ann Immunol* **125C**: 373-89

JOHNSON P.M., PHUA K.K. & EVANS H.B. (1985). An idiotypic complementarity between rheumatoid factor and anti-peptidoglycan antibodies? *Clin Exp Immunol* **61**(2): 373-8

JOHNSTON R. (2003). AIDSVAX results: an answer, or just more questions? *AIDS Patient Care STDS* **17**(2): 47-51

KALB E., FREY S. & TAMM L.K. (1992). Formation of supported planar bilayers by fusion of vesicles to supported phospholipid monolayers. *Biochim Biophys Acta* **1103**: 307-16

KANEDA K., NAITO S., IMAIZUMI S., YANO I., MIZUNO S., TOMIYASU I., BABA T., KUSUNOSE E. & KUSUNOSE M. (1986). Determination of molecular species composition

of C_{80} or longer-chain α-mycolic acids in *Mycobacterium* spp. by gas chromatography-mass spectrometry and mass chromatography. *J Clin Microbiol* **24**(6): 1060-70

KARLSSON K.-A. (1995). Microbial recognition of target-cell glycoconjugates. *Curr Opin Struct Biol* **5**: 622-35

KAROL R., REICHLIN M. & NOBLE R.W. (1978). Idiotypic cross-reactivity between antibodies of different specificities. *J Exp Med* **148**(6): 1488-97

KAZATCHKINE M.D. & COUTINHO A. (1993). Are lymphocytes concerned with our definition of idiotypes? *Immunol Today* **14**(10): 513-5

KEARNEY J.F., VAKIL M. & SOLVASON N. (1989). The role of idiotypic interactions and the B-cell subsets in development of the B-cell repertoire. Cold Spring Harbor symposia on quantitative biology, Cold Spring Harbor Laboratory Press

KENNERLY D.A. (1986). Improved analysis of species of phospholipids using argentation thin-layer chromatography. *J Chromatogr* **363**: 462-7

KIEBER-EMMONS T. (1998). Peptide mimotopes of carbohydrate antigens. *Immunol Res* **17**: 95-108

KIM J.H., CHO J.H., CHA G.S., LEE C.W., KIM H.B. & PAEK S.H. (2000). Conductimetric membrane strip immunosensor with polyaniline-bound gold colloids as signal generator. *Biosens Bioelectron* **14**(12): 907-15

KISHIMOTO K., URADE R., OGAWA T. & MORIYAMA T. (2001). Nondestructive quantification of neutral lipids by thin-layer chromatography and laser-fluorescent scanning: suitable methods for "lipidome" analysis. *Biochem Biophys Res Commun* **281**(3): 657-62

KLUSKENS L. & KÖHLER H. (1974). Regulation of immune response by autogenous antibody against receptor. *Proc Natl Acad Sci USA* **71**(12): 5083-7

KÖHLER H. (1975). The response to phosphorylcholine: dissecting an immune response. *Transplant Rev* **27**: 24-56

KRAIG E., KRONENBERG M., KAPP J.A., PIERCE C.W., ABRUZZINI A.F., SORENSEN C.M., SAMELSON L.E., SCHWARTZ R.H. & HOOD L.E. (1983). T and B cells that recognize the same antigen do not transcribe similar heavy chain variable region gene segments. *J Exp Med* **158**(1): 192-209

KULYS J. & VIDZIUNAITE R. (2003). Amperometric biosensors based on recombinant laccases for phenols determination. *Biosens Bioelectron* **18**(2-3): 319-25

KUROSAWA Y., VON BOEHMER H., HAAS W., SAKANO H., TRAUNEKER A. & TONEGAWA S. (1981). Identification of D segments of immunoglobulin heavy-chain genes and their rearrangement in T lymphocytes. *Nat* **290**(5807): 565-70

KURZCHALIA T.V. & PARTON R.G. (1999). Membrane microdomains and caveolae. *Curr Opin Cell Biol* **11**(4): 424-31

KUZIEMKO G.M., STROH M. & STEVENS R.C. (1996). Cholera toxin binding affinity and specificity for gangliosides determined by surface plasmon resonance. *Biochemistry* **35**: 6375-84

LACROIX-DESMAZES S., MOUTHON L., SPALTER S.H., KAVERI S. & KAZATCHKINE M.D. (1996). Immunoglobulins and the regulation of autoimmunity through the immune network. *Clin Exp Rheumatol* **14 (Suppl. 15)**: S9-15

LASTOVICA A.J., GODDARD E.A. & ARGENT A.C. (1997). Guillain-Barré syndrome in South Africa associated with *Campylobacter jejuni* O:41 strains. *J Infect Dis* **176 (Suppl 2)**: S139-43

LAVAL F., LANÉELLE M.-A., DÉON C., MONSARRAT B. & DAFFÉ M. (2001). Accurate molecular mass determination of mycolic acids by MALDI-TOF mass spectrometry. *Anal Chem* **73**: 4537-44

LEMKE H., LANGE H. & BEREK C. (1998). Maternal immunization modulates the primary immune response to 2-phenyl-oxazolone in BALB/c mice. *Eur J Immunol* **28**(5): 1743

LI J., WU Z.Y., XIAO L.T., ZENG G.M., HUANG G.H., SHEN G.L. & YU R.Q. (2002). A novel piezoelectric biosensor for the detection of phytohormone beta-indole acetic acid. *Anal Sci* **18**(4): 403-7

LIU J., BARRY C.E., BESRA G.S. & NIKAIDO H. (1996). Mycolic acid structure determines the fluidity of the mycobacterial cell wall. *J Biol Chem* **271**: 29 - 545, 551

LOSMAN M.J., LEUNG S.O., SHIH L.B., SHEVITZ J., SHUKLA R., HARAGA L., GOLDENBERG D.M. & HANSEN H.J. (1995). Development and evaluation of the specificity of a rat monoclonal anti-idiotype antibody, WN, to an anti-B-cell lymphoma monoclonal antibody, LL2. *Cancer Res* **55**(23 Suppl): 5978s-82s

LUNDKVIST I., VAN DOORN P.A., VERMEULEN M. & BRAND A. (1993). Spontaneous recovery from the Guillain-Barré Syndrome is associated with anti-idiotypic antibodies recognizing a cross-reactive idiotype on anti-neuroblastoma cell line antibodies. *Clin Immunol Immunopathol* **67**(3): 192-8

MACKENZIE C.R., HIRAMA T., LEE K.K., ALTMAN E. & YOUNG N.M. (1997). Quantitative analysis of bacterial toxin affinity and specificity for glycolipid receptors by surface plasmon resonance. *J Biol Chem* **272**(9): 5533-8

MARCHALONIS J.J., KAYMAZ H., DEDEOGLU F., SCHLUTER S.F., YOCUM D.E. & EDMUNDSON A.B. (1992). Human autoantibodies reactive with synthetic autoantigens from T-cell receptor beta chain. *Proc Natl Acad Sci USA* **89**(8): 3325-9

MARON R., ELIAS D., DE JONGH B.M., BRUINING G.J., VAN ROOD J.J., SHECHTER Y. & COHEN I.R. (1983). Autoantibodies to the insulin receptor in juvenile onset insulin-dependent diabetes. *Nat* **303**(5920): 817-8

MASSERINI M., FREIRE E., PALESTINI P., CALAPPI E. & TETTAMANTI G. (1992). Fuc-GM1 ganglioside mimics the receptor function of GM1 for cholera toxin. *Biochemistry* **31**: 2422-6

McIntyre C.W., Fluck R.J. & Lambie S.H. (2001). Steroid and cyclophosphamide therapy for IgA nephropathy associated with crescentric change: an effective treatment. *Clin Nephrol* **56**(3): 193-8

Meek K., Jeske D., Slaoui M., Leo O., Urbain J. & Capra J.D. (1984). Complete amino acid sequence of heavy chain variable regions derived from two monoclonal anti-p-azophenylarsonate antibodies of BALB/c mice expressing major cross-reactive idiotype of the A/J strain. *J Exp Med* **160**(4): 1070-86

Menze M.A., Hellmann N., Decker H. & Grieshaber M.K. (2001). Binding of urate and caffeine to haemocyanin analysed by isothermal titration calorimetry. *J Exp Biol* **204**: 1033-8

Merritt E.A., Sarfaty S., Van den Akker F., L'Hoir C., Martial J.A. & Hol W.G. (1994). Crystal structure of cholera toxin B-pentamer bound to receptor GM1 pentasaccharide. *Prot Sci* **3**(2): 166-75

Minnikin D.E. (1982). Lipids: complex lipids, their chemistry, biosynthesis and roles. New York, Academic Press

Moran A.P. (1997). Structure and conserved characteristics of *Campylobacter jejuni* lipopolysaccharides. *J Infect Dis* **176 (Suppl 2)**: S115-21

Munthe L.A., Kyte J.A. & Bogen B. (1999). Resting small B cells present endogenous immunoglobulin variable-region determinants to idiotope-specific $CD4^+$ T cells in vivo. *Eur J Immunol* **29**(12): 4043-52

Mustafa A.S. (2002). Development of new vaccines and diagnostic reagents against tuberculosis. *Mol Immunol* **39**(1-2): 113-9

Nakajima H., Kiyokawa N., Katagiri Y.U., Taguchi T., Suzuki T., Sekino T., Mimori K., Ebata T., Saito M., Nakao H., Takeda T. & Fujimoto J. (2001). Kinetic analysis of binding between Shiga toxin and receptor glycolipid Gb3Cer by surface plasmon resonance. *J Biol Chem* **276**(46): 42915-22

Naparstek Y., Duggan D., Schattner A., Madaio M.P., Goni F., Frangione B., Stollar B.D., Kabat E.A. & Schwartz R.H. (1985). Immunochemical similarities between monoclonal antibacterial Waldenstrom's macroglobulins and monoclonal anti-DNA lupus autoantibodies. *J Exp Med* **161**(6): 1525-38

Neisser A., Schwerer B., bernheimer H. & Moran A.P. (2000). Ganglioside-induced antiganglioside antibodies from a neuropathy patient cross-react with lipopolysaccharides of *Campylobacter jejuni* associated with Guillain-Barré syndrome. *J Neuroimmunol* **102**: 85-8

Nice E.C. & Catimel B. (1999). Instrumental biosensors: new perspectives for the analysis of biomolecular interactions. *BioEssays* **21**(4): 339-52

Nikolelis D.P., Hianik T. & Krull U.J. (1999). Biosensors based on thin lipid films and liposomes. *Electroanalysis* **11**(1): 7-15

NUTMAN T.B., OTTESEN E.A., FAUCI A.S. & VOLKMAN D.J. (1984). Parasite antigen-specific human T cell lines and clones. Major histocompatibility complex restriction and B cell helper function. *J Clin Invest* **73**(6): 1754-62

OLDSTONE M.B.A., SCHWIMMBECK P., DYRBERG T. & FUJINAMI R. (1986). Mimicry by virus of host molecules: implications for autoimmune disease. *Prog Immunol* **6**: 787-95

OLSSON N.U. (1992). Advances in planar chromatography for the separation of food lipids. *J Chromatogr* **624**(1-2): 11-9

OUCHTERLONY Ö. & HOLMGREN J. (1980). Cholera and related diarrheas : molecular aspects of a global health problem. New York, Karger

OUDIN J. & CAZENAVE P.A. (1971). Similar idiotypic specificities in immunoglobulin fractions with different antibody functions or even without detectable antibody function. *Proc Natl Acad Sci USA* **68**(10): 2616-20

PAGE N., MURRAY N., PERRUISSEAU G. & STECK A.J. (1985). A monoclonal anti-idiotypic antibody against a human monoclonal IgM with specificity for myelin-associated glycoprotein. *J Immunol* **134**(5): 3094-9

PAN J., FUJIWARA N., OKA S., MAEKURA R., OGURA T. & YANO I. (1999). Anti-cord factor (trehalose-6,6'-dimycolate) IgG antibody in tuberculosis patients recognizes mycolic acid subclasses. *Microbiol Immunol* **43**(9): 863-869

PAPAROUNAS K., O'HANLON G., O'LEARY C.P., ROWAN E.G. & WILLISON H.J. (1999). Anti-ganglioside antibodies can bind peripheral nerve nodes of Ranvier and activate the complement cascade without inducing acute conduction block *in vitro*. *Brain* **122**: 807-16

PASQUALI J.L., URLACHER A. & STORCK D. (1984). Idiotypic network: possible explanation of seronegativity in a patient with rheumatoid arthritis. *Clin Exp Immunol* **55**(2): 281-6

PATHAK S.S. (1995). Antibody affinity and affinity distributions: determination in ELISA and biosensor. PhD. Immunology, Erasmus University Rotterdam, Rotterdam

PERELSON A.S. (1989). Immune network theory. *Immunol Rev* **110**: 5-36

PEREZ A., MIER E.S., VISPO N.S., VAZQUEZ A.M. & PEREZ RODRIGUEZ R. (2002a). A monoclonal antibody against NeuGc-containing gangliosides contains a regulatory idiotope involved in the interaction with B and T cells. *Mol Immunol* **39**(1-2): 103-12

PEREZ C., GUARCH R., RODRIGO M., GALLEGO M. & ORMAZABAL O. (2002b). Successful treatment of leucocytoclastic vasculitis and pancytopenia secondary to systemic lupus erythematosus with intravenous immunoglobulin. *Br J Dermatol* **147**(1): 180-2

PLOTZ P.H. (1983). Autoantibodies are anti-idiotype antibodies to antiviral antibodies. *Lancet* **2**(8354): 824-6

PUU G. (2001). An approach for analysis of protein toxins based on thin films of lipid mixtures in an optical biosensor. *Anal Chem* **73**: 72-9

QUÉMARD A., LANÉELE M.-A., MARRAKCHI H., PROME D., DUBNAU E. & DAFFÉ M. (1997). Structure of a hydroxymycolic acid potentially involved in the synthesis of oxygenated mycolic acids of the *Mycobacterium tuberculosis* complex. *Eur J Biochem* **250**(3): 758-63

RAMANATHAN K. & DANIELSSON B. (2001). Principles and applications of thermal biosensors. *Biosens Bioelectron* **16**(6): 417-23

REDDY R.R., CHADHA A. & BHATTACHARYA E. (2001). Porous silicon based potentiometric triglyceride biosensor. *Biosens Bioelectron* **16**(4-5): 313-7

ROBINSON W.E.J., MONTEFIORI D.C. & MITCHELL W.M. (1988). Will antibody-dependent enhancement of HIV-1 infection be a problem with AIDS vaccines? *Lancet* **1**(8589): 830-1

RODKEY L.S. (1974). Studies of idiotypic antibodies. Production and characterization of autoantiidiotypic antisera. *J Exp Med* **139**(3): 712-20

ROIIT I.M. & COOKE A. (1986). Idiotypes and autoimmunity. *Prog Immunol* **6**: 512-35

ROOT-BERNSTEIN R.S. (1995). Preliminary evidence for idiotype-antiidiotype immune complexes cross-reactive with lymphocyte antigens in AIDS and lupus. *Med Hypotheses* **44**(1): 20-7

ROSSI F., DIETRICH G. & KAZATCHKINE M.D. (1989). Anti-idiotypes against autoantibodies in normal immunoglobulins: evidence for network regulation of human autoimmune responses. *Immunol Rev* **110**: 135-49

ROUDIER C., AUGER I. & ROUDIER J. (1996). Molecular mimicry reflected through database screening: serendipity or survival strategy? *Immunol Today* **17**(8): 357-8

ROUX K.H. & METZGER D.W. (1982). Immunoelectron microscopic localization of idiotypes and allotypes on immunoglobulin molecules. *J Immunol* **129**(6): 2548-53

RUBIO I., BUCKLE P., TRUTNAU H. & WETZKER R. (1997). Real-time assay of the interaction of a GST fusion protein with a protein ligate using a resonant mirror technique. *BioTechniques* **22**: 269-71

SADIQ S.A., THOMAS F.P., KILIDIREAS K., PROTOPSALTIS S., HAYS A.P., LEE K.W., ROMAS S.N., KUMAR N., VAN DEN BERG L., SANTORO M. & *AL. E.* (1990). The spectrum of neurologic disease associated with anti-GM1antibodies. *Neurology* **40**: 1067-72

SCHLEICHER G.K., FELDMAN C., VERMAAK Y. & VERSCHOOR J.A. (2002). Prevalence of anti-mycolic acid antibodies in patients with pulmonary tuberculosis co-infected with HIV. *Clin Chem Lab Med* **40**(9): 882-7

SCHNEIDER B.H., EDWARDS J.G. & HARTMAN N.F. (1997). Hartman interferometer: versatile integrated optic sensor for label-free, real-time quantification of nucleic acids, proteins, and pathogens. *Clin Chem* **43**(9): 1757-63

SCHWARTZ R.S. (1986). Autoantibodies and normal antibodies. *Prog Immunol* **6**: 478-82

SETO A. (1980). Cycling in the idiotypical proliferative response of peripheral blood lymphocytes in normal and *Salmonella typhi*-immunized rabbits. *Ann Immunol* **131C**(3): 289-309

SHENG N., FAIRBANKS M.B., HEINRIKSON R.L., CANZIANI G., CHAIKEN I.M., MOSSER D.M., ZHANG H. & COLMAN R.W. (2000). Cleaved high molecular weight kininogen binds directly to the integrin CD11b/CD18 (Mac-1) and blocks adhesion to fibrinogen and ICAM-1. *Blood* **95**(12): 3788-95

SIKO D.G.R. (1999). The effects of Mycobacterial mycolic acids on rodent tuberculosis and adjuvant arthritis. MSc. Department of Biochemistry, Faculty of Natural and Agricultural Sciences, University of Pretoria, Pretoria

SIKO D.G.R. (2002). Mycobacterial mycolic acids as immunoregulatory lipid antigens in the resistance to tuberculosis. PhD. Department of Biochemistry, Faculty of Natural and Agricultural Sciences, University of Pretoria, Pretoria

SIMONS K. & TOOMRE D. (2000). Lipid rafts and signal transduction. *Nat Rev Mol Cell Biol* **1**: 31-9

SINGER A., MIZUOCHI T., MUNITZ T.I. & GRESS R.E. (1986). Role of self antigens in the selection of the developing T cell repertoire. *Prog Immunol* **6**: 60-6

SIXMA T.K., PRONK S.E., KALK K.H., WARTNA E.S., VAN ZANTEN B.A., WITHOLT B. & HOL W.G. (1991). Crystal structure of a cholera toxin-related heat-labile enterotoxin from *E. coli*. *Nat* **351**(6325): 371-7

SKIPSKI V.P. & BARCLAY M. (1969). Thin-layer chromatography of lipids. Methods Enzymol. LOWENSTEIN J.M. New York, Academic Press. **14:** 530-98

SOMASUNDARAM R., ZALOUDIK J., JACOB L., BENDEN A., SPERLAGH M., HART E., MARKS G., KANE M., MASTRANGELO M. & HERLYN D. (1995). Induction of antigen-specific T and B cell immunity in colon carcinoma patients by anti-idiotypic antibody. *J Immunol* **155**(6): 3253-61

SPARBIER K. & WALDEN P. (1999). T-cell receptor specificity and mimotopes. *Curr Opin Immunol* **11**(2): 214-8

ST HILAIRE P.M., BOYD M.K. & TOONE E.J. (1994). Interaction of the Shiga-like toxin type 1 B-subunit with its carbohydrate receptor. *Biochemistry* **33**(48): 14452-63

STANNARD L.M. (1996). The bacterial cell wall. University of Cape Town. http://www.uct.ac.za/depts/mmi/lsteyn/cellwall.html: http://www.uct.ac.za/depts/mmi/lsteyn/cellwall.html

STEIN P.E., BOODHOO A., ARMSTRONG G.D., COCKLE S.A., KLEIN M.H. & READ R.J. (1994). The crystal structure of pertussis toxin. *Structure* **2**(1): 45-57

STOLTZ A.D. (2002). Immunological properties of mycolic acids, the major lipid cell wall component of *Mycobacterium tuberculosis*. PhD. Department of Biochemistry, University of Pretoria, Pretoria

STULNIG T.M., HUBER J., LEITINGER N., IMRE E.-M., ANGELISOVÁ P., NOWOTNY P. & WALDHÄUSL W. (2001). Polyunsaturated eicosapentanoic acid displaces proteins from membrane rafts by altering raft lipid composition. *J Biol Chem* **276**(40): 37335-40

SULTAN Y., KAZATCHKINE M.D., MAISONNEUVE P. & NYDEGGER U.E. (1984). Anti-idiotypic suppression of autoantibodies to factor VIII (antihaemophilic factor) by high-dose intravenous gammaglobulin. *Lancet* **2**(8406): 765-8

SÜSAL C., DANIEL V. & OPELZ G. (1996). Does AIDS emerge from a disequilibrium between two complementary groups of molecules that mimic MHC? *Immunol Today* **17**(3): 114-9

SÜSAL C., KROPELIN M., DANIEL V. & OPELZ G. (1993). Molecular mimicry between HIV-1 and antigen receptor molecules: a clue to the pathogenesis of AIDS. *Vox Sang* **65**(1): 10-7

SVENNERHOLM L., BOSTROM K., FREDMAN P., JUNGBJER B., LEKMAN A., MANSSON J.E. & RYNMARK B.M. (1994). Gangliosides and allied glycosphingolipids in human peripheral nerve and spinal cord. *Biochim Biophys Acta* **1214**: 115-23

THANYANE S.T. (2003). A novel application of affinity biosensor technology to detect antibodies to mycolic acids in tuberculosis patients. MSc. Department of Biochemistry, Faculty of Natural and Agricultural Sciences, University of Pretoria, Pretoria

THÉVENOT D.R., TOTH K., DURST R.A. & WILSON G.S. (2001). Electrochemical biosensors: recommended definitions and classification. *Biosens Bioelectron* **16**: 121-31

THURMOND L.M., REESE M.J., DONALDSON R.J. & ORBAN B.S. (1998). A kinetic enzyme immunoassay for the quantitation of antibodies to a humanized monoclonal antibody in human serum. *J Pharm Biomed Anal* **16**(8): 1317-28

TSUBOUCHI A., YOSHIOKA K. & KAKUMU S. (1985). Naturally occurring serum antiidiotypic antibody against antiliver-specific membrane lipoprotein in patients with hepatitis. *Hepatology* **5**(5): 752-7

VAN DER MECHÉ F.G.A., VISSER L.H., JACOBS B.C., ENDTZ H.P., MEULSTEE J. & VAN DOORN P.A. (1997). Guillain-Barré syndrome: multifactorial mechanisms versus defined subgroups. *J Infect Dis* **176 (Suppl 2)**: S99-102

VAN KONINGSVELD R., VAN DOORN P.A., SCHMITZ P.I.M., ANG C.W. & VAN DER MECHÉ F.G.A. (2000). Mild forms of Guillain-Barré syndrome in an epidemiologic survey in The Netherlands. *Neurology* **54**: 620-5

VAN LOGHEM E. & BIEWENGA J. (1983). Allotypic and isotypic aspects of human immunoglobulin A. *Mol Immunol* **20**(9): 1001-7

VAN REGENMORTEL M.H.V. (1998). From absolute to exquisite specificity. Reflections on the fuzzy nature of species, specificity and antigenic sites. *J Immunol Methods* **216**: 37-48

VARELA F., ANDERSSON A., DIETRICH G., SUNDBLAD A., HOLMBERG D., KAZATCHKINE M.D. & COUTINHO A. (1991). Population dynamics of natural antibodies in normal and autoimmune individuals. *Proc Natl Acad Sci USA* **88**(13): 5917-21

WATANABE M., AOYAGI Y., RIDELL M. & MINNIKIN D.E. (2001). Separation and characterization of individual mycolic acids in representative mycobacteria. *Microbiology* **147**: 1825-37

WILLISON H.J., O'HANLON G., PATERSON G., O'LEARY C.P., VEITCH J., WILSON G.S., ROBERTS M., TANG T. & VINCENT A. (1997). Mechanisms of action of anti-GM_1 and anti-GQ_{1b} ganglioside antibodies in Guillain-Barré syndrome. *J Infect Dis* **176 (Suppl 2)**: S144-9

WILSON R. & SARGENT J.R. (2001). Chain separation of monounsaturated fatty acid methyl esters by argentation thin-layer chromatography. *J Chromatogr A* **905**(1-2): 251-7

WINER J.B., HUGHES R.A.C., ANDERSON M.J., JONES D.M., KANGRO H. & WATKINS R.P.F. (1988). A prospective study of acute idiopathic neuropathy. II. Antecedent events. *J Neurol* **51**: 613-8

WOLFE G.I., BAROHN R.J., FOSTER B.M., JACKSON C.E., KISSEL J.T., DAY J.W., THORNTON C.A., NATIONS S.P., BRYAN W.W., AMATO A.A., FREIMER M.L. & PARRY G.J. (2002). Randomized, controlled trial of intravenous immunoglobulin in myasthenia gravis. *Muscle Nerve* **26**(4): 549-52

WUILMART C., WIKLER M. & URBAIN J. (1979). Induction of autoanti-idiotypic antibodies and effects on the subsequent immune response. *Mol Immunol* **16**(12): 1085-92

YU F.Y. & CHU F.S. (1999). Production and characterization of a monoclonal anti-anti-idiotype antibody against fumonisin B(1). *J Agric Food Chem* **47**(11): 4815-20

YUAN Y., CRANE D.C., MUSSER J.M., SREEVATSAN S. & BARRY C.E. (1997). MMAS-1, the branch point between *cis*- and *trans*-cyclopropane-containing oxygenated mycolates in *Mycobacterium tuberculosis*. *Biol Chem* **272**: 10041-10049

YUAN Y., LEE R.E., BESRA G.S., BELISLE J.T. & BARRY III C.E. (1995). Identification of a gene involved in the biosynthesis of cyclopropanated mycolic acids in *Mycobacterium tuberculosis*. *Proc Natl Acad Sci USA* **92**: 6630-4

YUKI N., ANG C.W., KOGA M., JACOBS B.C., VAN DOORN P.A., HIRATA K. & VAN DER MECHÉ F.G.A. (2000). Clinical features and response to treatment in Guillain-Barré syndrome associated with antibodies to GM1b ganglioside. *Ann Neurol* **47**: 214-21

ZHANG R.-G., SCOTT D.L., WESTBROOK M.L., NANCE S., SPANGLER B.D., SHIPLEY G.G. & WESTBROOK E.M. (1995). The three-dimensional crystal structure of cholera toxin. *J Mol Biol* **251**: 563-73

ZHANG W., FRANK M.B. & REICHLIN M. (2002). Production and characterization of human monoclonal anti-idiotype antibodies to anti-dsDNA antibodies. *Lupus* **11**(6): 362-9

ZOUALI M. & EYQUEM A. (1983). Expression of anti-idiotypic clones against auto-anti-DNA antibodies in normal individuals. *Cell Immunol* **76**(1): 137-47